Coupling of Redundant *gooseberry neuro* and *gooseberry* Functions in *Drosophila melanogaster*, an Evolutionary Strategy against an Intrinsic Haploinsufficiency of *gooseberry*?

Dissertation

zur

Erlangung der naturwissenschaftlichen Doktorwürde

(Dr. sc. nat.)

vorgelegt der

Mathematisch-naturwissenschaftlichen Fakultät

der

Universität Zürich

von

Haihuai He

aus der

Volksrepublik China

Promotionskomitee

Prof. Dr. Markus Noll
(Vorsitz und Leitung der Dissertation)

Prof. Dr. Walter Schaffner

Zürich 2007

Table of Contents

Summary

The *gooseberry* (*gsb*) and *gooseberry neuro* (*gsbn*) genes of *Drosophila*, together with *paired* (*prd*), are the founding members of the Pax gene family and part of the Pax-3/7 subfamily. *gsb* and *gsbn* are closely apposed and divergently transcribed. A similar situation has been found for several other *Drosophila* segmentation genes. The common feature of these "gene pairs" is that the expression patterns of the two genes of a pair are similar to and independent of each other, because of the capability of their enhancers to activate both genes of the pair. Therefore, the *gsb-gsbn* pair is unique in the sense that *gsb* and *gsbn* exhibit distinct, though overlapping expression patterns, and most importantly, *gsbn* expression is dependent on *gsb* activity. However, in the absence of mutant alleles specific for *gsbn*, it was not clear why *Drosophila* needs two *gooseberry* genes rather than only one, what is their functional relationship to each other, and furthermore how their functional link is established.

To address these questions, a series of *gsbn* mutations were generated by ends-in homologous recombination and Flipase-mediated homologous recombination. *gsbn* homozygous mutants are viable, but males are sterile and females barely fertile. Although *gsbn* is dispensable for viability, transheterozygotes of a *gsbn* allele over a large deficiency uncovering both *gsbn* and *gsb* are lethal at larval stages. This lethality is caused by the additional loss of one copy of *gsb* uncovered by the large deficiency. The *gsb* haploinsufficiency in *gsbn* mutants indicates that *gsbn* and *gsb* share overlapping function(s) required for postembryonic viability.

In the CNS, *gsbn* is expressed in the dorsal subset of SNa (segmental nerve branch a) motoneurons. In $gsbn^{-}$ $gsb^{-/+}$ mutant embryos, more than 80% of hemisegments exhibit a defective innervation of the lateral body wall muscles by SNa motor axons. This phenotype results from the inability of the dorsal SNa motor axons to extend into the lateral muscle field. The evidence presented suggests that *gsbn* and *gsb* act in a partially redundant manner at the early phase of the neuronal stage to control the differentiation of the dorsal SNa motoneurons.

To address the role of *gsbn* in segmentation, the cuticular phenotype of large deficiency mutants rescued by *gsbn* was examined. Furthermore, a new strong allele of *gsb*, generated by imprecise excision of the P-element insertion gsb^{P1155}, was isolated. The results presented support the idea that *gsbn* is partially redundant with *gsb* in the development of the epidermis.

Collectively, the analyses of the *gsbn* mutant phenotypes demonstrate that the functions of *gsbn* and *gsb* are intimately linked. The essential role of *gsbn* in both male and female fertility justifies its existence in *Drosophila*. Furthermore, the results from the analysis of the SNa phenotype in $gsbn^{-}$ $gsb^{-/+}$ mutants provide direct evidence that the functional link between *gsb* and *gsbn* is established through the *gsb-gsbn* hierarchy and that the establishment of this hierarchy is to prevent the deleterious effects caused by the *gsb* haploinsufficiency.

Zusammenfassung

Gooseberry (*gsb*) und *gooseberry neuro* (*gsbn*) sind, zusammen mit dem *paired* (*prd*) Gen, die Gründungsmitglieder der Pax Genfamilie und Teil der Pax-3/7 Subfamilie in *Drosophila melanogaster*. *Gsb* und *gsbn* liegen in unmittelbarer Nachbarschaft zueinander und werden divergierend transkribiert. Eine ähnliche Konstellation liegt bei mehreren anderen Segmentierungsgenen von *Drosophila* vor. Die allgemeine Eigenschaft solcher „Genpaare“ ist, dass die Expressionsmuster der beiden Gene eines Paars ähnlich und unabhängig von einander sind, weil ihre Enhancers beide Gene des Paares aktivieren. Das *gsb-gsbn* Paar ist in diesem Sinn einzigartig, weil sich die Expressionsmuster der beiden Gene zwar überlappen, aber doch klar unterscheiden. Zudem ist die Expression von *gsbn* abhängig von der Aktivität des *gsb* Gens. Wegen des Fehlens von mutanten Allelen, die spezifisch das *gsbn* Gen betreffen, war es nicht klar, weshalb in *Drosophila* nicht eines sondern zwei *gooseberry* Gene benötigt werden, was die funktionelle Beziehung zwischen diesen zwei paralogen Genen kennzeichnet und wie diese funktionelle Verbindung hergestellt wird.

Um diese Fragen anzugehen, wurden eine Reihe von Mutationen im *gsbn* Gen erzeugt, indem man zwei Methoden, die „ends-in“ homologe Rekombination und die „Flipase-vermittelte“ homologe Rekombination verwendete. Die solcherart erzeugten *gsbn* Nullmutanten sind zwar homozygot lebensfähig, aber die Männchen sind steril und die Weibchen nur stark reduziert fruchtbar. Obgleich *gsbn* für die Entwicklung und das Überleben der Taufliege entbehrlich zu sein scheint, ist die transheterozygote Kombination eines *gsbn* Allels mit einer großen Defizienz, die sowohl das *gsbn* als auch das *gsb* Gen deletiert, im Larvenstadium letal. Diese Letalität wird durch das zusätzliche Fehlen der einen *gsb* Genkopie verursacht, die durch die Defizienz eliminiert worden ist. Die *gsb* Haploinsuffizienz in der homozygoten *gsbn* Mutante weist darauf hin, dass sich *gsbn* und *gsb* gewisse Genfunktionen teilen, die für die postembryonale Entwicklung erforderlich sind.

Im zentralen Nervensystem wird das *gsbn* Gen in der dorsalen Subpopulation der SNa (segmentieller Nervenast a) Motorneuronen exprimiert. In homozygoten *gsbn* Embryonen, die zusätzlich eine mutierte Kopie des *gsb* Gens tragen, weisen mehr als

80% der Hämisegmente eine defekte Innervation der lateralen Körperwandmuskeln durch die SNa Motoraxone auf. Dieser Phänotyp ergibt sich aus dem Unvermögen der dorsalen SNa Motoraxone, sich auf das laterale Muskelfeld auszudehnen. Die gezeigten Beweise legen nahe, dass *gsbn* und *gsb* in einer zum Teil redundanten Weise an der frühen Phase der neuronalen Entwicklung mitwirken, um die Differenzierung der dorsalen SNa Motoneuron zu kontrollieren.

Um die Rolle von *gsbn* in der Segmentierung des Embryos zu studieren, wurde der cuticuläre Phänotyp der Mutanten überprüft, welche homozygot für die bereits weiter oben beschriebenen grossen Defizienzen sind und zusätzich ein *gsbn* Transgen tragen. Ausserdem wurde ein neues starkes *gsb* Allel durch die unpräzise Exzision der P-Element Insertion von gsb^{P1155} erzeugt. Die gezeigten Ergebnisse unterstützen die Hypothese, dass das *gsbn* Gen eine teilweise redundante Funktion mit *gsb* in der Entwicklung der Epidermis erfüllt.

In der vorliegenden Arbeit zeigt die Analyse der Phänotypen in *gsbn* Mutanten, dass die Funktionen von *gsbn* und *gsb* eng miteinander gekoppelt sind. Die Existenz des *gsbn* Gens in *Drosophila* wird durch seine essentielle Rolle sowohl in der männlichen wie auch weiblichen Fertilität gerechtfertigt. Die Analyse des Phänotyps in SNa Motorneuronen von *gsbn gsb/+* Mutanten liefern zusätzlich direkte Beweise dafür, dass die funktionelle Verbindung zwischen *gsb* und *gsbn* durch die *gsb-gsbn* Hierarchie begründet wird und dass die Aufrechterhaltung dieser Hierarchie die negativen Folgen einer *gsb* Haplo-Insuffizienz verhindern kann.

Chapter 1

General introduction

The *gooseberry* (*gsb*) and *gooseberry neuro* (*gsbn*) genes of *Drosophila*, together with *paired* (*prd*), are the founding members of the Pax gene family and part of the Pax-3/7 subfamily (Noll, 1993). The *gsb* locus was first identified by Nüsslein-Volhard and Wieschaus in a large screen for mutations affecting larval cuticle formation (Nüsslein-Volhard and Wieschaus, 1980). Later, in an attempt to search for homologous domains of *paired* (*prd*) as a test of the gene network hypothesis, *gsb* and *gsbn* were isolated, thus defining the *gsb* locus (Bopp et al., 1986). The N-terminal halves of the Prd, Gsb and Gsbn proteins are highly conserved, containing two DNA-binding domains: a 128-amino acid paired-domain and a 78-amino acid *paired*-type homeodomain, whereas the C-terminal halves are highly divergent and display no long stretches of homology among the three genes (Baumgartner et al., 1987).

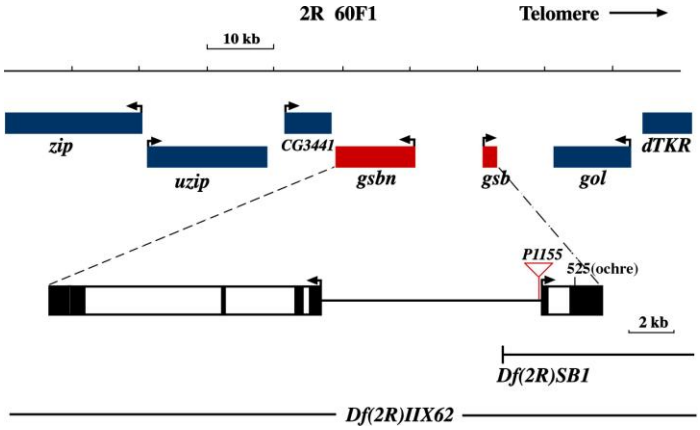

Fig. 1. Scheme of *gsbn-gsb* locus.

gsb and *gsbn* are closely apposed, separated by a 10 kb *cis*-regulatory region, and divergently transcribed (Fig. 1). In *Anopheles gambiae* and *Apis mellifera*, the two *gooseberry* genes are linked in a similar fashion to that in *Drosophila* (Osborne and Dearden, 2005). In addition to the close proximity of *gsb* and *gsbn*, the high conservation of the N-terminal halves of their proteins suggests that *gsb* and *gsbn* have descended from

an ancestral gene by duplication. It has been demonstrated that despite the considerably diverged coding sequences of *prd*, *gsb*, and *gsbn*, their proteins have conserved the same function and that the developmental functional difference between *prd*, *gsb*, and *gsbn* resides in their *cis*-regulatory regions acquired during evolution (Li and Noll, 1994).

During *Drosophila* embryogenesis, *gsb* expression begins at the end of cellularization in a segmentally repeated manner. Initially *gsb* is mainly expressed in the neuroectoderm. During germ band extension, some of the Gsb-expressing cells delaminate from the neuroectoderm to become neuroblasts, while the other Gsb-expressing cells remain in the ectodermal layer. After germ band retraction, *gsb* expression begins to diminish. *gsb* expression in the ectoderm is no longer detectable by the time of head involution, while very low levels of Gsb protein persist in the central nervous system (CNS) until head involution (Gutjahr et al., 1993).

Although *gsb* and *gsbn* share a common upstream region (Fig. 1), *gsbn* has an expression pattern distinct from that of *gsb*. *gsbn* expression starts at stage 10 in a small number of neuroblasts, ganglion mother cells, and neurons. As neurogenesis proceeds, the number of Gsbn-expressing cells in the CNS increases. Gsbn reaches its highest level before head involution and gradually diminishes afterwards. After germ band retraction, *gsbn* is also expressed in the epidermis, and its expression persists till the end of embryogenesis (Gutjahr et al., 1993). The temporal and spatial expression patterns of *gsb* and *gsbn* in the CNS suggest that the cells expressing Gsbn are derived from neuroblasts expressing Gsb. Indeed, it has been shown that expression of *gsbn* is dependent on *gsb* (Gutjahr et al., 1993).

gsb functions as a segment polarity gene in the epidermis and as a neuroblast identity gene in the CNS (Gutjahr et al., 1993; Zhang et al., 1994; Skeath et al., 1995; Duman-Scheel et al., 1997). However, nothing is known about the function(s) of *gsbn* in *Drosophila* development simply because no *gsbn* single mutation has been identified. All mutations of the *gsb* gene are either hypomorphic or large deficiencies uncovering *gsb*, *gsbn*, and several additional genes (Fig. 1). The lack of null alleles affecting only *gsbn* or *gsb* forces researchers to work with either large deficiencies uncovering other genes or with *gsb* hypomorphic alleles, whereby several aspects of *gsb* function remain

unresolved. As *gsb* activates *gsbn* expression in the CNS, it is not yet clear whether *gsb* executes its function exclusively through the activation of *gsbn* or not. Furthermore, the function of *gsb* at the postmitotic neuronal stage has not been assessed due to the severe neuronal precursor defects in *gsb* mutants. Other puzzling aspects of the *gsb* functions are the cuticular phenotype of *gsb* mutants. *gsb* deficiency mutants show a strong cuticular phenotype, whereas the gsb^{525} allele, which produces Gsb protein at undetectable levels, exhibits a very weak cuticular phenotype (Duman-Scheel et al., 1997). Despite a complete rescue of the cuticular phenotype by a *gsb* transgene in *gsb* deficiency mutants (Gutjahr et al., 1993), it is not certain that this phenotype could be attributed solely to the loss of *gsb*, because it is still formally possible that *gsbn* is redundant or partially redundant with *gsb*. Therefore, without mutations that affect only *gsbn*, it would be extremely difficult, if not impossible, to analyze the function of *gsbn* or to address the complex aspects of the role of *gsb* and its functional relationship to *gsbn*.

One of the most prominent features of the organization of *Drosophila* larval external structures is that the repeated segments are aligned along the anterior-posterior (A-P) axis. Within each segment, the posterior part is covered by smooth cuticle, whereas the anterior part is covered by denticles where each denticle row has a distinct morphology based on shape, size, and polarity of the denticles (Nüsslein-Volhard and Wieschaus, 1980).

The genetic program underlying the patterning of the *Drosophila* larval cuticle has been discovered and unraveled by Nüsslein-Volhard and Wieschaus through a systematic search for mutations that affect the segmental pattern (Nüsslein-Volhard and Wieschaus, 1980). In this study, the identification of three classes of zygotic mutants, gap, pair-rule, and segment polarity mutants, suggested that at least three levels of spatial regulation are involved in the patterning of segmentation. During the past two decades, extensive studies have been carried out to elucidate the molecular mechanisms by which segmentation is controlled. Now, it is clear that this process involves a cascade of transcription factor interactions as well as cell-cell interactions through signaling pathways (Sanson, 2001). The progressive subdivision of the A-P axis is initiated at mid-oogenesis through the localization of maternal transcripts of the maternal coordinate genes to the anterior and posterior ends, which generates an embryonic polarity along the

A-P axis by the establishment of transcription factor gradients. In response to the gradients of maternal transcription factors, gap genes are transcribed in discrete stripes spanning several segments to further subdivide the A-P axis. Subsequently, through complex regulations by gap genes and maternal transcription factor gradients, the aperiodic gap gene patterns are converted into evenly spaced periodic pair-rule gene stripes at double-segment intervals. Pair-rule genes are the first set of genes to define segmental regions, establish polarity within each segment, and to properly initiate the expression of segment polarity genes in portions of every segment (Fig. 2). Finally, segment polarity genes interact with each other to maintain the A-P polarity within each segment.

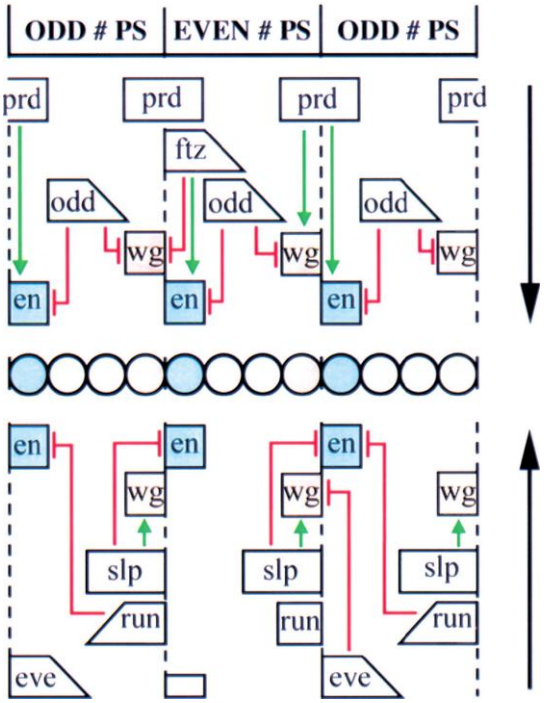

Fig. 2. Initial regulation of *engrailed* (*en*) and *wingless* (*wg*) (Adapted from Nasiadka and Krause, 2002). Expression of *en* and *wg* begins at the end of cellular blastoderm (stage 5) as a result of complex gene-regulatory interactions mediated by pair-rule gene products. A schematic representation of three consecutive parasegments is shown. The circles in the center represent a row of cells along the anterior–posterior axis. These are placed in the center of the figure for clarity with gene interactions diagramed both above and below. Stripes of gene expression are depicted as boxes or trapezoids. Sloped sides indicate decreasing levels of expression. Positive gene-regulatory interactions are marked in green and negative interactions in red. Stripes of *en* and *wg* initiate in single rows on either side of the parasegmental border.

One of the key steps in the hierarchical regulation of segmentation is the establishment and maintenance of the parasegment boundary (Nasiadka and Krause, 2002). Parasegments are the first morphologically distinct metameric units that appear during stage 10 (Martinez-Arias and Lawrence, 1985). Parasegments have the same width as segments, but are shifted anteriorly by two cells. The establishment of the parasegment boundary is achieved through complex interactions of pair-rule genes. Among pair-rule genes, *fushi tarazu* (*ftz*) and *even-skipped* (*eve*) play particularly important roles in determining the size, identity, and boundaries of parasegments. *ftz* and *eve* are expressed precisely in register with parasegments: *ftz* is expressed in even-numbered, *eve* in odd-numbered parasegments. It has been shown that at the stripe junction, the relative levels of *ftz* and *eve* expression define the parasegment width (Hughes and Krause, 2001). Changing these levels results in alternating wide and narrow parasegments. A major role for many of the remaining pair-rule genes is to ensure that *ftz* and *eve* are precisely positioned, and then to define the polarity within each parasegment.

Three segment polarity genes, *wingless* (*wg*), *engrailed* (*en*), and *hedgehog* (*hh*), play important roles in the maintenance of the parasegment boundary (Sanson, 2001). *wg* is initially expressed in one row of cells immediately anterior to the parasegment boundary, while *en* is expressed in two rows immediately posterior to the parasegment boundary. *hh* is expressed in the cells expressing *en*, and indirectly activated by *en*. *wg* stripes are positively regulated by *prd* and *odd-paired* (*opa*), but negatively regulated by *ftz* and *eve*. *prd* directly activates *wg* in odd-numbered stripes of *wg* (in even-numbered parasegments), and also indirectly activates *wg* by negative regulation of *odd-skipped* (*odd*), a repressor of *wg* (Mullen and DiNardo, 1995; Saulier-Le Drean et al., 1998; Nasiadka and Krause, 1999). *en* is positively regulated by *ftz* and *opa* for even-numbered *en* stripes, and by *prd* and *eve* for odd-numbered *en* stripes (Fig. 2). Kinetic studies suggest that the positive regulations of *prd* and *ftz* on *en* are direct, whereas *eve* acts positively on *en* indirectly by repression of *runt*, *odd*, and *sloppy-paired* (Manoukian and Krause, 1993).

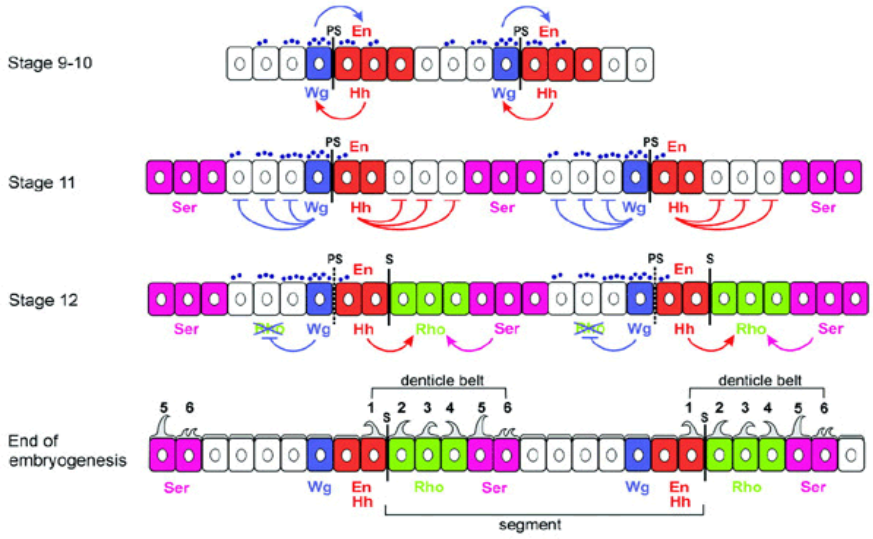

Fig. 3. Generation of an intrasegmental pattern in the *Drosophila* embryo (from Sanson, 2001). This sequence is accurate for the ventral side of the abdomen. PS designates the parasegmental boundaries and S the segmental boundaries. The anterior of the embryo is to the left, the posterior to the right. The apical side of the cells is up, and the basal side is down. Small violet dots represent the extracellular gradient of Wg protein. At stage 9–10, Wg and En/Hh expression is interdependent, and the Wg gradient symmetrical. At stage 11, Wg and En/Hh expression become independent, and the Wg gradient becomes asymmetric. At the same time, the Ser domain is delimited by the repressive action of both Wg and Hh. This generates one Ser stripe, two to three cells wide, per parasegment. At stage 12, Hh activates Rho expression in two rows of cells posterior to the En/Hh domain, and Ser activates Rho in one row of cells anterior to its domain. This results in a stripe of Rho expression precisely three cells wide. Anterior to the En/Hh domain, Wg signaling represses Rho expression. At the end of stage 12, the PS boundaries are no longer visible, and the segment grooves have formed immediately posterior to the En cells. At the end of embryogenesis, the posterior row of En cells and the Rho and Ser cells secrete denticles that make up the ventral denticle belts of the larval abdomen. Wg signaling specifies smooth cuticle in asymmetric fashion, three to four cell diameters in the anterior direction, but only extending through the first row of En cells to the posterior. The Ser-expressing cells secrete rows 5 and 6 of the denticle belts

Once the expression of *wg* and *en* at the parasegment boundary is initiated by pair-rule genes, the mutual stabilization of *wg* and *hh* expression is crucial for the maintenance of parasegment boundary and specification of epidermal cell types within each parasegment (Sanson, 2001). The major role of other segment polarity genes is to either positively or negatively regulate the Wg or Hh signaling pathways. The maintenance of *hh* expression is through the stabilization of *en* expression by Wg signaling. At 3-5 h AEL (after egg laying), *en* expression is dependent on *wg*. From 5-7

h AEL, *en* expression becomes independent of *wg* and is maintained by *en* autoregulation (Heemskerk et al., 1991). The maintenance of *wg* stripes from stage 8 to stage 10 requires Hh signaling activities. It has been suggested that *wg* also autoregulates itself in a Hh-independent way before stage 9 (Hooper, 1994). From stage 11, *wg* expression depends on *gsb* (Li et al., 1993; Li and Noll, 1993).

In addition to their functions in maintaining the parasegment boundary, *wg* and *hh* are also essential for the intrasegmental patterning after *en* expression becomes independent of *wg*. *Serrate* (*Ser*), encoding a membrane-bound ligand of the Notch receptor, is activated in a single stripe by the Hox genes at stage 11 (Fig. 3). Both *wg* and *hh* are repressors of *Ser* expression. *hh* represses *Ser* in the posterior direction, two to three cell-diameters away, thereby delimiting the anterior border of the *Ser* domain (Fig. 3). In the anterior direction, *wg* also represses *Ser* two to three cells away, thus defining the posterior border of the *Ser* domain (Sanson, 2001). Simultaneously, *wg*, *hh*, and *Ser* refine the expression of *rhomboid* (*rho*), a transmembrane protein required for the activation of the EGFR ligand *spitz* (*spi*), into a stripe pattern. As for *Ser*, the Hox genes activate *rho* in the ventral ectoderm. At stage 12, Hh signaling induces the first and second stripe of *rho*, while *Ser* induces the third *rho* stripe immediately adjacent to the *Ser* domain through activation of the Notch receptor (Fig. 3). Anterior to the parasegment boundary, *rho* activation is counteracted by the repressive action of Wg signaling (O'Keefe et al., 1997).

At the end of *Drosophila* embryogenesis, the differentiation of ventral epidermal cells is revealed by two distinct cuticle patterns within each segment: denticle belts in the anterior portion, and smooth cuticle in the posterior portion. *shaven baby* (*svb*), a zinc-finger domain transcription factor, is necessary and sufficient for denticle formation in the embryo. It appears that the EGFR signaling pathway activates *svb*, whereas *wg* specifies smooth cuticle by the repression of *svb* (Payre et al., 1999).

Similar to *wg* and *en*, the initiation of *gsb* expression is controlled by pair-rule genes. At least two pair-rule genes, *prd* and *opa*, positively regulate *gsb* expression in the odd- (even-numbered parasegments) and even-numbered stripes, respectively (Li et al., 1993). After 4 h AEL, *gsb* expression is maintained by *wg*. At 6 h AEL, *wg* expression

depends on *gsb*. The major function of *gsb* in segmentation is to maintain the *wg-gsb* autoregulatory loop after 6 h AEL (Li and Noll, 1993).

The *Drosophila* ventral nerve cord (VNC) arises from neuroectodermal cells located in the ventral-lateral region of the embryo. During the blastoderm stage the orchestration of the Dpp gradient from the dorsal region and of the Dorsal gradient from the ventral region establish the border of the neuroectoderm region along the dorsal-ventral (D-V) axis. Ventral cells expressing *twist* (*twi*) and *snail* (*sna*) develop into mesoderm and midline CNS; ventral-lateral cells express *short gastrulation* (*sog*) and form the neuroectoderm, which gives rise to the VNC; dorsal cells express Dpp and produce dorsal epidermis and the amnioserosa.

Genetic studies suggest that neuroblast (NB) formation in the neuroectoderm is controlled by two groups of genes with antagonistic functions: proneural genes and neurogenic genes (Campos-Ortega, 1993). Proneural genes include four basic helix-loop-helix transcription factors in the *achaete-scute* complex (*AS-C*): *archaete* (*ac*), *scute* (*sc*), *lethal of scute* (*l'sc*), and *asense* (*ase*). The neurogenic genes include *Notch* (*N*), *Delta* (*Dl*), *mastermind* (*mam*), *neuralized* (*neu*), and the *Enhancer-of-split* (*E(spl)*) complex. In the proneural gene mutants, the number of NBs is dramatically reduced, but not all NBs are missing, indicating that other genes are also involved in the NB formation. In the neurogenic gene mutants, the number of NBs is increased at the expense of epidermal cells. A "lateral inhibition" model has been proposed to account for the selection of NBs from proneural clusters in the neuroectoderm. All cells of a proneural cluster acquire the potential to be committed to a NB fate by the expression of proneural genes. Within each proneural cluster, the cell that expresses the proneural genes at the highest level is singled out and maintains proneural gene expression to become a NB. This cell expresses Dl, a membrane-bound ligand for the N receptor, and Dl triggers the N signaling pathway in the surrounding cells to inhibit their neural competence by down-regulating the proneural genes.

The unique identity of each NB is revealed by its characteristic lineage of ganglion mother cells (GMCs) and neurons as well as by the spectrum of genes it expresses. Genetic studies suggest that positional cues from A-P axis and D-V axis play

important roles in defining the identity of each NB. Along the A-P axis, the segment polarity genes *wg*, *gsb*, *patched* (*ptc*), and *hh* are redeployed to specify NB identity (Skeath, 1999). It has been shown that *gsb* expression directs row 5 cells to acquire fates different from row 3/4 cells, while *wg* activity endows NBs with row 3, 4, and 6 fates (Chu-LaGraff and Doe, 1993). However, the regulatory interactions between segment polarity genes in conferring NB identity is distinct from that used in the epidermis for segmentation. For example, one of the functions of *wg* in segmentation is to maintain *en* expression. In contrast, loss of *wg* in the CNS leads to the loss of row 4, 5, and 6 NBs, whereas loss of *en* does not affect the formation of these NBs (Chu-LaGraff and Doe, 1993; Bhat and Schedl, 1997). Along the D-V axis, the EGFR signaling pathway and three homeodomain transcription factors, *ventral nerve cord defective* (*vnd*), *intermediate nerve cord defective* (*ind*), and *msh* (mesoderm-specific homeobox-containing gene), control the NB fate (Skeath and Thor, 2003). The expression and activities of *vnd*, *ind*, and *msh* subdivide the neuroectoderm into a parallel array of three adjacent longitudinal columns. *vnd* is expressed in the medial column (closest to the ventral midline), *ind* in the intermediate column next to it, and *msh* in the lateral column, while EGFR activity acts in the medial and intermediate columns. *vnd* functions in the medial columns to promote the formation of proneural clusters and NBs with medial fates and represses intermediate fates of NBs. *ind* promotes the formation of proneural clusters and NBs with intermediate fates and represses lateral fates of NBs. EGFR signaling promotes intermediate column NB formation and helps specifying the fate of medial column NBs by activating *ind* expression, repressing *msh* in the intermediate column, and maintaining *vnd* expression. Thus, the combination of activities of columnar and segment polarity genes determines the fates of NBs within each cluster. After gastrulation, NBs delaminate from the neuroectoderm in five spatiotemporally distinct waves (SI-SV) to form an invariant and roughly orthogonal pattern of 30 NBs aligned in seven rows per hemisegment (Skeath, 1999).

After formation, each NB undergoes a series of asymmetric divisions, regenerating itself and producing a largely invariant numbers of GMCs. The key outcome of these asymmetric divisions is the exclusive localization of Prospero (*pros*), a homeobox transcription factor, into the nucleus of the GMCs. As GMCs divide only

once to produce two terminally differentiating neurons or glial cells, it is thought that Pros regulates the proliferative capabilities of GMCs. The identification of the *in vivo* targets of Pros suggests that *pros* acts as a binary switch between self-renewal and differentiation in neuronal precursors (Choksi et al., 2006). Pros not only represses genes required for self-renewal, such as NB identity genes and cell cycle genes, but it is also required to activate genes for terminal differentiation, as in *pros* mutants GMCs can divide several times to produce non-differentiating offspring cells.

Since each NB has a unique identity, it is conceivable that GMCs produced from different NBs will aquire different fates as well. However, the question arises how cell fates of GMCs derived from a common NB are specified. The recent discovery of a "temporal gene network" suggests that the temporal transitions in the expression of a set of transcription factors in almost all NB lineages play a key role in enabling GMCs born at different times in a lineage to aquire different fates (Isshiki et al., 2001; Pearson and Doe, 2003; Grosskortenhaus et al., 2005). This temporal cascade involves the sequential expression of five transcription factors: *hunckback* (*hb*), *Krüppel* (*Kr*), *pdm*, *castor* (*cas*), and *grainyhead* (*grh*). *hb* is expressed in NBs when they delaminate and during their first round of division. GMCs and neurons produced by NBs expressing *hb* maintain *hb* expression and require *hb* for proper fate specification. During the next division of the NBs, *hb* is down-regulated while *Kr* is activated. As with *hb*, GMCs and neurons produced by NBs expressing *Kr* maintain *Kr* expression and require *Kr* for proper fate specification. The operation of this network requires the ability of each temporal factor to activate the next gene in the cascade and to repress the "next plus one" gene. For example, *hb* activates *Kr* expression in the next time window and simultaneously represses *pdm* expression to ensure that *Kr* but not *pdm* is expressed during this window.

Each GMC divides asymmetrically to give rise to two terminally differentiating neurons or to two glial cells that acquire distinct fates. Genetic studies suggest that the N signaling pathway and *numb* function antagonistically to enable most, if not all, GMCs to produce two sibling neurons with distinct fates. The key outcome of a GMC division is that Numb segregates exclusively into one daughter cell to prevent this cell from adopting the fate of its sibling, in part by promoting the endocytosis of the N receptor.

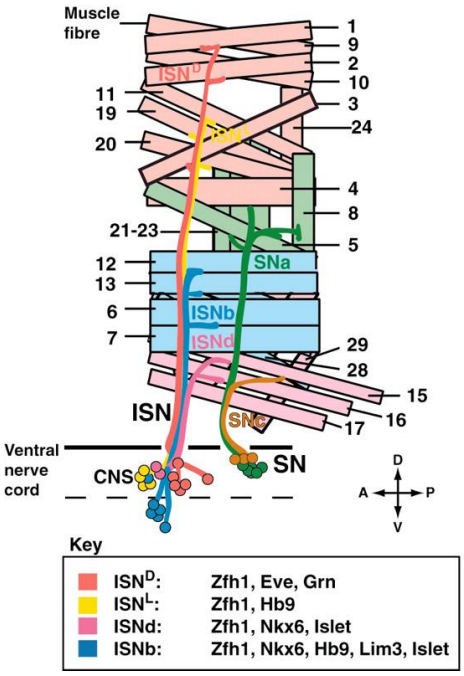

Fig. 4. *Drosophila* motor axon projections and their innervating body wall muscles (from Butler and Tear, 2007). In *Drosophila*, most MNs exit from the ventral nerve cord along two major nerve routes, the segmental nerve (SN) and intersegmental nerve (ISN), from which they defasciculate to innervate discreet populations of muscles (represented by numbers 1-29). The MNs express different combinations of transcription factors that appear to dictate which muscle fields they innervate, as shown in the key.

In the *Drosophila* ventral nerve cord, there are about 36 motoneurons (MNs) per hemisegment that innervate peripheral larval body wall muscles. The motor axons project through three main routes: the intersegmental nerve (ISN), the segmental nerve (SN), and the transverse nerve (TN) projecting along the segment border (Johansen et al., 1989; Van Vactor et al., 1993). Outside the ventral nerve cord, the ISN and SN converge at the exit junction, where some axons selectively fasciculate, switch pathways and branch further into the ISN, ISNb, ISNd, SNa, and SNc (Fig. 4). The ISN branch projects into dorsal muscles, whereas the other five branches project ventrally or laterally (Fig. 4). Axon outgrowth begins with the extension of the growth cone, a structure at the leading edge of the axon. To find the correct target muscle fibers that motor axons innervate, the growth cone senses and processes multiple molecular guidance cues from the cell surfaces along which it navigates. Guidance signals include differential adhesion, chemo-attraction, and repulsion. Developing larval muscles, body wall glia, and trachea have been suggested as the sources presenting the guidance signals. During the last decade, significant progress has been made in the identification of the ligands, receptors, and their downstream components that dictate and detect the trajectory taken by an individual axon (Butler and Tear, 2007). Diffusible ligand/receptor pairs include the

Slit/Robo, the Netrin/UNC5 and the Semaphorin/Plexin families. Recent studies in vertebrates suggest that morphogens, like BMPs, Wnt, and Hedgehog can function as axon guidance molecules as well (Butler and Tear, 2007). Guidance receptors function through activation of second messenger systems to locally rearrange the cytoskeleton to promote the growth towards or away from the target. Guidance molecules can also act by mediating differential adhesion.

Drosophila motoneurons can be subdivided into six distinct subclasses (ISN, ISNb, ISNd, SNa, SNc, TN) on the basis of their projection pathways (Fig. 4). Lineage analyses showed that *Drosophila* motoneurons are produced from a number of different Nbs (Landgraf et al., 1997; Schmidt et al., 1997; Schmid et al., 1999). The NBs that generate motoneurons are not distributed in a particular domain, but rather along both the mediolateral and dorsoventral axes of the ventral nerve cord (Landgraf et al., 1997). Moreover, these NBs do not exhibit any obvious common gene expression pattern. So far, no pan-motoneuron transcription factors in *Drosophila* have been identified that regulate common properties of motoneuron development. Instead, genes controlling the specification of motoneuronal subtypes have been found. These genes include *lim3*, *islet* (*isl*), *zfh1*, *eve*, *grain* (*grn*), *dHb9*, and *Nkx6*. *lim3* and *isl* are Lim-homeodomain transcription factors. *isl* is expressed in ISNb, ISNd and TN motoneurons, and in *isl* mutants ISNb motoneurons fail to innervate the neuromuscular junction of muscles 12 and 13 (Thor and Thomas, 1997). *lim3* is co-expressed by all of the *isl*-expressing motoneurons except those projecting through ISNd. *lim3* mutants display a lack of normal innervation at the neuromuscular junction of mucles 12 and 13 as well. Instead of taking their normal trajectory, these ISNb motoneurons ectopically project into the ISNd pathway (Thor et al., 1999). It is suggested that *isl* is necessary for the identity of both ISNb and ISNd motoneurons and *lim3*, in combination with *isl*, subdivides these motoneurons into the individual ISNb and ISNd classes. *dHb9* and *Nkx6* are homeodomain transcription factors. *dHb9*-expressing motoneurons populate the majority of motor axon branches, including ISN, ISNb, ISNd, SNa, and SNc. In the absence of *dHb9*, the ISNb fails to defasciculate from the ISN or projects aberrantly after defasciculating from ISN. At least part of the functions of *dHb9* is to repress *eve* in ISNb motoneurons (Broihier and Skeath, 2002; Odden et al., 2002). *Nkx6* is co-expressed with

dHb9 and *lim3* in the motoneurons innervating ventral muscles. *Nkx6* acts in parallel with *dHb9* to regulate the motoneuron fate and promote axonogenesis (Broihier et al., 2004; Cheesman et al., 2004). *eve* is a key regulator for motoneurons projecting to the dorsal muscles (Landgraf et al., 1999; Fujioka et al., 2003). *eve* executes its function by regulating the expression of UNC5, a repulsive receptor for Netrin (Labrador et al., 2005). The specification of the aCC neuron, an ISN motoneuron, is governed by *eve*, *grn*, a GATA transcription factor, and *zfh1* through the *eve-grn-zfh1* code (Certel and Thor, 2004). *zfh1*, a zinc-finger homeodomain transcription factor, is expressed in all motoneurons. In *zfh1* mutants, motoneuron identity is not affected. However, motor axons projecting ventrally often stall at the edge of the CNS, which suggests that *zfh1* controls the axon exit from the CNS (Layden et al., 2006).

References

Baumgartner, S., Bopp, D., Burri, M. and Noll, M. (1987). Structure of two genes at the *gooseberry* locus related to the paired gene and their spatial expression during *Drosophila* embryogenesis. *Genes Dev* **1**, 1247-1267.

Bhat, K. M. and Schedl, P. (1997). Requirement for *engrailed* and *invected* genes reveals novel regulatory interactions between *engrailed/invected*, *patched*, *gooseberry* and *wingless* during *Drosophila* neurogenesis. *Development* **124**, 1675-1688.

Bopp, D., Burri, M., Baumgartner, S., Frigerio, G. and Noll, M. (1986). Conservation of a large protein domain in the segmentation gene *paired* and in functionally related genes of *Drosophila*. *Cell* **47**, 1033-1040.

Broihier, H. T., Kuzin, A., Zhu, Y., Odenwald, W. and Skeath, J. B. (2004). *Drosophila* homeodomain protein Nkx6 coordinates motoneuron subtype identity and axonogenesis. *Development* **131**, 5233-5242.

Broihier, H. T. and Skeath, J. B. (2002). *Drosophila* homeodomain protein dHb9 directs neuronal fate via crossrepressive and cell-nonautonomous mechanisms. *Neuron* **35**, 39-50.

Butler, S. J. and Tear, G. (2007). Getting axons onto the right path: the role of transcription factors in axon guidance. *Development* **134**, 439-448.

Campos-Ortega, J. (1993). Early neurogenesis in *Drosophila melanogaster*. In *The Development of Drosophila melanogaster*, (ed. M. Bate and A. Martinez-Arias), pp. 1091-1131. New York: Cold Spring Harbor Laboratory Press.

Certel, S. J. and Thor, S. (2004). Specification of *Drosophila* motoneuron identity by the combinatorial action of POU and LIM-HD factors. *Development* **131**, 5429-5439.

Cheesman, S. E., Layden, M. J., Von Ohlen, T., Doe, C. Q. and Eisen, J. S. (2004). Zebrafish and fly Nkx6 proteins have similar CNS expression patterns and regulate motoneuron formation. *Development* **131**, 5221-5232.

Choksi, S. P., Southall, T. D., Bossing, T., Edoff, K., de Wit, E., Fischer, B. E., van Steensel, B., Micklem, G. and Brand, A. H. (2006). Prospero acts as a binary switch between self-renewal and differentiation in *Drosophila* neural stem cells. *Dev Cell* **11**, 775-789.

Chu-LaGraff, Q. and Doe, C. Q. (1993). Neuroblast specification and formation regulated by *wingless* in the *Drosophila* CNS. *Science* **261**, 1594-1597.

Duman-Scheel, M., Li, X., Orlov, I., Noll, M. and Patel, N. H. (1997). Genetic separation of the neural and cuticular patterning functions of *gooseberry*. *Development* **124**, 2855-2865.

Fujioka, M., Lear, B. C., Landgraf, M., Yusibova, G. L., Zhou, J., Riley, K. M., Patel, N. H. and Jaynes, J. B. (2003). Even-skipped, acting as a repressor, regulates axonal projections in *Drosophila*. *Development* **130**, 5385-5400.

Grosskortenhaus, R., Pearson, B. J., Marusich, A. and Doe, C. Q. (2005). Regulation of temporal identity transitions in *Drosophila* neuroblasts. *Dev Cell* **8**, 193-202.

Gutjahr, T., Patel, N. H., Li, X., Goodman, C. S. and Noll, M. (1993). Analysis of the *gooseberry* locus in *Drosophila* embryos: *gooseberry* determines the cuticular pattern and activates *gooseberry neuro*. *Development* **118**, 21-31.

Heemskerk, J., DiNardo, S., Kostriken, R. and O'Farrell, P. H. (1991). Multiple modes of *engrailed* regulation in the progression towards cell fate determination. *Nature* **352**, 404-410.

Hooper, J. E. (1994). Distinct pathways for autocrine and paracrine Wingless signalling in *Drosophila* embryos. *Nature* **372**, 461-464.

Hughes, S. C. and Krause, H. M. (2001). Establishment and maintenance of parasegmental compartments. *Development* **128**, 1109-1118.

Isshiki, T., Pearson, B., Holbrook, S. and Doe, C. Q. (2001). *Drosophila* neuroblasts sequentially express transcription factors which specify the temporal identity of their neuronal progeny. *Cell* **106**, 511-521.

Johansen, J., Halpern, M. E. and Keshishian, H. (1989). Axonal guidance and the development of muscle fiber-specific innervation in *Drosophila* embryos. *J Neurosci* **9**, 4318-4332.

Labrador, J. P., O'Keefe, D., Yoshikawa, S., McKinnon, R. D., Thomas, J. B. and Bashaw, G. J. (2005). The homeobox transcription factor *even-skipped* regulates *netrin*-receptor expression to control dorsal motor-axon projections in *Drosophila*. *Curr Biol* **15**, 1413-1419.

Landgraf, M., Bossing, T., Technau, G. M. and Bate, M. (1997). The origin, location, and projections of the embryonic abdominal motorneurons of *Drosophila*. *J Neurosci* **17**, 9642-9655.

Landgraf, M., Roy, S., Prokop, A., VijayRaghavan, K. and Bate, M. (1999). *even-skipped* determines the dorsal growth of motor axons in *Drosophila*. *Neuron* **22**, 43-52.

Layden, M. J., Odden, J. P., Schmid, A., Garces, A., Thor, S. and Doe, C. Q. (2006). Zfh1, a somatic motor neuron transcription factor, regulates axon exit from the CNS. *Dev Biol* **291**, 253-263.

Li, X., Gutjahr, T. and Noll, M. (1993). Separable regulatory elements mediate the establishment and maintenance of cell states by the *Drosophila* segment-polarity gene *gooseberry*. *Embo J* **12**, 1427-1436.

Li, X. and Noll, M. (1993). Role of the *gooseberry* gene in *Drosophila* embryos: maintenance of *wingless* expression by a *wingless--gooseberry* autoregulatory loop. *Embo J* **12**, 4499-4509.

Li, X. and Noll, M. (1994). Evolution of distinct developmental functions of three *Drosophila* genes by acquisition of different *cis*-regulatory regions. *Nature* **367**, 83-87.

Manoukian, A. S. and Krause, H. M. (1993). Control of segmental asymmetry in *Drosophila* embryos. *Development* **118**, 785-796.

Martinez-Arias, A. and Lawrence, P. A. (1985). Parasegments and compartments in the *Drosophila* embryo. *Nature* **313**, 639-642.

Mullen, J. R. and DiNardo, S. (1995). Establishing parasegments in *Drosophila* embryos: roles of the *odd-skipped* and *naked* genes. *Dev Biol* **169**, 295-308.

Nasiadka, A. and Krause, H. M. (1999). Kinetic analysis of segmentation gene interactions in *Drosophila* embryos. *Development* **126**, 1515-1526.

Noll, M. (1993). Evolution and role of Pax genes. *Curr Opin Genet Dev* **3**, 595-605.

Nusslein-Volhard, C. and Wieschaus, E. (1980). Mutations affecting segment number and polarity in *Drosophila*. *Nature* **287**, 795-801.

O'Keefe, L., Dougan, S. T., Gabay, L., Raz, E., Shilo, B. Z. and DiNardo, S. (1997). Spitz and Wingless, emanating from distinct borders, cooperate to establish cell fate across the Engrailed domain in the *Drosophila* epidermis. *Development* **124**, 4837-4845.

Odden, J. P., Holbrook, S. and Doe, C. Q. (2002). *Drosophila* HB9 is expressed in a subset of motoneurons and interneurons, where it regulates gene expression and axon pathfinding. *J Neurosci* **22**, 9143-9149.

Osborne, P. W. and Dearden, P. K. (2005). Expression of Pax group III genes in the honeybee (*Apis mellifera*). *Dev Genes Evol* **215**, 499-508.

Payre, F., Vincent, A. and Carreno, S. (1999). *ovo/svb* integrates Wingless and DER pathways to control epidermis differentiation. *Nature* **400**, 271-275.

Pearson, B. J. and Doe, C. Q. (2003). Regulation of neuroblast competence in *Drosophila*. *Nature* **425**, 624-628.

Sanson, B. (2001). Generating patterns from fields of cells. Examples from *Drosophila* segmentation. *EMBO Rep* **2**, 1083-1088.

Saulier-Le Drean, B., Nasiadka, A., Dong, J. and Krause, H. M. (1998). Dynamic changes in the functions of Odd-skipped during early *Drosophila* embryogenesis. *Development* **125**, 4851-4861.

Schmid, A., Chiba, A. and Doe, C. Q. (1999). Clonal analysis of *Drosophila* embryonic neuroblasts: neural cell types, axon projections and muscle targets. *Development* **126**, 4653-4689.

Schmidt, H., Rickert, C., Bossing, T., Vef, O., Urban, J. and Technau, G. M. (1997). The embryonic central nervous system lineages of *Drosophila melanogaster*. II. Neuroblast lineages derived from the dorsal part of the neuroectoderm. *Dev Biol* **189**, 186-204.

Skeath, J. B. (1999). At the nexus between pattern formation and cell-type specification: the generation of individual neuroblast fates in the *Drosophila* embryonic central nervous system. *Bioessays* **21**, 922-931.

Skeath, J. B. and Thor, S. (2003). Genetic control of *Drosophila* nerve cord development. *Curr Opin Neurobiol* **13**, 8-15.

Skeath, J. B., Zhang, Y., Holmgren, R., Carroll, S. B. and Doe, C. Q. (1995). Specification of neuroblast identity in the *Drosophila* embryonic central nervous system by *gooseberry-distal*. *Nature* **376**, 427-430.

Thor, S., Andersson, S. G., Tomlinson, A. and Thomas, J. B. (1999). A LIM-homeodomain combinatorial code for motor-neuron pathway selection. *Nature* **397**, 76-80.

Thor, S. and Thomas, J. B. (1997). The *Drosophila islet* gene governs axon pathfinding and neurotransmitter identity. *Neuron* **18**, 397-409.

Van Vactor, D. V., Sink, H., Fambrough, D., Tsoo, R. and Goodman, C. S. (1993). Genes that control neuromuscular specificity in *Drosophila*. *Cell* **73**, 1137-1153.

Zhang, Y., Ungar, A., Fresquez, C. and Holmgren, R. (1994). Ectopic expression of either the *Drosophila gooseberry-distal* or *proximal* gene causes alterations of cell fate in the epidermis and central nervous system. *Development* **120**, 1151-1161.

Chapter 2

Generation and phenotypic analysis of *gooseberry neuro* mutants

Summary

To analyze the functions of *gsbn* during *Drosophila* development and address its complex functional relationship to *gsb*, two *gsbn* nonsense alleles were generated by ends-in homologous recombination. Both *gsbn* alleles have nonsense mutations followed by a shift in the open reading frame and were verified by PCR, Southern blot, and immunostaining. In addition, a deletion allele of *gsbn* was generated by Flipase-mediated homologous recombination. Homozygous *gsbn* mutants are viable but males are sterile and females barely fertile. However, transheterozygotes of a *gsbn* allele over a large deficiency uncovering both *gsbn* and *gsb* are lethal. This *gsb* haploinsufficiency in *gsbn* mutants indicates that *gsbn* and *gsb* share overlapping function(s) required for viability. Moreover, the evidence presented supports the previously proposed explanation why *gsb* and *gsbn* remained intimately linked during evolution. Phenotypic analysis of the *gsbn* mutants strongly suggests that the two *gsbn* nonsense alleles generated by ends-in homologous recombination are strong, if not null, alleles of *gsbn* and thus constitute decisive genetic tools for the functional analysis of *gsbn* and *gsb*.

Introduction

The *gooseberry* (*gsb*) and *gooseberry neuro* (*gsbn*) genes of *Drosophila*, together with *paired* (*prd*), are the founding members of the Pax gene family and part of the Pax-3/7 subfamily (Noll, 1993). The N-terminal halves of Gsb and Gsbn are highly conserved, containing two DNA-binding domains, the paired-domain and the *paired*-type homeodomain, whereas the C-terminal moieties are highly divergent and display no long stretches of homology among the three genes (Baumgartner et al., 1987).

gsb and *gsbn* are closely apposed, separated by a 10 kb *cis*-regulatory region, and divergently transcribed. In *Anopheles gambiae* and *Apis mellifera*, the two *gooseberry* genes are linked in a similar fashion (Osborne and Dearden, 2005). Despite the considerably diverged coding sequences of *prd*, *gsb*, and *gsbn*, their proteins have conserved the same function. The developmental functional difference between *prd*, *gsb*, and *gsbn* resides in their *cis*-regulatory regions acquired during evolution (Li and Noll, 1994b).

During *Drosophila* embryogenesis, *gsb* expression starts at the end of cellularization in a segmentally repeated manner. Initially *gsb* is expressed mainly in the neuroectoderm. During germ band extension, some of the Gsb-expressing cells delaminate from the neuroectoderm to become neuroblasts, while the other Gsb-expressing cells remain in the epidermal layer. After germ band retraction, *gsb* expression starts to diminish. *gsb* expression in the ectoderm is no longer detectable by the time of head involution, while very low levels of *gsb* persists in the CNS until head involution (Gutjahr et al., 1993).

Although *gsb* and *gsbn* share a common upstream region, *gsbn* has an expression pattern distinct from that of *gsb*. *gsbn* expression starts at stage 10 in a small number of neuroblasts, ganglion mother cells, and neurons. As neurogenesis proceeds, the number of Gsbn-expressing cells in the CNS increases. Gsbn reaches its highest level by head involution, and gradually diminishes afterwards. After germ band retraction, *gsbn* is expressed in the epidermis, and its expression persists till the end of embryogenesis (Gutjahr et al., 1993). It has been shown that the Gsbn-expressing cells descend from the

neuroblasts expressing Gsb (Gutjahr et al., 1993; Buenzow and Holmgren, 1995) and that the embryonic *gsbn* expression is largely dependent on *gsb* (Gutjahr et al., 1993).

It is not uncommon in *Drosophila* that two genes arising by duplication are closely linked. Among *Drosophila* segmentation genes, in addition to *gsb* and *gsbn*, other known examples of such "gene pairs" are *engrailed* (*en*) and *invected* (*inv*) (Gustavson et al., 1996), *sloppypaired 1* (*slp1*) and *2* (*slp2*) (Grossniklaus et al., 1992), or *knirps* (*kni*) and *knirps related* (*knrl*) (Gonzalez-Gaitan et al., 1994). The common feature of these gene pairs is that the expression patterns of the two genes of a pair are similar to and independent of each other. This feature appears to result from the capability of their *cis*-regulatory sequences to activate both genes of the pair (Gustavson et al., 1996). Therefore, the *gsb-gsbn* pair is unique in the sense that *gsb* and *gsbn* exhibit distinct, although overlapping expression patterns, and most importantly, *gsbn* expression is dependent on *gsb* activity (Gutjahr et al., 1993). Furthermore, the enhancers of *gsb* and *gsbn* cannot activate the heterologous promoters properly (Li and Noll, 1994a), which implies that the *gsb* locus has evolved, after the event of gene duplication, through a fundamentally different mechanism from that of the other gene pairs.

gsb functions as a segment polarity gene in the epidermis and as a neuroblast identity gene in the CNS (Gutjahr et al., 1993; Zhang et al., 1994; Skeath et al., 1995; Duman-Scheel et al., 1997). However, nothing is known about the function(s) of *gsbn* in *Drosophila* development simply because no single mutation affecting only *gsbn* has been identified. All mutations of the *gsb* gene are either hypomorphic or large deficiencies uncovering *gsb*, *gsbn*, and a few neighboring genes. The lack of null mutations affecting only *gsbn* or *gsb* has induced researchers to work with large deficiencies or *gsb* hypomorphic alleles, whereby several aspects of *gsb* functions remain unresolved. As *gsb* activates *gsbn* expression in the CNS, it is not yet clear whether *gsb* executes its function in the CNS exclusively through the activation of *gsbn*. Furthermore, the function of *gsb* at the postmitotic neuronal stage has not been assessed because of the severe defects in neuronal precursors of *gsb* mutants. Another puzzling aspect of the *gsb* functions is the cuticular phenotype of *gsb* mutants. *gsb* deficiency mutants show a strong cuticular phenotype, whereas the gsb^{525} allele, which produces Gsb protein by readthrough at the ochre codon at undetectable levels, exhibits a very weak cuticular

phenotype (Duman-Scheel et al., 1997). Despite the complete rescue of the cuticular phenotype by a *gsb* transgene in *gsb* deficiency mutants (Gutjahr et al., 1993), it is not certain that this mutant phenotype can be attributed solely to the loss of *gsb* because it is still possible that *gsbn* fulfills a function that is redundant or partially redundant with that of *gsb*. Therefore, without mutations that affect only *gsbn*, it is extremely difficult, if not impossible, to analyze the function of *gsbn* or to address the complex aspects of the role of *gsb* and its functional relationship to *gsbn*.

In order to unravel the complexity of the *gsb* locus, we generated a series of new *gsbn* alleles by ends-in homologous recombination and Flipase-mediated homologous recombination. The isolation of new *gsbn* alleles allows us not only to assess the functions of *gsbn* and *gsb*, but also to address the functional interaction between *gsbn* and *gsb* in *Drosophila* development.

Results

Generation and characterization of two *gsbn* nonsense alleles by ends-in homologous recombination

As homologous recombination does not require *a priori* knowledge about the functions of the target gene and as the nature of the mutation it generates is predictable, we decided to employ the method of ends-in homologous recombination to isolate *gsbn* mutants. A 14 kb *Avr*II-*Hpa*I fragment containing the entire *gsbn* coding region was used as donor construct for gene targeting after its introduction into the germline through the pTV2 P-element vector (Fig. 1A). Three modifications were introduced into the donor construct. Two nonsense mutations, both of which are followed by frame-shifts, are introduced into exon 1 and exon 4 of *gsbn*, creating an *Apa*I site and a *Spe*I site, respectively. In addition, into intron 3 an I-*Sce* I site was introduced, which is cleaved by heat-shock activated I-*Sce* I to generate a linear substrate for homologous recombination (Fig. 1A). The screening for targeting events essentially followed the procedure previously described (Fig. 2) (Rong et al., 2002; Egli et al., 2003). Among 49,208 flies screened,

four potential recombinants were isolated (Fig. 2A). The ends-in homologous recombination at the *gsbn* locus results in a tandem-duplication with two *gsbn* genes, one mutated in exon 1, the other in exon 4 (Fig. 1A). The correct targeting of the *gsbn* locus was verified by PCR as well as staining with anti-Gsbn of the four recombinants (data not shown). Subsequently, the two mutated *gsbn* alleles, $gsbn^{D\text{-}19A}$ and $gsbn^{D\text{-}25A}$, were separated through I-*Cre*I -induced recombination (Fig. 1B) and isolated (Fig. 2B).

PCR analysis showed that there is only a single mutated copy of *gsbn* present at each recombined *gsb* locus (Fig. 3A), which suggests that the I-*Cre*I-mediated reduction step was successful. Sequence analysis of the genomic regions containing the expected mutation sites confirmed that the mutations have been correctly introduced. Furthermore, Southern blot analysis showed that no obvious genomic rearrangement is present at the *gsbn* locus for both *gsbn* alleles (Fig. 3B). Since the stop codons and frame-shifts introduced are located in the N-terminal half of Gsbn, both alleles were expected to produce a truncated Gsbn protein (Fig. 2C). To confirm this expectation, embryos homozygous for each mutant allele were stained with an anti-Gsbn antiserum that recognizes only the C-terminal half of Gsbn. As expected, Gsbn protein is not detectable in $gsbn^{D\text{-}19A}$ embryos (cf. Fig. 4B with 4A). However, a weak signal appears in $gsbn^{D\text{-}25A}$ mutants (cf. Fig. 4D with 4C). Nevertheless, the subsequent phenotypic analysis of $gsbn^{D\text{-}25A}$ mutants suggested that the Gsbn protein detected in $gsbn^{D\text{-}25A}$ mutants is not functional (see Discussion).

Generation and characterization of a *gsbn* deletion allele

In addition to the two *gsbn* alleles obtained by homologous recombination, a *gsbn* deficiency allele was generated by Flipase-mediated recombination between two insertions of transposable elements into *gsbn*, $gsbn^{f06670}$ and $gsbn^{d07597}$, available from the Exelixis Collection (Parks et al., 2004; Thibault et al., 2004). The insertion sites of $gsbn^{f06670}$ and $gsbn^{d07597}$ were confirmed by PCR analysis of both ends of each insertion (data not shown). $gsbn^{f06670}$ is a piggyBac element inserted into intron 3 of *gsbn*, while $gsbn^{d07597}$ is a P-element insertion in the 5'UTR of *gsbn*. The presence of FRT sites with the same orientation in both $gsbn^{f06670}$ and $gsbn^{d07597}$ permits the generation of a deletion

allele of *gsbn*, $gsbn^{del}$, through Flipase-mediated recombination (Fig. 5) (Thibault et al., 2004). DNA sequence analysis showed that $gsbn^{del}$ has the expected deletion, extending from the 5'UTR to intron 3 of *gsbn* (data not shown). Furthermore, Gsbn protein was not detectable by anti-Gsbn staining in $gsbn^{del}$ embryos (cf. Fig. 3F with 3E). Similarly, the deficiency, $Df(2R)GGG^{d13}$, which uncovers *gsbn*, *gsb*, and *gol*, was generated by Flipase-mediated recombination between the FRT sites of the piggyBac-element insertions $gsbn^{f06670}$ and *f06661*, which is inserted in the region upstream of the *goliath* (*gol*) transcription start site. The genomic lesion of $Df(2R)GGG^{d13}$ was confirmed by DNA sequence analysis of the breaking points and immunostaining with antibodies against Gsbn and Gsb (data not shown).

Phenotypic analysis of *gsbn* mutants

Homozygous mutants of $gsbn^{D\text{-}19A}$, $gsbn^{f06670}$, and $gsbn^{del}$ can survive to adulthood, but all males are sterile and females are barely fertile. However, the survival rate of the homozygotes of the three alleles exhibits a large degree of variability (Table 1). Notably, the fraction of surviving $gsbn^{del}$ homozygotes is considerably lower than that of $gsbn^{D\text{-}19A}$ homozygotes. The survival rate of $gsbn^{del}$ homozygotes is essentially the same as that of $gsbn^{del}$ transheterozygotes while that of $gsbn^{D\text{-}19A}/gsbn^{f06670}$ transheterozygotes is similar to that of $gsbn^{D\text{-}19A}$ homozygotes (Table 1). All three *gsbn* alleles are completely lethal over one of the two large deficiencies, $Df(2R)GGG^{d13}$ and *Df(2R)IIX62*, uncovering both *gsb* and *gsbn* (Table 1). Their lethal phase occurs largely during larval stages. Only under non-crowded conditions, less than 5% of the $gsbn^{D\text{-}19A}/Df(2R)GGG^{d13}$ or $gsbn^{D\text{-}19A}/Df(2R)IIX62$ transheterozygotes survived to adulthood. But these escapers were extremely weak, hardly able to move, and died within one day after eclosion.

Rescue of the fertility defects of $gsbn^{-}$ mutants and the lethality of $gsbn^{-}$ $gsb^{-/+}$ mutants

To confirm that the defective fertility of *gsbn* homozygous mutants and the lethality of $gsbn^{-}$ $gsb^{-/+}$ mutants result from the loss of *gsbn*, an attempt was made to rescue the

fertility and viability by a *gsbn* transgene, *gsbnRes-deltaIN3*, which includes the full upstream and transcribed region of *gsbn* except introns 3 and 4 (Fig. 4I). *gsbnRes-deltaIN3* exhibited similar expression patterns to those of endogenous *gsbn* during embryogenesis (cf. Fig. 4G with 4A,E). As *gsbn* expression is largely dependent on *gsb* **(**Gutjahr et al., 1993**)**, it was also tested whether *gsbnRes-deltaIN3* expression depends on *gsb*. Indeed, in *Df(2R)IIX62* embryos, *gsbnRes-deltaIN3* expression is drastically reduced, but not completely abolished (cf. Fig. 4H with 4G), which indicates that *gsbnRes-deltaIN3* is transcriptionally regulated as endogenous *gsbn*. One copy of *gsbnRes-deltaIN3* rescues male and female fertility of *gsbn* homozygotes completely and the lethality of $gsbn^{-}$ $gsb^{-/+}$ mutants partially. Two copies of *gsbnRes-deltaIN3* (scored for two independent *gsbnRes-deltaIN3* lines), rescued 74% (n=538) and 81% (n=603) of $gsbn^{D\text{-}19A}$/*Df(2R)IIX62* transheterozygotes to fertile adults.

Discussion

Classification of the new *gsbn* alleles

Since $gsbn^{del}$ is a deficiency extending from the 5'UTR to intron 3 of *gsbn* and since no Gsbn protein encoded by the remaining exons 4 and 5 are detectable in $gsbn^{del}$ mutants by an anti-Gsbn antiserum prepared against this part of Gsbn, $gsbn^{del}$ should be considered to be a null allele of *gsbn*. However, in light of previous work suggesting that intron 2 of *gsbn* contains a *gsb* enhancer required for the viability function of *gsb* **(**Liu, 2003**)**, $gsbn^{del}$ does not only abolish *gsbn*, but is probably also a hypomorphic allele for *gsb*. In agreement with this interpretation, only 14% of $gsbn^{del}$ homozygotes survived to adulthood, whereas 58% of $gsbn^{D\text{-}19A}$ homozygotes survived. The reduction of the survival rate of $gsbn^{del}$ as compared to $gsbn^{D\text{-}19A}$ homozygotes most probably results from the additional deletion in $gsbn^{del}$ of this *gsb* enhancer in intron 2 of *gsbn*.

$gsbn^{D\text{-}19A}$ has a stop codon in the second amino acid of the extended homeodomain followed by a frame-shift. Thus, $gsbn^{D\text{-}19A}$ produces a truncated Gsbn protein, which includes the entire paired-domain, the linker region between the paired-

domain and homeodomain, and the first amino acid of the extended homeodomain. The question thus arises whether this truncated protein retains a residual function. A similar situation exists for *gsb*^{525}, in which the first codon of the homeobox is mutated to a stop codon, producing a truncated Gsb protein consisting of the paired-domain and the entire linker region (Duman-Scheel et al., 1997). The hypomorphic nature of *gsb*^{525} results from read-through at the ochre codon rather than a residual function of the truncated protein since the truncated Gsb^{525} protein is unable to rescue the *gsb* cuticular phenotype (Liu, 2003). As the N-termini of Gsb and Gsbn are highly conserved, it is improbable that the similarly truncated Gsbn protein produced by *gsbn*$^{D\text{-}19A}$ has any residual function.

gsbn$^{D\text{-}25A}$ was expected to be a null allele of *gsbn* because two stop codons followed by a frame-shift have been introduced N-terminal to the paired-domain. However, the assessment of the nature of this allele was complicated by the observation that *gsbn*$^{D\text{-}25A}$ embryos show weak staining with anti-Gsbn. Nevertheless, *gsbn*$^{D\text{-}25A}$ males are sterile and females are barely fertile, while *gsbn*$^{D\text{-}25A}$*/Df(2R)IIX62* or *gsbn*$^{D\text{-}25A}$*/Df(2R)GGG*^{d13} mutants are lethal (data not shown). Furthermore, the survival rate of *gsbn*$^{D\text{-}25A}$ is similar to that of *gsbn*$^{D\text{-}19A}$ (data not shown). Thus, *gsbn*$^{D\text{-}25A}$ behaves in all phenotypic aspects tested as *gsbn*$^{D\text{-}19A}$, which suggests that the detected Gsbn protein produced by *gsbn*$^{D\text{-}25A}$ is nonfunctional. Since the two stop codons are followed by a frame-shift mutation in *gsbn*$^{D\text{-}25A}$, read-through at both stop codons cannot explain the detection of very low levels of Gsbn antigens. Therefore, these low levels probably result from internal re-initiation of translation on the *gsbn*$^{D\text{-}25A}$ mRNA. In the coding region downstream of the *gsbn*$^{D\text{-}25A}$ mutations, there are several methionine codons in the Gsbn reading frame that might be used as internal re-initiation sites. These methionine codons are located within the N-terminal moiety of the paired-domain or the C-terminal half of Gsbn. In either case, the Gsbn$^{D\text{-}25A}$ protein which is truncated in its N-terminal part does not contain a complete paired-domain and hence is probably not functional, in agreement with the phenotypic analysis of *gsbn*$^{D\text{-}25A}$.

gsbn^{f06670} has a piggyBac-element insertion in intron 3 of *gsbn*. Therefore, *gsbn*^{f06670} might produce a truncated Gsbn protein like Gsbn$^{D\text{-}19A}$, including the paired-domain and the linker region but lacking the entire extended homeodomain. In *gsbn*^{f06670} embryos, the Gsbn protein is not detectable with an antiserum directed against the C-

terminal half of Gsbn (data not shown), which suggests that *gsbn*^{f07770} is a strong allele of *gsbn*. In agreement with this interpretation, the phenotypic analysis showed that *gsbn*^{f06670} behaved in the same manner as *gsbn*$^{D\text{-}19A}$ with respect to viability and fertility phenotypes.

gsbn^{d07597} has a P-element inserted in the 5'UTR of *gsbn*. *gsbn*^{d07597} homozygotes are viable and fertile although male fertility is reduced compared to that of the wild type. Male transheterozygotes of *gsbn*^{d07597} with either *gsbn*$^{D\text{-}19A}$ or *gsbn*^{f06670} are fertile and *gsbn*^{d07597}/*Df(2R)IIX62* and *gsbn*^{d07597}/*Df(2R)GGG*^{d13} transheterozygotes can survive to adulthood (data not shown). Moreover, there is a weak anti-Gsbn staining in *gsbn*^{d07597} embryos (data not shown). Since the P-element of *gsbn*^{d07597} does not disrupt the coding region of *gsbn*, it is conceivable that the detected Gsbn protein produced by *gsbn*^{d07597} is functional. Taken together, the phenotypic analysis and the immunostaining suggest that *gsbn*^{d07597} is a hypomorphic allele of *gsbn*.

In summary, based on the results from the phenotypic analysis and immunostaining of *gsbn* mutants, *gsbn*^{del} is a null allele for *gsbn*, but also a hypomorphic allele for *gsb*, while *gsbn*$^{D\text{-}19A}$, *gsbn*$^{D\text{-}25A}$ and *gsbn*^{f06670} are strong, if not null, alleles whereas *gsbn*^{d07597} is a hypomorphic allele.

gsb haploinsufficiency in *gsbn* mutants

Surprisingly, all *gsbn* alleles obtained except *gsbn*^{d07597} are lethal over a large deficiency uncovering both *gsbn* and *gsb*. One explanation is that a *gsbn* null allele is homozygous lethal and all *gsbn* alleles obtained are hypomorphic. It would follow that *gsb*^{del} is a hypomorphic allele, which is highly unlikely based on the preceding phenotypic analysis as well as the molecular lesion of *gsbn*^{del}. Another possibility is that the lethality of *gsbn*$^{-}$ *gsb*$^{-/+}$ mutants results from a mutation outside of the *gsbn* locus but uncovered by the large deficiencies. Since *Df(2R)GGG*^{d13} uncovers only *gsb* and *gol* in addition to *gsbn*, the most likely candidate is *gsb*. In agreement with this interpretation, one copy of *gsbres2* (Liu, 2003) rescued 12% (n=311) of *gsbn*$^{D\text{-}19A}$/*Df(2R)IIX62* transheterozygotes to adulthood.

The *gsb* haploinsufficiency in *gsbn* mutants suggests that *gsbn* and *gsb* share overlapping function(s) required for viability. The lethal phase of $gsbn^{-}$ $gsb^{-/+}$ mutants appears to occur during larval stages. Since *gsb* alleles are lethal during embryogenesis, it is not clear whether the *gsb* postembryonic function required for viability is completely or partially redundant with that of *gsbn*. Although *gsbn* is not essential for viability in the presence of two copies of *gsb*, it does have crucial functions for both male and female fertility. $gsbn^{-}$ males have accessory glands and an ejaculatory duct. They can initiate courtship, but fail to copulate with females, probably due to neuronal and/or muscular defects. It has been shown that the impairment of *gsb* function(s) leads to partial male sterility as well. The defective male fertility of partially rescued *gsb* mutants can be explained at least in part by the improper development of the ejaculatory duct (Liu, 2003). It would be interesting to examine whether the partially rescued *gsb* mutants, like $gsbn^{-}$ males, cannot copulate successfully with females.

The close link of the two *gooseberry* genes

In view of the similar genomic organizations of the *gsbn-gsb* locus in *Drosophila*, *Anopheles*, and *Apis*, the intriguing question arises why *gsbn* and *gsb* have remained closely linked during evolution. Previous work suggested that intron 2 of *gsbn* contains a *gsb* enhancer required for the viability function of *gsb* and that, to properly activate *gsb*, this enhancer must be located in the vicinity of *gsb* (Liu, 2003). However, the fact that $gsbn^{del}$, in which intron 2 of *gsbn* is completely deleted, is not homozygous lethal casts doubt on this interpretation and suggests that intron 2 of *gsbn* is not absolutely required for survival to adulthood. Nevertheless, the survival rate of $gsbn^{del}$ is considerably lower than that of $gsbn^{D\text{-}19A}$. It should be noticed that $gsbn^{del}$, like $gsbn^{D\text{-}19A}$, abolishes all *gsbn* functions. It follows that the reduced survival rate of $gsbn^{del}$ mutants may result from the impairment of a *gsb* function either redundant with *gsbn* or independent of *gsbn*. The assessment of the viability of $gsbn^{del}$ mutants rescued by a *gsbn* transgene will resolve this issue. Another scenario is that intron 2 of *gsbn* contains a *gsb* enhancer required for the *gsb* fertility function. Although the previous work on partially rescued *gsb* mutants suggested that this enhancer is not absolutely required for the male fertility function of

gsb (Liu, 2003), the partial penetrance of the male sterility phenotype could result from the residual *gsb* function from the hypomorphic *gsb* allele used in that study. Therefore, to clarify this issue, it would be desirable to examine the male fertility of partially rescued *gsb* mutants in combination with a *gsb* null allele.

Materials and methods

1. Preparation of the targeting donor construct for homologous recombination

a. Cloning of the 14 kb *gsbn* genomic region into the plasmid pBS (NA)

The plasmid "*gsbn*-3'*Avr*II 5 kb in pBS (NA)" was constructed by cloning the 5 kb *Avr*II fragment from the BSH4 λ-phage clone containing the genomic *gsbn* DNA (Bopp et al., 1986) into the vector pBS(NA), which was derived from pBS(*Not*I) (Rong and Golic, 2001) by the insertion of a *Hin*dIII-*Avr*II-*Hpa*I-*Sal*I linker between the *Hin*dIII and *Sal*I sites of the polylinker in pBS (*Not*I). Subsequently, a 3 kb *Hpa*I fragment was removed from the 3' downstream region of *gsbn* by digestion of "*gsbn*-3'*Avr*II 5 kb in pBS (NA)" DNA with *Hpa*I and religation to generate the plasmid "*gsbn*-3'*Avr*II-*Hpa*I 2 kb in pBS (NA)." Finally, the 11 kb *Avr*II fragment from BSH4 was inserted into the *Avr*II site of the plasmid "*gsbn*-3'*Avr*II-*Hpa*I 2 kb in pBS (NA)" in the appropriate orientation to generate the plasmid "*gsbn Avr*II-*Hpa*I 14 kb in pBS (NA)."

b. Introducing nonsense and frame-shift mutations into *gsbn* coding region

The plasmid "*gsbn Pst*I-*Hpa*I 12 kb in pBS (NA)" was derived from the plasmid "*gsbn Avr*II-*Hpa*I 14 kb in pBS (NA)" by replacing of the 1.5 kb *Xba*I-*Fse*I fragment with the 0.5 kb *Xba*I-*Fse*I fragment of "c4Z3-3.1in pKSpL2" (Li and Noll, 1994a). The plasmids "*gsbn Pst*I-*Sph*I 1.5 kb in pGEM-3" and "*gsbn Sph*I-*Sac*I 9 kb in pGEM-3" were obtained by cloning of the 1.5 kb *Sac*I-*Sph*I and the 9 kb *Sph*I-*Sac*I fragments of "*gsbn Pst*I-*Hpa*I 12 kb in pBS (NA)," respectively, between the *Sac*I and *Sph*I sites of pGEM-3.

The plasmid "*gsbn Sac*I-*Hpa*I 3 kb in pBS (NA)" was derived by the removal of the 9 kb *Sac*I fragment from "*gsbn Pst*I-*Hpa*I 12 kb in pBS (NA)."

5'-GAACT*A*GT*A*G.GGCCCCTTTTCGCAGGGTATCCCTTTC-3' (*gsbn*-Mu-up1) and 5'-GGGCC.C*T*AC*T*AGTTCGCGCTGGACATATCCATGGT-3' (*gsbn*-Mu-up2) were used as primers in PCR reactions with "*gsbn Pst*I-*Sph*I 1.5 kb in pGEM-3" DNA to generate the plasmid "Mu *gsbn Pst*I-*Sph*I 1.5 kb in pGEM-3." This procedure introduces into exon 1 of *gsbn* two consecutive stop codons (by mutating the codons for amino acids 8 and 9 (Ser-Leu) into amber codons; mutations underlined) followed by a single base-pair deletion (indicated by dot and gerating an *Apa*I site) resulting in a shift of the reading frame.

5'-AGACT.AG*T*TATAAGTGACACGGAATCGGAGCCTGGG-3' (*gsbn*-Mu-down3) and 5'-TTATA*A*CT.AGTCTCGCCCTGCAAACGATGTGAAAAGG-3' (*gsbn*-Mu-down4) were used as primers in PCR reactions with "*gsbn Sac*I-*Hpa*I 3 kb in pBS(NA)" DNA to generate the plasmid "Mu *gsbn Sac*I-*Hpa*I 3 kb in pBS(NA)." This procedure introduces into exon 4 of *gsbn* a single base-pair deletion (indicated by dot and generating together with an additional underlined point mutation a *Spe*I site), resulting in a frame-shift and two closely spaced in-frame amber and ochre codons that truncate the encoded Gsbn protein after the first amino acid of the extended homeodomain, Asp164.

5'-CGCGGTAGGGATAACAGGGTAATC-3' (*Mlu*I-I-*Sce*I-1) and 5'-CGCGGATTACCCTGTTATCCCTA-3' (*Mlu*I-I-*Sce* I-2) were annealed and then inserted into the unique *Mlu*I site of "*gsbn Sph*I-*Sac*I (I-*Sce* I) 9 kb in pGEM-3" to generate the plasmid "Mu *gsbn Sph*I-*Sac*I (I-*Sce*I) 9 kb in pGEM-3." This procedure replaces the unique *Mlu*I site of intron 3 of *gsbn* by an I-*Sce* I site.

To construct the plasmid "Mu *gsbn Pst*I-*Hpa*I 12 kb in pBS (NA)" that consists of the contiguous *gsbn* genomic DNA including all three mutated regions (exon1, intron 3, and exon 4), the 1.5 kb *Sac*I-*Sph*I fragment of "Mu *gsbn Pst*I-*Sph*I 1.5 kb in pGEM-3" and the 9 kb *Sph*I-*Sac*I fragment of "Mu *gsbn Sph*I-*Sac*I (I-*Sce*I) 9 kb in pGEM-3" were cloned into the *Sac*I site of "Mu *gsbn Sac*I-*Hpa*I 3 kb in pBS (NA)."

From the "Mu *gsbn Pst*I-*Hpa*I 12 kb in pBS (NA)" plasmid "Mu *gsbn Avr*II-*Hpa*I 14 kb in pBS (NA)" was constructed by replacing the *Xba*I-*Fse*I fragment of "Mu *gsbn*

*Pst*I-*Hpa*I 12 kb in pBS (NA)" with the *Xba*I-*Fse*I fragment of "*gsbn Avr*II-*Hpa*I 14kb in pBS (NA)."

Finally, the 14 kb *Not*I fragment of the *gsbn* targeting sequences from the mutated plasmid "Mu *gsbn Avr*II-*Hpa*I 14 kb in pBS (NA)" was inserted into the *Not*I site of the P-element vector pTV2 (Rong and Golic, 2001) to generate the targeting donor construct "Mu *gsbn Avr*II-*Hpa*I 14 kb in pTV2." This targeting donor construct contains a 14 kb fragment of the *gsbn* gene, including 1.5 kb of the upstream region, the entire transcribed region, and about 0.5 kb of the downstream region.

2. Construction of "*gsbnRes-deltaIN3* in pW8"

The plasmid "*gsbn* fullRes in pBS (NA)" was obtained by replacing the 1.5 kb *Xba*I-*Fse*I fragment of "*gsbn Avr*II-*Hpa*I 14 kb in pBS (NA)" with the 9 kb *Xba*I-*Fse*I fragment of *4Z1*, consisting of *gsbn* upstream and part of the leader sequences (Li and Noll, 1994a). To generate the plasmid "*gsbnRes-deltaIN3* in pBS(NA)," the 13 kb *Xba*I-*Asi*SI fragment of "*gsbn* fullRes in pBS (NA)" and the 0.7 kb *Asi*SI-*Bgl*II fragment of the *gsbn*-cDNA BSH4c4 (Baumgartner et al., 1987) were combined with the *Bgl*II-*Xba*I fragment of "*gsbn*-3'*Avr*II-*Hpa*I 2 kb in pBS (NA)," which includes most of exon 5, the adjacent 0.5 kb of the downstream region and the vector. Finally, the insert of "*gsbnRes-deltaIN3* in pBS (NA)," a 16 kb *Xba*I-*Not*I fragment, was inserted between the *Xba*I and *Not*I sites of the polylinker of the P-element vector pW8 (Klemenz et al., 1987) to generate the rescue construct "*gsbnRes-deltaIN3* in pW8."

Transgenic flies were obtained by injecting the targeting donor construct and the rescue construct together with helper plasmid pUChspΔ2-3 into *y w* embryos according to standard procedures. 18 and 6 independent transgenic lines were obtained for the *gsbn* targeting donor construct and the *gsbnRes-deltaIN3* rescue construct, respectively.

3. *Drosophila* stocks

y w; *P{hs-FLP}P{hs-I-Sce I}/TM6* (Rong et al., 2002),

y w; P*{hs-I-Cre I} Sb/TM6* (Rong et al., 2002),

w; *gsbn*^{f06670}*/CyO* (Parks et al., 2004),

w; *gsbn*^{d07597}*/CyO* (Parks et al., 2004),

w; *Df(2R)IIX62/SM6B*,

y w; *Df(2R)IIX62*/*CyO, Kr-GFP*; *gsb-res2* (Liu, 2003),

w; *gsbn*$^{M7\text{-}B1}$*/SM6B*,

w; *gsbn*$^{D\text{-}19A}$*/SM6B*,

w; *gsbn*$^{D\text{-}25A}$*/SM6B*,

w; *gsbn*^{del}*/SM6B*,

w; *Df(2R)GGG*^{d13}*/SM6B*,

y *w*; *gsbn*$^{D\text{-}19A}$*/CyO, y*$^{+}$; *gsbnRes-deltaIN3*,

y w; *gsbn*$^{D\text{-}19A}$*/CyO, hb-LacZ*; *gsbnRes-deltaIN3*,

y w; *Df(2R)GGG*^{d13}*/CyO, y*$^{+}$; *gsbnRes-deltaIN3*,

y w; *Df(2R)GGG*^{d13}*/CyO, hb-LacZ*; *gsbnRes-deltaIN3*,

y w; *Df(2R)IIX62 /CyO, y*$^{+}$; *gsbnRes-deltaIN3*,

y w; *Df(2R)IIX62/CyO, hb-LacZ*; *gsbnRes-deltaIN3*.

y w; *ey-flp* (Egli et al., 2003)

hs-flp w; *Adv*^{1}*/CyO* (Thibault et al., 2004)

4. Genetic procedures for gene targeting

a. Targeting crosses for homologous recombination at the *gsbn* locus

Three independent targeting donor lines, *P{w*$^{+}$; *donor 7}*, *P{w*$^{+}$; *donor 12}*, and *P{w*$^{+}$; *donor 17}*, all inserted on the X-chromosome, were used for targeting crosses. Male targeting donor flies were crossed to *y w*; *P{hs-FLP} P{hs-I-Sce I}/TM6* virgins (Fig. 2). After 1 day of egg laying at 25°C, parents were removed and transferred to new tubes. On days 2, 3, and 4, the progeny were given a heat shock at 38°C for 1 hour. The eclosed *y w P{w*$^{+}$; *donor}/y w*; *P{hs-FLP} P{hs-I-Sce I}/+* virgins were test-crossed with *y w; ey-FLP* males individually and their progeny were screened for the presence of the *w*$^{+}$ marker. The presence of the *w*$^{+}$ marker indicates that the donor targeting transgene must have undergone homologous recombination (after excision from the X-chromosome) with the *gsbn* target gene, during which the *w*$^{+}$ marker is tramsferred to the *gsbn* locus

and can no longer be excised by Flipase (Fig. 1A). For donor M7, 15,505 flies were screened, and three targeting events were identified. For donor M12, 16,886 flies were screened, and one targeting event was identified. For donor M17, 16,817 flies were screened, and no targeting event was identified.

b. Reduction of tandem-duplication of *gsbn* mutant alleles to single copies by I-*Cre*I-mediated recombination

w; gsbn$^{M7\text{-}B1}$*/SM6B* males carrying duplicated *gsbn* mutant alleles after targeted homologous recombination (Fig. 1A) were crossed with *w*; *P{hs-I-CreI} Sb/TM6* virgins (Fig. 2B). After 1 day of egg laying, parents were removed and transferred to new tubes and the progeny were heat-shocked at 36°C for 1 hour on day 3 or 4. Eclosing *w*; *gsbn*$^{M7\text{-}B1}$/+; *P{hs-I-CreI} Sb*/+ males with w^{+}/w^{-} mosaic eyes were individually mated with *y w*; *Gla/CyO, hb-LacZ* virgins (Fig. 2B). A white-eyed Sb^{+} son (*y w*; *gsbn*^{reduced}*/CyO, hb-LacZ*) from a given father was crossed to *y w*; *Gla/CyO, hb-LacZ* virgins to establish stocks of the reduced single *gsbn* mutant alleles (Fig. 2B). Once the stocks were established, the flies were analyzed for the presence of the *gsbn* mutant allele by PCR (Fig. 3A).

5. Genetic crosses for the generation of *gsbn*^{del} and *Df(2R)GGG*^{d13}

gsbn^{del} and *Df(2R)GGG*^{d13} were generated by a procedure described previously (Thibault et al., 2004). To generate *gsbn*^{del}, piggyBac transposon insertion *f06670* and P-element insertion *P{d07597}* were used (Fig. 5). The original *piggyBac{f06670}* insertion is homozygous lethal. After removal of the lethal(s) on the *piggyBac{f06670}* chromosome by recombination, a homozygous viable *piggyBac{f06670}* chromosome was obtained. The lethal-free *piggyBac{f06670}* chromosome was used in all subsequent crosses. Males carrying *P{d07597}* (*w*; *P{d07597}/CyO*) were crossed to *P{hs-FLP} w*; *Adv*^{1}*/CyO* virgins. *P{hs-FLP} w; P{d07597}/CyO* male progeny were crossed to *w*; *piggyBac{f06670}/CyO* virgins. After 2 days of egg laying, the parents were removed and the progeny were heat-shocked for 1 hour at 37°C on five consecutive days. *P{hs-*

FLP} *w/w*; *piggyBac{f06670}/P{d07597}* female progeny with w^+/w^- mosaic eyes were crossed to *y w*; *Gla/CyO*, y^+ males. The white-eyed male progeny (*y w*; $gsbn^{del}$/*CyO*, y^+) were kept for further verification. $Df(2R)GGG^{d13}$ was obtained by using two *piggyBac* insertions, *f06670* and *f06661*, in a crossing scheme analogous to that used to generate $gsbn^{del}$.

6. Verification and identification of *gsbn* nonsense alleles

Two primers, *gsbn* exon 1-2 (5'-GAGAGTTGCAAAGTACCGTCGG-3') and *gsbn* exon 2 (5'-CGGGAGAGGTCACCTTGGGCTTAG-3'), were used in PCR reactions for the amplification of the *gsbn* genomic region into which the upstream stop codons and frame-shift in exon 1 of *gsbn* had been introduced. For the amplification by PCR of the *gsbn* genomic region into which the frame-shift in exon 4 of *gsbn* had been introduced, generating two closely spaced in frame stop codons, the primers BSH4 intron 3 (5'-TTCAAGCCCGATTGCCGATGACG-3') and Rgsbn-3'UTR (5'-AAGCCATGTAATGCACATGCAGC-3') were used. The PCR products were gel-purified and digested with *Apa*I or *Spe*I for the detection of the presence of the upstream and downstream stop codons, respectively (Fig. 3A).

7. Verification of *gsbn* nonsense alleles by Southern blot analysis

Genomic DNA was extracted as described (Steller, 1990). For each genotype, 1 μg of genomic DNA digested with *Avr*II was separated on a 0.8% agarose gel by electrophoresis and blotted to Hybond-N+ membranes (Amersham Pharmacia Biotech) for hybridization. The probe was a 14 kb *Avr*II-*Hpa*I fragment of *gsbn*, labeled with [α-^{32}P]dATP by random primers and Klenow enzyme (Stratagene random primer labeling kit). Transfer and hybridization occurred according to standard procedures.

8. Immunostaining of embryos

Collection, fixation, and immunostaining of embryos were carried out as previously described (Gutjahr et al., 1993). Antisera were used at a 1:50 dilution (rabbit anti-Gsbn;

Gutjahr et al., 1993), 1:100 dilution (rabbit anti-Gsb; Gutjahr et al., 1993) and 1:1,500 dilution (rabbit anti-β-galactosidase from Cappel).

References

Baumgartner, S., Bopp, D., Burri, M. and Noll, M. (1987). Structure of two genes at the *gooseberry* locus related to the paired gene and their spatial expression during *Drosophila* embryogenesis. *Genes Dev* **1**, 1247-1267.

Bopp, D., Burri, M., Baumgartner, S., Frigerio, G. and Noll, M. (1986). Conservation of a large protein domain in the segmentation gene *paired* and in functionally related genes of *Drosophila*. *Cell* **47**, 1033-1040.

Buenzow, D. E. and Holmgren, R. (1995). Expression of the *Drosophila gooseberry* locus defines a subset of neuroblast lineages in the central nervous system. *Dev Biol* **170**, 338-349.

Duman-Scheel, M., Li, X., Orlov, I., Noll, M. and Patel, N. H. (1997). Genetic separation of the neural and cuticular patterning functions of *gooseberry*. *Development* **124**, 2855-2865.

Egli, D., Selvaraj, A., Yepiskoposyan, H., Zhang, B., Hafen, E., Georgiev, O. and Schaffner, W. (2003). Knockout of 'metal-responsive transcription factor' MTF-1 in *Drosophila* by homologous recombination reveals its central role in heavy metal homeostasis. *EMBO J* **22**, 100-108.

Gonzalez-Gaitan, M., Rothe, M., Wimmer, E. A., Taubert, H. and Jackle, H. (1994). Redundant functions of the genes *knirps* and *knirps-related* for the establishment of anterior *Drosophila* head structures. *Proc Natl Acad Sci U S A* **91**, 8567-8571.

Grossniklaus, U., Pearson, R. K. and Gehring, W. J. (1992). The *Drosophila sloppy paired* locus encodes two proteins involved in segmentation that show homology to mammalian transcription factors. *Genes Dev* **6**, 1030-1051.

Gustavson, E., Goldsborough, A. S., Ali, Z. and Kornberg, T. B. (1996). The *Drosophila engrailed* and *invected* genes: partners in regulation, expression and function. *Genetics* **142**, 893-906.

Gutjahr, T., Patel, N. H., Li, X., Goodman, C. S. and Noll, M. (1993). Analysis of the *gooseberry* locus in *Drosophila* embryos: *gooseberry* determines the cuticular pattern and activates *gooseberry neuro*. *Development* **118**, 21-31.

Klemenz, R., Weber, U. and Gehring, W. J. (1987). The *white* gene as a marker in a new P-element vector for gene transfer in *Drosophila*. Nucleic *Acids Res* **15**, 3947-3959.

Li, X., Gutjahr, T. and Noll, M. (1993). Separable regulatory elements mediate the establishment and maintenance of cell states by the *Drosophila* segment-polarity gene *gooseberry*. *EMBO J* **12**, 1427-1436.

Li, X. and Noll, M. (1993). Role of the *gooseberry* gene in *Drosophila* embryos: maintenance of *wingless* expression by a *wingless--gooseberry* autoregulatory loop. *EMBO J* **12**, 4499-4509.

Li, X. and Noll, M. (1994a). Compatibility between enhancers and promoters determines the transcriptional specificity of *gooseberry* and *gooseberry neuro* in the *Drosophila* embryo. *EMBO J* **13**, 400-406.

Li, X. and Noll, M. (1994b). Evolution of distinct developmental functions of three *Drosophila* genes by acquisition of different *cis*-regulatory regions. *Nature* **367**, 83-87.

Liu, W. (2003). Redundancy in enhancers and functions of the *Drosophila gooseberry* gene. Ph.D. thesis. University of Zurich.

Noll, M. (1993). Evolution and role of Pax genes. *Curr Opin Genet Dev* **3**, 595-605.

Nüsslein-Volhard, C. and Wieschaus, E. (1980). Mutations affecting segment number and polarity in *Drosophila*. *Nature* **287**, 795-801.

Osborne, P. W. and Dearden, P. K. (2005). Expression of Pax group III genes in the honeybee (*Apis mellifera*). *Dev Genes Evol* **215**, 499-508.

Parks, A. L., Cook, K. R., Belvin, M., Dompe, N. A., Fawcett, R., Huppert, K., Tan, L. R., Winter, C. G., Bogart, K. P., Deal, J. E. et al. (2004). Systematic generation of high-resolution deletion coverage of the *Drosophila melanogaster* genome. *Nat Genet* **36**, 288-292.

Rong, Y. S. and Golic, K. G. (2001). A targeted gene knockout in *Drosophila*. *Genetics* **157**, 1307-1312.

Rong, Y. S., Titen, S. W., Xie, H. B., Golic, M. M., Bastiani, M., Bandyopadhyay, P., Olivera, B. M., Brodsky, M., Rubin, G. M. and Golic, K. G. (2002). Targeted mutagenesis by homologous recombination in *D. melanogaster*. *Genes Dev* **16**, 1568-1581.

Skeath, J. B., Zhang, Y., Holmgren, R., Carroll, S. B. and Doe, C. Q. (1995). Specification of neuroblast identity in the *Drosophila* embryonic central nervous system by *gooseberry-distal*. *Nature* **376**, 427-430.

Steller, H. (1990). Rubin Lab Methods Book, Second ed.

Thibault, S. T., Singer, M. A., Miyazaki, W. Y., Milash, B., Dompe, N. A., Singh, C. M., Buchholz, R., Demsky, M., Fawcett, R., Francis-Lang, H. L. et al. (2004). A complementary transposon tool kit for *Drosophila melanogaster* using P and piggyBac. *Nat Genet* **36**, 283-287.

Zhang, Y., Ungar, A., Fresquez, C. and Holmgren, R. (1994). Ectopic expression of either the *Drosophila gooseberry-distal* or *proximal* gene causes alterations of cell fate in the epidermis and central nervous system. *Development* **120**, 1151-1161.

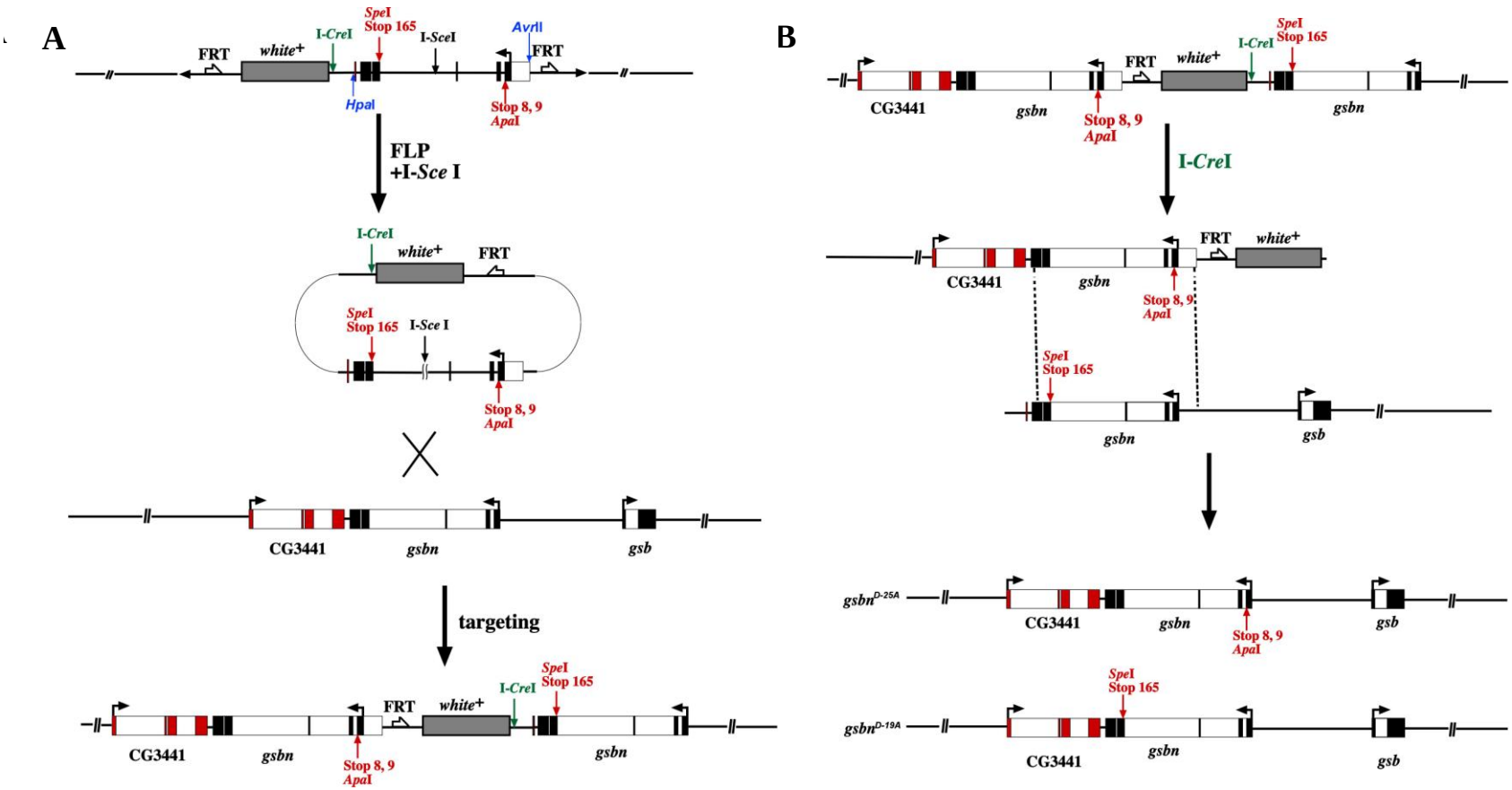

Fig. 1. Strategy of generating two *gsbn* nonsense alleles by ends-in homologous recombination. The method for gene targeting of *gsbn* followed the strategy described previously (Rong et al., 2002). As a result of gene targeting in *gsbn*, the intermediate product, a tandem duplication of *gsbn* in which both *gsbn* copies are mutated, is generated (A). Through I-*Cre*I-induced recombination, the two *gsbn* mutant alleles were reduced to single copies of two different *gsbn* alleles (B).

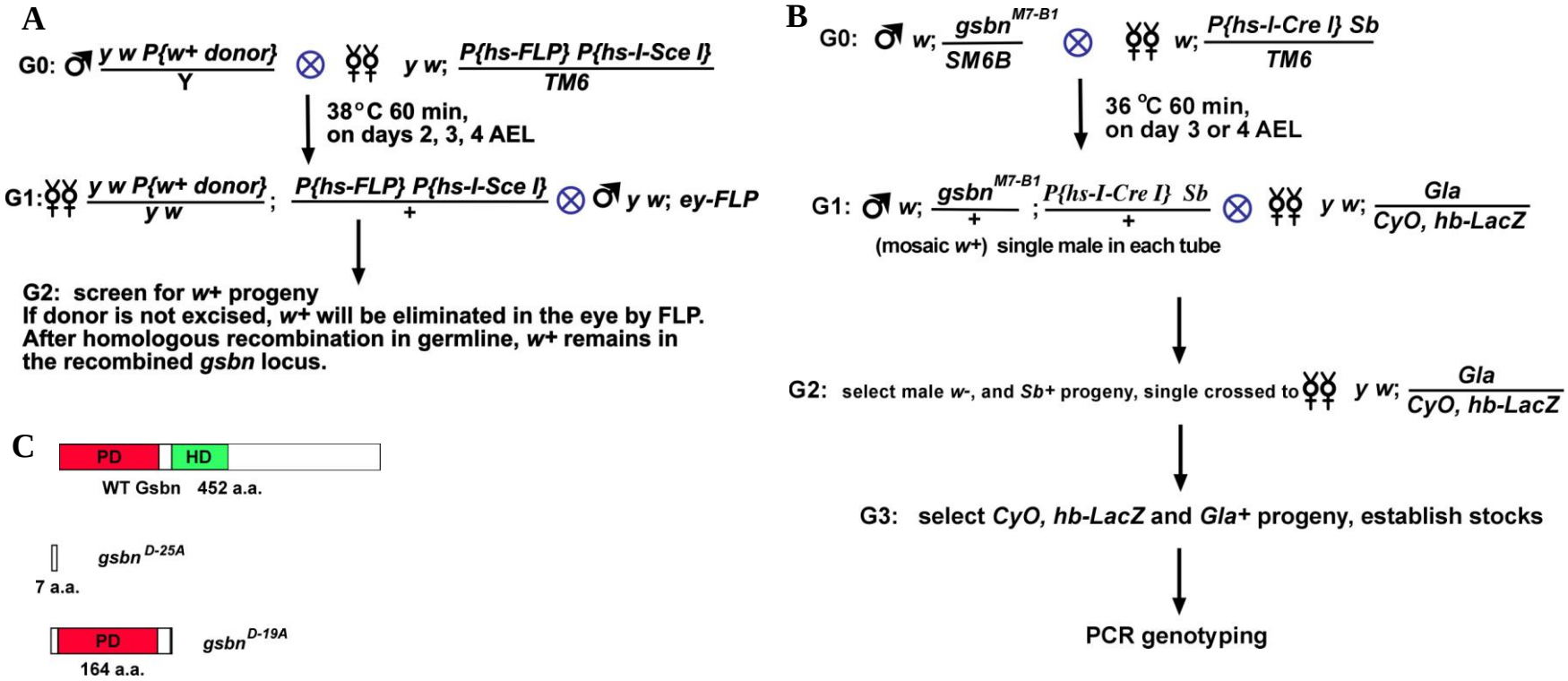

Fig. 2. Crosses to generate two *gsbn* nonsense alleles by homologous recombination. Crosses for gene targeting (A) and I-*Cre*I-induced recombination (B) essentially followed the procedure described previously (Rong et al., 2002; Egli et al., 2003). Three donor lines on the X-chromosome were used for gene targeting (A), and four targeting events were isolated. One targeting line, $gsbn^{M7\text{-}B1}$, was chosen for I-*Cre*I-induced recombination (B). After the I-*Cre*I-mediated reduction step, two different *gsbn* alleles, $gsbn^{D\text{-}25A}$ and $gsbn^{D\text{-}19A}$, were isolated. $gsbn^{D\text{-}25A}$ is expected to produce a truncated heptapeptide, while $gsbn^{D\text{-}19A}$ is expected to produce a truncated protein of 164 amino acids, containing the whole paired-domain and the linker region between the paired-domain and *prd*-type homeodomain (C).

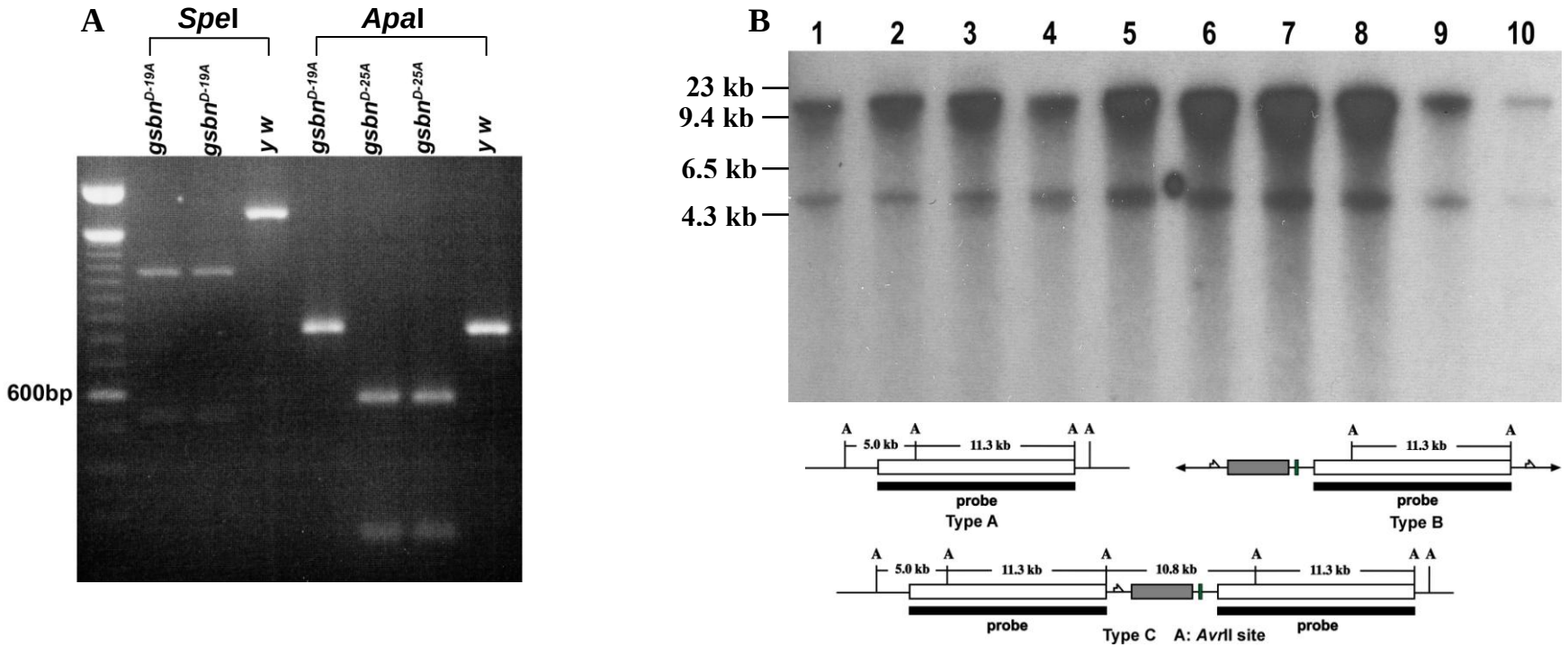

Fig. 3. Characterization of the two new *gsbn* alleles by PCR and Southern blot. According to the design of gene targeting of *gsbn*, a new *Spe*I site should be created in exon 4 of $gsbn^{D\text{-}19A}$ and a new *Apa*I site in exon 1 of $gsbn^{D\text{-}25A}$. The PCR products amplified by using the primers flanking the designed mutation sites were digested with either *Spe*I or *Apa*I to indicate the presence or absence of the introduced mutations. The PCR products of $gsbn^{D\text{-}19A}$ were completely digested with *Spe*I, whereas the PCR products of the *y w* control were not (A). Similarly, the PCR products of $gsbn^{D\text{-}25A}$ were completely digested with *Apa*I, whereas the PCR products of the *y w* and $gsbn^{D\text{-}19A}$ controls were not (A). In (B), genomic DNA of each genotype was digested with *Avr*II, the fragments were separated on a 0.8% agarose gel, and the Southern blot was hybridized with the probe covering the 14 kb *Avr*II-*Hpa*I fragment of the *gsbn* genomic region. The genotypes of the samples are: lane 1, *y w*; lane 2, *P{donor 7}*; lane 3, *P{donor 12}*; lane 4, *Df(2R)IIX62/CyO*; lane 5, $gsbn^{M7\text{-}A1}$*/CyO, y*$^{+}$; lane 6, $gsbn^{M7\text{-}B1}$; lane 7, $gsbn^{M7\text{-}C2}$; lane 8, $gsbn^{M12\text{-}A1}$; lane 9, $gsbn^{D\text{-}19A}$; lane 10, $gsbn^{D\text{-}25A}$. The hybridization patterns can be classified into three distinct patterns of bands. Type A (5.0 kb, 11.3 kb in lanes 1, 4, 9, and 10) is produced by DNA from the two *gsbn* mutant alleles and from the *y w* and *Df(2R)IIX62/CyO* controls. Type B (5.0 kb, 2x11.3 kb, and > 7.2 kb in lanes 2 and 3) is produced by DNA from two independent donor lines, carrying the double mutant *gsbn* donor allele (cf. top of Fig. 1A) on the X-chromosome. Type C (5.0 kb, 10.8 kb, 2x11.3 kb in lanes 5-8) is produced by DNA from four independent lines, carrying the two *gsbn* mutant alleles before their resolution by I-*Cre*I (cf. top of Fig. 1B). In none of the DNAs aberrant bands were detected. A, *Avr*II sites.

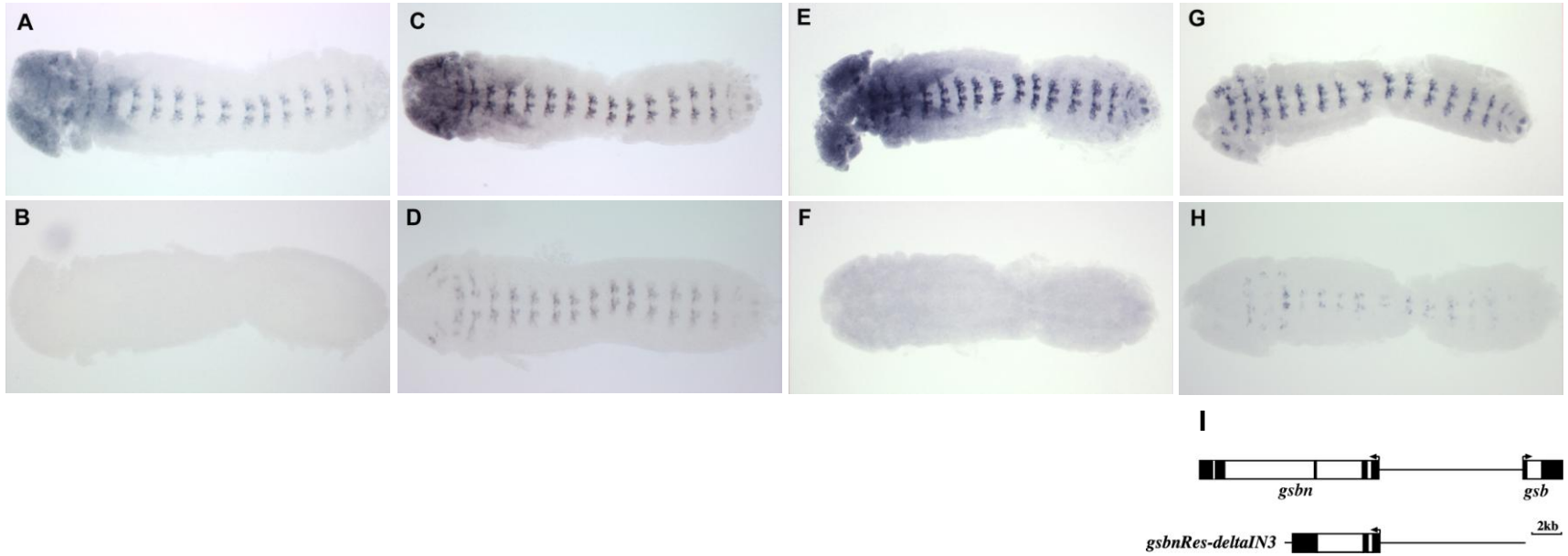

Fig. 4. Gsbn patterns in embryos mutant for *gsbn* or transgenic for *gsbnRes-deltaIN3*. Stage 11 embryos of different genotypes were stained for Gsbn and β-galactosidase. *gsbn*$^{D\text{-}19A}$*/CyO, hb-LacZ* (A), *gsbn*$^{D\text{-}19A}$ (B), *gsbn*$^{D\text{-}25A}$*/CyO, hb-LacZ* (C), *gsbn*$^{D\text{-}25A}$ (D), *gsbn*^{del}*/CyO, hb-LacZ* (E), *gsbn*^{del} (F), *gsbn*$^{D\text{-}19A}$; *gsbnRes-deltaIN3* (G), and *Df(2R)IIX62*; *gsbnRes-deltaIN3* (H) embryos are shown unfolded with their anterior to the left. In *gsbn*$^{D\text{-}19A}$ (B) and *gsbn*^{del} (F) embryos, Gsbn protein is not detectable, whereas in *gsbn*$^{D\text{-}25A}$ embryos (D) there is weak staining with anti-Gsbn in comparison with heterozygous *gsbn*$^{D\text{-}25A}$ embryos (E). In (G), the anti-Gsbn staining is exclusively from Gsbn protein expressed by *gsbnRes-deltaIN3*. The expression of *gsbnRes-deltaIN3* is dramatically down-regulated in embryos homozygous for *Df(2R)IIX62*, uncovering both *gsb* and *gsbn* (H). The *cis*-regulatory region included in *gsbnRes-deltaIN3* is illustrated in (I).

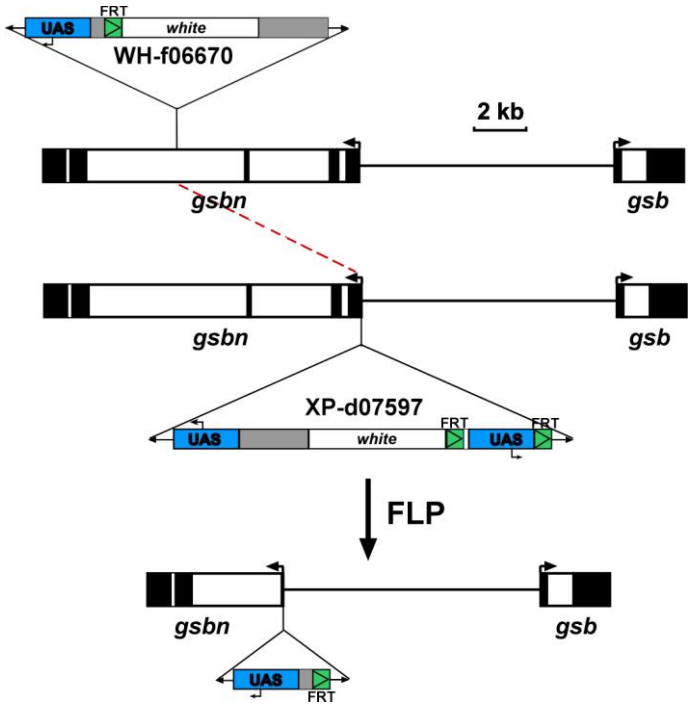

Fig. 5. Generation of a *gsbn* deficiency allele by Flipase-mediated recombination. A *gsbn* deficiency was produced by following the strategy of Flipase-mediated recombination described previously (Thibault et al., 2004). *piggyBac{f06670}* is a piggyBac element inserted in intron 3 of *gsbn*, while *P{d07597}*is a P-element insertion in the 5'UTR of *gsbn*. Both *piggyBac{f06670}* and *P{d07597}* contain FRT sites in the same orientation. The Flipase-mediated recombination between *piggyBac{f06670}* and *P{d07597}*, illustrated above, results in a *gsbn* deletion spanning the region between the FRT sites, as shown at the bottom.

	$gsbn^{D-19A}$	$gsbn^{f06670}$	$gsbn^{del}$	$Df(2R)GGG^{d13}$
$gsbn^{D-19A}$	**0.59±0.27 (n=2349)**	**0.67±0.19 (n=1361)**	**0.14±0.14 (n=950)**	**0**
$gsbn^{f06670}$		**0.32±0.23 (n=492)**	**0.22±0.09 (n=1348)**	**0**
$gsbn^{del}$			**0.16±0.14 (n=719)**	**0**
$Df(2R)GGG^{d13}$				**0**

Table 1. Survival rates of *gsbn* alleles. Survival rates were calculated based on the assumption that 100% of the $gsbn^{-/+}$ heterozygotes survive adulthood. Numbers in parentheses refer to the total numbers of surviving flies (including *gsbn* heterozygotes) scored from more than 10 tubes for each genotype. All homozygous and transheterozygous combinations of these *gsbn* alleles result in complete male sterility.

Chapter 3

gooseberry and *gooseberry neuro* control axonogenesis of a subset of motoneurons in *Drosophila*

Summary

The use of *gsbn* alleles in combination with a large deficiency uncovering both *gsb* and *gsbn* circumvents the complications of the severe neuronal precursor defects of the *gsb* homozygotes. This allows us to analyze the functions of both *gsbn* and *gsb* during neurogenesis, and to assess their functional relationship. We found that *gsbn* is expressed in the dorsal subset of SNa motoneurons. In $gsbn^{-}$ $gsb^{-/+}$ embryos, more than 80% of hemisegments showed a defective innervation of lateral body wall muscles by the SNa motor axons. This SNa phenotype results from the inability of the dorsal SNa motor axons to extend into the lateral muscle field, which suggests that *gsb* and *gsbn* control the axon growth of the dorsal SNa motoneurons. In addition, both *gsbn* and *gsb* act in a redundant manner to execute their functions in the CNS. The analysis of the SNa phenotype implies that the functional link between *gsb* and *gsbn* is established through the *gsb–gsbn* hierarchy and that the establishment of this hierarchy is to prevent the deleterious effects caused by a *gsb* haploinsufficiency.

Introduction

In the *Drosophila* ventral nerve cord (VNC), there are about 36 motoneurons (MNs) per hemisegement that innervate the stereotypically aligned peripheral larval body wall muscles. The motor axons project through three main routes: the intersegmental nerve (ISN), the segmental nerve (SN), and the transverse nerve (TN) projecting along the segment border (Johansen et al., 1989; Van Vactor et al., 1993). Outside the ventral nerve cord, the ISN and SN converge at the exit junction, where some axons selectively fasciculate, switch pathways and branch further into the ISN, ISNb, ISNd, SNa, and SNc. The ISN branch projects into the dorsal muscles, whereas the other four branches and the TN project laterally or ventrally.

Drosophila MNs can be subdivided into six distinct subclasses (ISN, ISNb, ISNd, SNa, SNc, TN) on the basis of their projection pathways. Lineage analyses showed that *Drosophila* MNs are produced from a number of different NBs (Bossing et al., 1996; Landgraf et al., 1997; Schmidt et al., 1997; Schmid et al., 1999). The NBs that generate MNs are not distributed in a particular domain, but rather along both the mediolateral and dorsoventral axes of the VNC. Moreover, these NBs do not exhibit any obvious common gene expression pattern. So far, no pan-motoneuron transcription factors in *Drosophila* have been found that regulate common properties of MN development. Instead, during the last decade progress has been made to identify the genes controlling the specification of motoneuronal subtypes. These genes include *lim3*, *islet* (*isl*), *zfh1*, *evenskipped* (*eve*), *grain* (*grn*), *dHb9*, and *Nkx6*. *lim3* and *isl* are Lim-homeodomain transcription factors. *isl* is expressed in ISNb, ISNd, and TN MNs, and in *isl* mutants ISNb MNs fail to innervate the neuromuscular junction of muscles 12 and 13 (Thor and Thomas, 1997). *lim3* is co-expressed by all of the *isl*-expressing MNs except those projecting through ISNd. *lim3* mutants display a lack of normal innervation at the neuromuscular junction of muscles 12 and 13 as well. Instead of taking their normal trajectory, these ISNb MNs ectopically project into the ISNd pathway (Thor et al., 1999). It is suggested that *isl* is necessary for the identity of both ISNb and ISNd MNs, and *lim3*, in combination with *isl*, subdivides these MNs into the individual ISNb and ISNd classes. *dHb9* and *Nkx6* are homeodomain transcription factors. *dHb9*-expressing MNs populate the majority of motor axon branches, including ISN, ISNb, ISNd, SNa, and SNc. In the absence of

dHb9, the ISNb fails to defasciculate from the ISN or projects aberrantly after defasciculating from ISN. At least part of the functions of *dHb9* is to repress *eve* in ISNb MNs (Broihier and Skeath, 2002; Odden et al., 2002). *Nkx6* is co-expressed with *dHb9* and *lim3* in the MNs innervating ventral muscles. *Nkx6* acts in parallel with *dHb9* to regulate the MN fate and promote axonogenesis (Broihier et al., 2004; Cheesman et al., 2004). *eve* is a key regulator for MNs projecting to the dorsal muscles (Landgraf et al., 1999; Fujioka et al., 2003). *eve* executes its function by regulating the expression of UNC5, a repulsive receptor for Netrin (Labrador et al., 2005). The specification of the aCC neuron, an ISN MN, is governed by *eve*, *grn*, a GATA transcription factor, and *zfh1* through the *eve-grn-zfh1* code (Certel and Thor, 2004). *zfh1*, a zinc-finger homeodomain transcription factor, is expressed in all MNs. In *zfh1* mutants, MN identity is not affected. However, motor axons projecting ventrally often stall at the edge of the CNS, which suggests that *zfh1* controls the axon exit from the CNS (Layden et al., 2006).

Curiously, so far no transcription factors have been identified that regulate the fate specification and differentiation of the MNs projecting through the SN branch, another main branch of the *Drosophila* motor axons. In this study, we present evidence that *gooseberry neuro* (*gsbn*) is expressed in the dorsal subset of SNa MNs and that *gsbn* and *gooseberry* (*gsb*) act in a redundant manner to control the differentiation of these MNs. Moreover, the results reveal how the functional link between *gsb* and *gsbn* is established as well as the consequences of this functional interaction.

Results

Expression of Gsbn in neuronal precursors and postmitotic neurons

To investigate the functions of *gsbn* in the development of the CNS, we extended our previous analysis of the *gsbn* expression pattern in the CNS with respect to neural cell type molecular markers. On the basis of cell morphology, it has been suggested that at stage 10-12 *gsbn* is mainly expressed in the Gsb-expressing neuroblasts (NBs) and the ganglion mother cells (GMCs) derived from the neuroblasts expressing Gsb (Gutjahr et

al., 1993; Buenzow and Holmgren, 1995). In agreement with this previous description, *gsbn* is first expressed at stage 10 in two rows of cells in each segment. These cells have large and round nuclei, which indicates that they are NBs (Fig. 1A). At stage 11, some of the Gsbn-expressing cells were labeled by anti-phospho-Histone3, a specific marker for dividing cells, which suggests that these cells are undergoing cell division and hence are either NBs or GMCs (Fig. 1D-F). The presence of Prospero (Pros), localized in GMCs and immature neurons but not in NBs (Spana and Doe, 1995), in the nuclei of most Gsbn-expressing cells at stage 12 (Fig. 1G-I), with the exception of a few cells in the lateral region of the ventral nerve cord, indicates that at this stage Gsbn is expressed mainly in the progeny of the Gsbn-expressing NBs. As neurogenesis proceeds, *gsbn* is expressed predominantly in the terminal differentiating neurons, as revealed by its co-expression with Elav (Fig. 1J-L), but is not expressed in the Repo-positive glial cells (data not shown).

Gsbn is expressed in the dorsal subset of SNa motoneurons

One of the key distinguishing features of neurons is their axonal trajectory. Therefore, to initiate functional analysis of *gsbn* in neurogenesis, it is important to trace the axonal projections of the neurons expressing Gsbn. To this end, two *gsbn* reporter transgenes, *gsbn-mCD8::GFP* and *gsbn-Gal4*, were constructed. The expression of both transgene products, the membrane-bound CD8-GFP fusion protein and Gal4, are under the control of the entire *gsbn* upstream *cis*-regulatory sequences and its cognate *gsbn* promoter. *gsbn-mCD8::GFP* faithfully recapitulates the expression pattern of *gsbn* in the CNS throughout embryogenesis, although in the dorsal region mCD8-GFP is expressed at lower levels and barely detectable because of its diffusion in the membrane (Fig. 2). Moreover, the expression of *gsbn-mCD8::GFP* is largely abolished in a $Df(2R)GGG^{d13}$ background (data not shown), which indicates that *gsbn-mCD8::GFP* is transcriptionally regulated as endogenous *gsbn*. To examine the expression patterns of *gsbn-Gal4*, we placed *UAS-nlsGFP* under its control and examined the expression of GFP in the CNS. As evident from Fig. 3, the GFP expression domain is restricted to the cells expressing Gsbn. Because of the temporal delay of the GAL4/UAS system, the number of GFP-

expressing cells is smaller than that of the Gsbn-positive cells, particularly at the early stages (Fig. 3A-C). Since the same *cis*-regulatory region is used in *gsbn-Gal4* and *gsbn-mCD8::GFP*, it is probable that, like *gsbn-mCD8::GFP*, *gsbn-Gal4* reflects the endogenous *gsbn* expression pattern.

In the abdominal hemisegments A2-A7, the pioneer SN motor axons exit the CNS through the segmental nerve root at stage 13 (Nose et al., 1992). By late stage 16, the SNa motor axons have extended into the lateral muscle field (Johansen et al., 1989; Nose et al., 1992). SNa bifurcates at its target region into two branches, the anterior SNa branch, innervating muscles 21-24, and the posterior branch, innervating muscles 5 and 8. The axons of the Gsbn-expressing interneurons project into the longitudinal pathways and the posterior commissures (Fig. 4A). In the periphery, a branch of the GFP-positive axons exit the CNS, project into the lateral muscle field, and appear to innervate, after a bifurcation, the body wall muscles 5, 8, and 24, but not 21-23 (Fig. 4B,C). Double-labeling with anti-GFP and anti-Fasciclin II, a marker for motor axons, confirmed that the GFP-positive axons project through the SNa branch, which suggests that *gsbn* is expressed in the SNa MNs (Fig. 3D-F).

It has recently been reported that SNa MNs, based on the positions of their cell bodies within the CNS, can be divided into a ventral subset and dorsal subset (Garces et al., 2006). To investigate in which subset of SNa MNs *gsbn* is expressed, we used the *BarH1-LacZ* enhancer-trap line and *BarH1-Gal4* which label the SNa MNs. *BarH1-LacZ* labels consistently two of the three dorsal SNa MNs and one tyrosine hydroxylase (TH)-positive cell in each abdominal hemisegment, and one ventral midline TH-positive cell (the ventral midline unpaired dopaminergic neuron). By double labeling with anti-LacZ and anti-Gsbn, we found that the two *BarH1-LacZ* positive SNa MNs in the dorsal-lateral region of the VNC co-express Gsbn (Fig. 5A-C). In addition, the three TH-positive cells in the medial region of the abdominal segments express *gsbn* as well (Fig. 5A-C). However, it appears that *gsbn* is not expressed in the ventral SNa MNs because Gsbn does not colocalize in these MNs with GFP driven by *BarH1-Gal4* (Fig. 5D-F). Collectively, these data establish that endogenous *gsbn* is expressed in the dorsal SNa motoneurons as well as in the three TH-positive cells of each abdominal segment, but not in the ventral SNa MNs.

Defective innervation of lateral body wall muscles by SNa branch in *gsbn*$^{-}$ *gsb*$^{-/+}$ embryos

The expression of *gsbn* in the dorsal SNa MNs raises the question whether *gsbn* controls the differentiation of these MNs. To address this question, we used anti-Fasciclin II to visualize motor axon projections in *gsbn*$^{-}$ embryos. Surprisingly, in *gsbn*$^{D\text{-}19A}$ or *gsbn*^{del} homozygotes, no obvious abnormalities were observed in the projections of SNa motor axons (cf. Fig. 6B,C with 6A; Table 1), or in the overall axonal organization (data not shown).

Since *gsbn* and *gsb* may have partially redundant functions in the CNS (as shown for the viability in Chapter 2), embryos were examined that were deficient for *gsbn* and haploid for *gsb*. In such *gsbn*$^{D\text{-}19A}$*/Df(2R)IIX62* or *gsbn*^{del}*/Df(2R)GGG*^{d13} embryos, the overall organization of motor axon projections is normal, and no aberrant projection is observed in the ISN or its ISNb, ISNd, or SNc branches. However, the SNa branch exhibits two phenotypes of a defective innervation of the lateral muscles. In more than 70% of the hemisegments examined, the anti-Fasciclin II staining of the SNa branch is very weak, but the stereotypic bifurcation of the SNa is still recognizable, displaying a "thin" SNa phenotype (cf. arrows in Fig. 6D,E with arrow in Fig. 6A; Table 1). The remaining of the SNa branch appears to innervate only muscles 21, 22, and 5. In more than 10% of the hemisegments, the anti-Fasciclin II staining of the SNa branch is very weak as well but, unlike in the "thin" phenotype, the SNa motor axons appear to project inappropriately into the lateral muscle field after the bifurcation point, generating a "bifurcation missing" phenotype (cf. arrowhead in Fig. 6D with arrow in Fig. 6A; Table 1). The SNa phenotype in *gsbn*$^{-}$ *gsb*$^{-/+}$ mutants does not result from the transcriptional down-regulation of Fasciclin II because the anti-HRP staining, which labels all neuropils, showed similar defects in SNa (cf. arrows in Fig. 6I and 6H).

The SNa phenotype is caused by the *gsb* haploinsufficiency in *gsbn* mutants

Two lines of evidence suggest that the SNa phenotype in *gsbn*$^{-}$ *gsb*$^{-/+}$ mutants results from the loss of *gsbn*. First, a *gsbn* transgene can completely rescue the SNa phenotype of *gsbn*$^{D\text{-}19A}$*/Df(2R)IIX62* embryos (cf. Fig. 6F with Fig. 6A,D). Second, the SNa

phenotype is not observed in either *Df(2R)IIX62*/+ or *Df(2R)GGG*^{d13}/+ embryos (Table 1). However, the SNa phenotype cannot be attributed solely to the loss of *gsbn* because the projections of the SNa motor axons are normal in *gsbn*$^{D\text{-}19A}$ and *gsbn*^{del} homozygous mutant embryos (Fig. 6B,C and Table 1). It follows that the removal of one copy of another gene uncovered by *Df(2R)GGG*^{d13} and *Df(2R)IIX62* also contributes to the SNa phenotype. Because *Df(2R)GGG*^{d13} deletes, in addition to *gsbn*, only *gsb* and *gol*, the most likely candidate is *gsb* for the following reasons. First, *gsbn* and *gsb* exhibit overlapping expression patterns in the CNS during embryogenesis, and *gsbn* expression is dependent on *gsb* (Gutjahr et al., 1993; Buenzow and Holmgren, 1995). Second, as previously demonstrated, Gsb and Gsbn proteins are to a large extent functionally equivalent to each other (Li and Noll, 1994b). Third, a similar situation has been found in the preceding analysis of the viability function(s) of *gsbn*, where *gsbn* mutants are viable, whereas *gsbn*$^{-}$ *gsb*$^{-/+}$ mutants die as larvae (Chapter 2). This *gsb* haploinsufficiency in *gsbn* mutants resulting in the SNa phenotype suggests that not only *gsbn*, but also *gsb* is involved in the differentiation of the dorsal SNa MNs. As *gsb* activates *gsbn* in the CNS, it is expected that *gsb* mutants also exhibit the SNa phenotype. Indeed, *gsb*^{525} homozygotes showed defective SNa projections (cf. Fig. 6G with 6A).

Essential role of *gsbn* and *gsb* in the axonogenesis of the dorsal SNa motoneurons

To study in detail the behavior of the dorsal SNa motor axons in *gsbn*$^{-}$ *gsb*$^{-/+}$ mutants, *gsbn-Gal4* and *UAS-mCD8::GFP* were crossed into a *gsbn*$^{D\text{-}19A}$/*Df(2R)GGG*^{d13} background. In the CNS, the overall *gsbn-Gal4* expression pattern revealed by anti-GFP staining is normal in comparison to a wild-type and a *Df(2R)GGG*^{d13}/+ background (data not shown). However, the *gsbn-Gal4*-positive SNa motor axons fail to extend into the lateral muscle field (cf. Fig. 7B with 7A and Fig. 4C). Similar results were obtained by using *gsbn-mCD8::GFP* (data not shown). Furthermore, the *gsbn-Gal4*-positive SNa motor axons did not aberrantly project into the other non-SNa branch, which suggests that the fate of the dorsal SNa MNs is not transformed into that of other MNs in *gsbn*$^{D\text{-}19A}$/*Df(2R)GGG*^{d13} embryos. Since the expression of *gsbn-Gal4* in the glia enwrapping the SNa motor axons masks the trajectory of SNa (see thin arrow in Fig. 4C), it is not

clear whether these dorsal SNa motor axons stall before they exit the CNS or only in the ventral muscle field.

It has been reported that *gsb* is expressed transiently in the mesoderm at stage 12 (Gutjahr et al., 1993). To exclude the possibility that the SNa phenotype results from an indirect effect of possible muscle defects, $gsbn^{D\text{-}19A}/Df(2R)GGG^{d13}$ embryos were stained with anti-Myosin heavy chain to examine whether the body wall muscles develop properly. All the muscle fibers of such embryos appear to have normal shape and attach to the epidermis at the correct sites (cf. Fig. 8C with 8A, and Fig. 8D with 8B). This implies that the SNa phenotype is a direct effect of the neuronal defects. In agreement with this interpretation, *BarH1-LacZ* expression in the dorsal SNa MNs is dramatically down-regulated in $gsbn^{D\text{-}19A}/Df(2R)GGG^{d13}$ embryos (Fig. 7D, arrow) as compared to wild-type embryos (Fig. 7C, arrow). In addition, *BarH1-LacZ* expression in the three TH-positive cells of each abdominal segment is almost abolished (cf. Fig. 7D with 7C, asterisks), which suggests that *gsb* and *gsbn* may play a role in cell fate specification for these cells.

gsbn and *gsb* are not sufficient to specify the fate of the dorsal SNa motoneurons

Since *gsb* functions as a neuroblast identity gene (Skeath et al., 1995; Duman-Scheel et al., 1997), it seemed important to determine whether *gsb* or *gsbn* is sufficient to direct the identity of the dorsal SNa MNs. To this end, Gsbn or Gsb was overexpressed in all postmitotic neurons through the control of *elav-Gal4* (Lin and Goodman, 1994). Although the gross organization of the CNS is disrupted, staining of SNa with anti-Fasciclin II is not significantly increased in either *elav-Gal4/UAS-gsbn* (cf. Fig. 9B with 9A) or *elav-Gal4/UAS-gsb* embryos (data not shown), which indicates that no other neurons are transformed into dorsal SNa MNs. Similar results were obtained by using two copies of *UAS-gsbn* under the control of either *elav-Gal4* (cf. Fig. 9C with 9A), or *ftz-Gal4* (cf. Fig. 9D with 9A) that is expressed in most of the MNs (Thor et al., 1999). Furthermore, the expression patterns of *dHb9* and *even-skipped* (*eve*), which are known to be expressed in many MNs (Landgraf et al., 1999; Broihier and Skeath, 2002), are not obviously altered when *gsbn* is over-expressed (cf. Fig. 9F with 9E, and 9H with 9G).

These results imply that neither *gsb* nor *gsbn* is sufficient to specify the fate of the dorsal SNa MNs.

gsbn and *gsb* act at the postmitotic stage to control differentiation of the dorsal SNa motoneurons

The fact that both *gsb* and *gsbn* are expressed in the neuronal precursors and that *gsb* functions as a neuroblast identity gene raises the question whether the SNa phenotype results from the loss of *gsb* and *gsbn* at the neuronal precursor stage or at the postmitotic neuron stage. To answer this question, we assayed for the SNa phenotype of $gsbn^{D\text{-}19A}/Df(2R)GGG^{d13}$ embryos expressing a *gsbn* transgene at the neuron stage. As shown in Fig. 10, the neuronal expression of *gsbn* almost completely rescued the SNa defects (Fig. 10). Since ectopic expression of *gsbn* driven by *elav-Gal4* is unable to transform the fate of non-SNa MNs into that of the SNa MNs (Fig. 9B-D), the rescue of the SNa phenotype must result from the expression of *gsbn* in the dorsal SNa MNs. Moreover, duplication of the RP2 neurons and the missing posterior commissure, the two phenotypes observed in *gsb* mutants (Patel et al., 1989; Duman-Scheel et al., 1997), were not detected in $gsbn^{-}$ $gsb^{-/+}$ mutants (Fig. 11). This implies that, in contrast to *gsb* homozygotes, no gross neural defects occur in $gsbn^{-}$ $gsb^{-/+}$ mutants at the neuronal precursor stage.

Discussion

Establishment of *gsb-gsbn* hierarchy to prevent *gsb* haploinsufficiency

The fact that the SNa phenotype is observed in $gsbn^{-}$ $gsb^{-/+}$ embryos, but not in $gsbn^{-}$ or $gsb^{-/+}$ embryos, suggests that both *gsbn* and *gsb* are involved in the differentiation of the dorsal SNa MNs. In the CNS, *gsb* is expressed mainly in the neuronal precursors and its protein levels begin to decrease at stage 12 (Gutjahr et al., 1993). However, considering that undetectable levels of *gsb* are able to rescue its segmentation function (Duman-Scheel et al., 1997; Liu, 2003), it may not be surprising that the extremely low level of Gsb in the dorsal SNa MNs renders *gsbn* dispensable for the normal development of these cells. In the absence of *gsbn*, the amount of Gsb protein may be close to the

threshold, but still can execute its function fully in the dorsal SNa MNs. However, when in addition one copy of *gsb* is removed, the amount of Gsb protein is below the threshold sufficient for its function.

The evidence suggests that the functional link between *gsb* and *gsbn* is established through the activation of *gsbn* by *gsb*, forming a *gsb-gsbn* hierarchy. When *gsbn* is expressed, *gsb*, together with *gsbn*, activates their target genes in a redundant fashion probably because of their two highly conserved DNA-binding domains, the paired-domain and the *paired*-type homeodomain (Baumgartner et al., 1987). It appears that the establishment of the *gsb-gsbn* hierarchy ensures at least the normal differentiation of the dorsal SNa MNs in case one copy of *gsb* is lost. It is well possible that *gsb* might exert its many other functions, such as the postembryonic viability function(s) as revealed by the analysis in Chapter 2, through the *gsb-gsbn* hierarchy as well.

In *Drosophila*, one common feature of many gene-pairs is "enhancer sharing." Two genes in a pair are activated by the same enhancer(s), which leads to similar expression patterns of the two genes. As a consequence, one gene could be completely redundant with the other. Indeed, this is the case for the *invected* gene of *Drosophila* at the *engrailed-invected* locus. Therefore, the *gsb-gsbn* pair is unique in the sense that *gsb* and *gsbn* exhibit distinct, although overlapping expression patterns, and most importantly, *gsbn* expression is dependent on *gsb* activity (Gutjahr et al., 1993). It is not clear what evolution pressures force the *gsb* locus to adopt the hierarchy mode, rather than the "enhancer sharing" mode. Nevertheless, it seems very unlikely that the *gsb-gsbn* hierarchy arises only by chance during evolution because *gsb* is also subjected to the hierarchical control established by *paired*, another member of the *Drosophila* Pax3/7 subfamily (Li et al., 1993; Noll, 1993; Li and Noll, 1994b). Furthermore, the enhancers of *gsb* and *gsbn* cannot activate the heterologous promoters properly (Li and Noll, 1994a). One possible advantage of the hierarchy mode is that it is more economical than the "enhancer sharing" mode in that *gsb* and *gsbn* are expressed only at the time when they are needed. As long as *gsb* alone can accomplish its function fully, there is no necessity to express *gsbn*, and *vice versa*.

gsbn and *gsb* directly control the axonogenesis of the dorsal SNa motoneurons

It is conceivable that the SNa phenotype observed in *gsbn*$^{-}$ *gsb*$^{-/+}$ mutants arises from the loss of *gsb* and *gsbn* either in the dorsal SNa MNs or in the development of cell lineages producing these neurons. Two lines of evidence strongly support a role for *gsb* and *gsbn* function in the dorsal SNa MNs. First, the normal SNa motor axon projections are restored in *gsbn*$^{-}$ *gsb*$^{-/+}$ mutants by postmitotic expression of *gsbn*. Second, the severe neuronal precursor defects observed in the *gsb* homozygous mutants were not detected in the *gsbn*$^{-}$ *gsb*$^{-/+}$ mutants.

The weak anti-Fasciclin II staining of the SNa branch in *gsbn*$^{-}$ *gsb*$^{-/+}$ embryos indicates that the dorsal SNa motor axons are unable to extend into the exit junction region. Since in wild-type embryos the SNa motor axons leave the CNS at stage 13, it follows that *gsb* and *gsbn* act at an early phase of neuronal differentiation of the dorsal SNa MNs. In agreement with this argument, *gsb* expression in the CNS begins to decay at stage 12 (Gutjahr et al., 1993). Moreover, the down-regulation of the *BarH1-LacZ* in the dorsal SNa MNs is detected already at stage 14 (data not shown). The inability of the dorsal SNa MNs to elongate their axons raises several possibilities. It could be that some axon guidance molecules are mis-regulated or the fate of these cells is transformed into that of interneurons, or these cells undergo apoptosis.

The lineage of the dorsal SNa motoneurons

The analysis of expression patterns and the loss-of-function studies of *gsbn*$^{-}$ *gsb*$^{-/+}$ mutants demonstrate that *gsbn* and *gsb* are expressed in the dorsal SNa MNs. It has been shown that all *gsbn*-expressing neurons are derived from the *gsb*-expressing neuroblasts in a lineage–specific manner (Buenzow and Holmgren, 1995). It follows that the NB(s) giving rise to the dorsal SNa MNs should be assigned to the NBs of row 5 or 6 where *gsb* is expressed. Three comprehensive studies have been carried out to identify the NB lineages in the embryonic CNS of *Drosophila* (Landgraf et al., 1997; Schmidt et al., 1997; Schmid et al., 1999). Due to the inherent technical difficulties of the methodology, the interpretation of the data from one study is not always consistent with that from other studies. With regard to the origin of the dorsal SNa MNs, the results from Landgraf *et al*.

(1997) and Schmid *et al*. (1999) suggested that the dorsal SNa MNs might be derived from NB3-2 or NB3-3. However, Schmidt *et al*. (1997) reported that the NB5-4 clone consists of three to four neurons whose axons project through the segmental nerve. In addition, the position of the cell bodies from the NB5-4 clone are also located at the dorsal-lateral edge of the CNS, which is consistent with our observation as well as a previous study (Buenzow and Holmgren, 1995). Although it could be that NBs other than NB5-4 produce the dorsal SNa MN(s) as well, we favor the idea that the dorsal SNa MNs expressing Gsbn are derived from NB5-4.

It should be noted that in the absence of the dorsal SNa motor axons, the ventral SNa motor axons sometimes cannot follow their normal trajectory after bifurcation to innervate the target muscles, resulting in a "bifurcation missing" phenotype. This non-autonomous effect implies that the dorsal SNa MNs might be the pioneer neurons in the SNa. Cell ablation experiments carried out in several organisms showed that pioneer neurons in some cases appear to be required for normal pathfinding by later outgrowing neurons, whereas the later outgrowing neurons in general do not seem to influence pioneer neurons (du Lac et al., 1986; Klose and Bentley, 1989). It has been proposed that pioneer neurons may have intrinsic pathfinding abilities that distinguish them from follower neurons, although the mechanism and molecules involved are still not clear.

The functions of *gsb* and *gsbn* in the development of the CNS midline

Using the *BarH1-LacZ* enhancer-trap line, we found that *gsbn* is expressed in the three TH-positive cells in each segment. Among the three TH-positive cells, the ventral midline unpaired dopaminergic neuron is well characterized. This cell is derived from the unpaired median neurons (UMIs) (Wheeler et al., 2006). In the CNS midline, *gsb* is expressed in the UMIs and their progeny from stage 7 to 11 (Gutjahr et al., 1993; Bossing and Brand, 2006). It has been speculated that *gsb* is crucial for the determination of the UMIs (Bossing and Brand, 2006). Indeed, the *BarH1-LacZ* expression in the unpaired dopaminergic neurons as well as the other two TH-positive neurons are almost eliminated in $gsbn^{D\text{-}19A}/Df(2R)GGG^{d13}$ embryos (Fig. 7D). The fact that in two different cell types

BarH1-LacZ expression depends on both *gsb* and *gsbn* implies that *BarH1* might be a direct target of *gsb* and *gsbn*.

Materials and methods

Construction of *gsbn-Gal4*

The plasmid "*gsbn-Gal4* in pDA187" was constructed by the insertion of the 9 kb blunt-ended *Xba*I-*Nco*I fragment of the plasmid "*gsbnRes-deltaIN3* in pW8" into the blunt-ended *Spe*I site of the polylinker of the plasmid pDA187 (kindly provided by K. Basler).

Construction of *gsbn-mCD8::GFP*

The 1.4 kb *Xho*I-*Xba*I fragment from "*mCD8::GFP* in pBS" (Lee and Luo, 1999) and the 600 bp *Xba*I-*Eco*RI fragment of "*gsbn*-3'UTR," which was obtained by PCR of "BSH4c4 in pGEM-1" DNA and the primers *gsbn*-3'up (5'-GCTCTAGATCATGATTTAATGAATCGCCGACG-3') and *gsbn*-3'down (5'-CGGAATTCTTACCTGTTTGTTCCCATA-3'), were cloned between the *Xho*I and *Eco*RI sites of the polylinker of pW8 to generate the plasmid "*mCD8::GFP-gsbn* 3'UTR in pW8." Finally, the plasmid "*gsbn-mCD8::GFP*" was obtained by the insertion of the 9 kb blunt-ended *Xba*I-*Nco*I fragment from the plasmid "*gsbnRes-deltaIN3* in pW8" into the blunt-ended *Xho*I site of "*mCD8::GFP-gsbn* 3'UTR in pW8" to generate *gsbn-mCD8::GFP*.

Construction of UAS-*gsbn*

The plasmid "pUAST-*gsbn*" was constructed by the insertion of the 1.7 kb blunt-ended *Bss*HII-*Nsi*I fragment from the plasmid "BSH4c4 in pGEM-1" into the blunt-ended *Eco*RI site of the polylinker of pUAST and screening for the correct orientation (Brand and Perrimon, 1993).

Fly stocks

y w; *Df(2R)IIX62/CyO, hb-LacZ*,
y w; *Df(2R)GGG^{d13}/CyO, hb-LacZ*,
y w; *gsbn^{D-19A}/CyO, hb-LacZ*,
y w; *gsbn^{del}/CyO, hb-LacZ*,
y w; *gsbn-mCD8::GFP*,
y w; *gsbn-Gal4*,
y w; *UAS-mCD8::GFP/CyO* (Lee and Luo, 1999),
w; *UAS-nlsGFP*,
y w; *UAS-gsbn*,
y w BarH1-LacZ (PL9 line) (Bourbon et al., 2002),
w BarH1-Gal4 (Garces et al., 2006),
elav-Gal4 (C155 line) (Lin and Goodman, 1994),
w; *ftz-Gal4* (Thor et al., 1999),
gsbn-lacZ (*4Z1*) (Li and Noll, 1994a).

Immunostaining of embryos

Embryos were fixed and stained as previously described (Gutjahr et al., 1993) and photographed under a Zeiss Axiophot microscope or a Leica TCS SP confocal microscope. The following antibodies were used at the dilutions indicated in parentheses: rabbit anti-Gsbn (Gutjahr et al., 1993; 1:50), rabbit anti-Gsb (Gutjahr et al., 1993; 1:100), rabbit anti-β-galactosidase (Cappel; 1:1,500), mouse anti-β-galactosidase (Promega; 1:500), rabbit anti-phospho-Histone3 (Ser10) (Upstate; 1:1,000), rabbit anti-GFP (MBL; 1:500), chicken anti-GFP (Abcam; 1:500), rabbit anti-HRP (Jackson ImmunoReserch; 1:2,000), mouse anti-Fasciclin II MAb 1D4 (Developmental Studies Hybridoma Bank, University of Iowa; 1:4), mouse MAb BP102 (Developmental Studies Hybridoma Bank, The University of Iowa; 1:50), mouse anti-Prospero MAb MR1A (Developmental Studies Hybridoma Bank, The University of Iowa; 1:4), mouse anti-Elav MAb 9F8A9 (Developmental Studies Hybridoma Bank, The University of Iowa; 1:100),

rabbit anti-Eve (Frasch et al., 1987; 1:3,000 dilution), guinea pig anti-dHb9 (Broihier and Skeath, 2002; 1:1,000), rabbit anti-MHC (Kiehart and Feghali, 1986; 1:500), biotinylated goat anti-rabbit IgG (VectorLab; 1:300), biotinylated goat anti-mouse IgG (VectorLab; 1:300), biotinylated goat anti-guinea pig IgG (VectorLab; 1:300), Alexa488 conjugated goat anti-rabbit IgG (Invitrogen; 1:500), Alexa594 conjugated goat anti-rabbit IgG (Invitrogen; 1:500), Alexa488 conjugated goat anti-mouse IgG (Invitrogen; 1:500), Alexa594 conjugated goat anti-mouse IgG (Invitrogen; 1:500), and Alexa488 conjugated goat anti-chicken IgG (Invitrogen; 1:500).

The signals of anti-GFP staining in Fig. 2 and anti-β-galactosidase staining in Fig. 5 were enhanced by the use of the TSA^{TM} kit (Invitrogen).

References

Baumgartner, S., Bopp, D., Burri, M. and Noll, M. (1987). Structure of two genes at the *gooseberry* locus related to the paired gene and their spatial expression during *Drosophila* embryogenesis. *Genes Dev* **1**, 1247-1267.

Bossing, T. and Brand, A. H. (2006). Determination of cell fate along the anteroposterior axis of the *Drosophila* ventral midline. *Development* **133**, 1001-1012.

Bossing, T., Udolph, G., Doe, C. Q. and Technau, G. M. (1996). The embryonic central nervous system lineages of *Drosophila melanogaster*. I. Neuroblast lineages derived from the ventral half of the neuroectoderm. *Dev Biol* **179**, 41-64.

Bourbon, H. M., Gonzy-Treboul, G., Peronnet, F., Alin, M. F., Ardourel, C., Benassayag, C., Cribbs, D., Deutsch, J., Ferrer, P., Haenlin, M. et al. (2002). A P-insertion screen identifying novel X-linked essential genes in *Drosophila*. *Mech Dev* **110**, 71-83.

Brand, A. H. and Perrimon, N. (1993). Targeted gene expression as a means of altering cell fates and generating dominant phenotypes. *Development* **118**, 401-415.

Broihier, H. T., Kuzin, A., Zhu, Y., Odenwald, W. and Skeath, J. B. (2004). *Drosophila* homeodomain protein Nkx6 coordinates motoneuron subtype identity and axonogenesis. *Development* **131**, 5233-5242.

Broihier, H. T. and Skeath, J. B. (2002). *Drosophila* homeodomain protein dHb9 directs neuronal fate via crossrepressive and cell-nonautonomous mechanisms. *Neuron* **35**, 39-50.

Buenzow, D. E. and Holmgren, R. (1995). Expression of the *Drosophila gooseberry* locus defines a subset of neuroblast lineages in the central nervous system. *Dev Biol* **170**, 338-349.

Certel, S. J. and Thor, S. (2004). Specification of *Drosophila* motoneuron identity by the combinatorial action of POU and LIM-HD factors. *Development* **131**, 5429-5439.

Cheesman, S. E., Layden, M. J., Von Ohlen, T., Doe, C. Q. and Eisen, J. S. (2004). Zebrafish and fly Nkx6 proteins have similar CNS expression patterns and regulate motoneuron formation. *Development* **131**, 5221-5232.

du Lac, S., Bastiani, M. J. and Goodman, C. S. (1986). Guidance of neuronal growth cones in the grasshopper embryo. II. Recognition of a specific axonal pathway by the aCC neuron. *J Neurosci* **6**, 3532-3541.

Duman-Scheel, M., Li, X., Orlov, I., Noll, M. and Patel, N. H. (1997). Genetic separation of the neural and cuticular patterning functions of *gooseberry*. *Development* **124**, 2855-2865.

Frasch, M., Hoey, T., Rushlow, C., Doyle, H. and Levine, M. (1987). Characterization and localization of the even-skipped protein of *Drosophila*. *Embo J* **6**, 749-759.

Fujioka, M., Lear, B. C., Landgraf, M., Yusibova, G. L., Zhou, J., Riley, K. M., Patel, N. H. and Jaynes, J. B. (2003). Even-skipped, acting as a repressor, regulates axonal projections in *Drosophila*. *Development* **130**, 5385-5400.

Garces, A., Bogdanik, L., Thor, S. and Carroll, P. (2006). Expression of *Drosophila* BarH1-H2 homeoproteins in developing dopaminergic cells and segmental nerve a (SNa) motoneurons. *Eur J Neurosci* **24**, 37-44.

Gutjahr, T., Patel, N. H., Li, X., Goodman, C. S. and Noll, M. (1993). Analysis of the *gooseberry* locus in *Drosophila* embryos: *gooseberry* determines the cuticular pattern and activates *gooseberry neuro*. *Development* **118**, 21-31.

Johansen, J., Halpern, M. E. and Keshishian, H. (1989). Axonal guidance and the development of muscle fiber-specific innervation in *Drosophila* embryos. *J Neurosci* **9**, 4318-4332.

Kiehart, D. P. and Feghali, R. (1986). Cytoplasmic myosin from *Drosophila melanogaster*. *J Cell Biol* **103**, 1517-1525.

Klose, M. and Bentley, D. (1989). Transient pioneer neurons are essential for formation of an embryonic peripheral nerve. *Science* **245**, 982-984.

Labrador, J. P., O'Keefe, D., Yoshikawa, S., McKinnon, R. D., Thomas, J. B. and Bashaw, G. J. (2005). The homeobox transcription factor *even-skipped* regulates *netrin*-receptor expression to control dorsal motor-axon projections in *Drosophila*. *Curr Biol* **15**, 1413-1419.

Landgraf, M., Bossing, T., Technau, G. M. and Bate, M. (1997). The origin, location, and projections of the embryonic abdominal motorneurons of *Drosophila*. *J Neurosci* **17**, 9642-9655.

Landgraf, M., Roy, S., Prokop, A., VijayRaghavan, K. and Bate, M. (1999). *even-skipped* determines the dorsal growth of motor axons in *Drosophila*. *Neuron* **22**, 43-52.

Layden, M. J., Odden, J. P., Schmid, A., Garces, A., Thor, S. and Doe, C. Q. (2006). Zfh1, a somatic motor neuron transcription factor, regulates axon exit from the CNS. *Dev Biol* **291**, 253-263.

Lee, T. and Luo, L. (1999). Mosaic analysis with a repressible cell marker for studies of gene function in neuronal morphogenesis. *Neuron* **22**, 451-461.

Li, X., Gutjahr, T. and Noll, M. (1993). Separable regulatory elements mediate the establishment and maintenance of cell states by the *Drosophila* segment-polarity gene *gooseberry*. *Embo J* **12**, 1427-1436.

Li, X. and Noll, M. (1994a). Compatibility between enhancers and promoters determines the transcriptional specificity of *gooseberry* and *gooseberry neuro* in the *Drosophila* embryo. *Embo J* **13**, 400-406.

Li, X. and Noll, M. (1994b). Evolution of distinct developmental functions of three *Drosophila* genes by acquisition of different *cis*-regulatory regions. *Nature* **367**, 83-87.

Lin, D. M. and Goodman, C. S. (1994). Ectopic and increased expression of Fasciclin II alters motoneuron growth cone guidance. *Neuron* **13**, 507-523.

Liu, W. (2003). Redundancy in enhancers and functions of the *Drosophila gooseberry* gene. Ph.D. thesis. University of Zurich.

Noll, M. (1993). Evolution and role of Pax genes. *Curr Opin Genet Dev* **3**, 595-605.

Nose, A., Mahajan, V. B. and Goodman, C. S. (1992). Connectin: a homophilic cell adhesion molecule expressed on a subset of muscles and the motoneurons that innervate them in *Drosophila*. *Cell* **70**, 553-567.

Odden, J. P., Holbrook, S. and Doe, C. Q. (2002). *Drosophila* HB9 is expressed in a subset of motoneurons and interneurons, where it regulates gene expression and axon pathfinding. *J Neurosci* **22**, 9143-9149.

Patel, N. H., Schafer, B., Goodman, C. S. and Holmgren, R. (1989). The role of segment polarity genes during *Drosophila* neurogenesis. *Genes Dev* **3**, 890-904.

Schmid, A., Chiba, A. and Doe, C. Q. (1999). Clonal analysis of *Drosophila* embryonic neuroblasts: neural cell types, axon projections and muscle targets. *Development* **126**, 4653-4689.

Schmidt, H., Rickert, C., Bossing, T., Vef, O., Urban, J. and Technau, G. M. (1997). The embryonic central nervous system lineages of *Drosophila melanogaster*. II. Neuroblast lineages derived from the dorsal part of the neuroectoderm. *Dev Biol* **189**, 186-204.

Spana, E. P. and Doe, C. Q. (1995). The prospero transcription factor is asymmetrically localized to the cell cortex during neuroblast mitosis in *Drosophila*. *Development* **121**, 3187-3195.

Thor, S., Andersson, S. G., Tomlinson, A. and Thomas, J. B. (1999). A LIM-homeodomain combinatorial code for motor-neuron pathway selection. *Nature* **397**, 76-80.

Thor, S. and Thomas, J. B. (1997). The *Drosophila islet* gene governs axon pathfinding and neurotransmitter identity. *Neuron* **18**, 397-409.

Van Vactor, D. V., Sink, H., Fambrough, D., Tsoo, R. and Goodman, C. S. (1993). Genes that control neuromuscular specificity in *Drosophila*. *Cell* **73**, 1137-1153.

Wheeler, S. R., Kearney, J. B., Guardiola, A. R. and Crews, S. T. (2006). Single-cell mapping of neural and glial gene expression in the developing *Drosophila* CNS midline cells. *Dev Biol* **294**, 509-524.

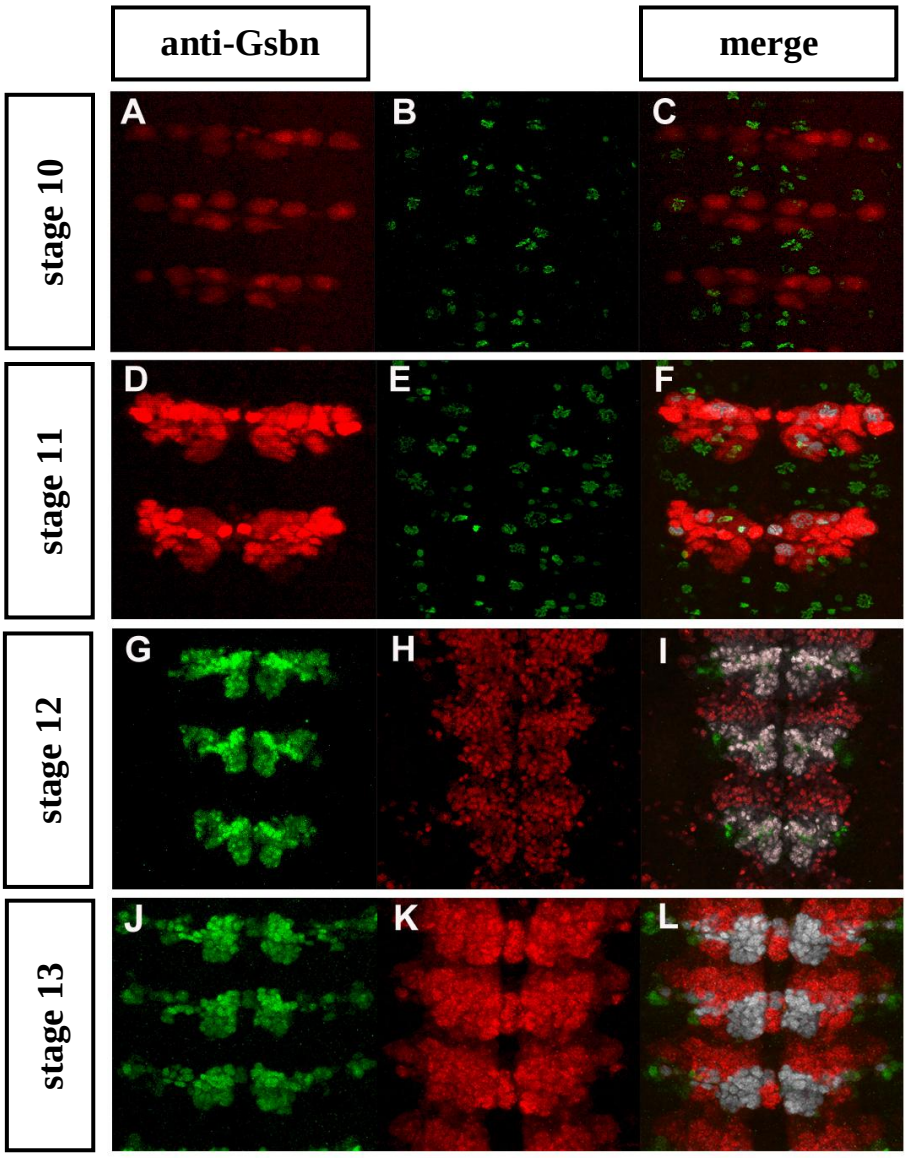

Fig. 1. *gsbn* is expressed in the neuronal precursors and neurons during embryogenesis. Ventral views of VNCs of dissected, flat mounted embryos are shown with anterior up. Wild-type embryos carrying the *lacZ* reporter transgene of *gsbn*, *4Z1* (Li and Noll, 1994a), were double-stained with anti-β-galactosidase and anti-phospho-Histone3 (A-F). *4Z1* recapitulates the *gsbn* expression pattern during embryogenesis (data not shown). A lateral Gsbn-expressing cell in the most anterior segment stains weakly for phospho-H3 while the strong label in the middle segment does not stain. Wild-type embryos (G-L) were double-stained with anti-Gsbn and anti-Prospero (G-I) or with anti-Gsbn and anti-Elav (J-L). The grey-colored cells in (F), (I), and (L) indicate colocalization of Gsbn with phosphoHistone3 (F), Prospero (I), and Elav (L).

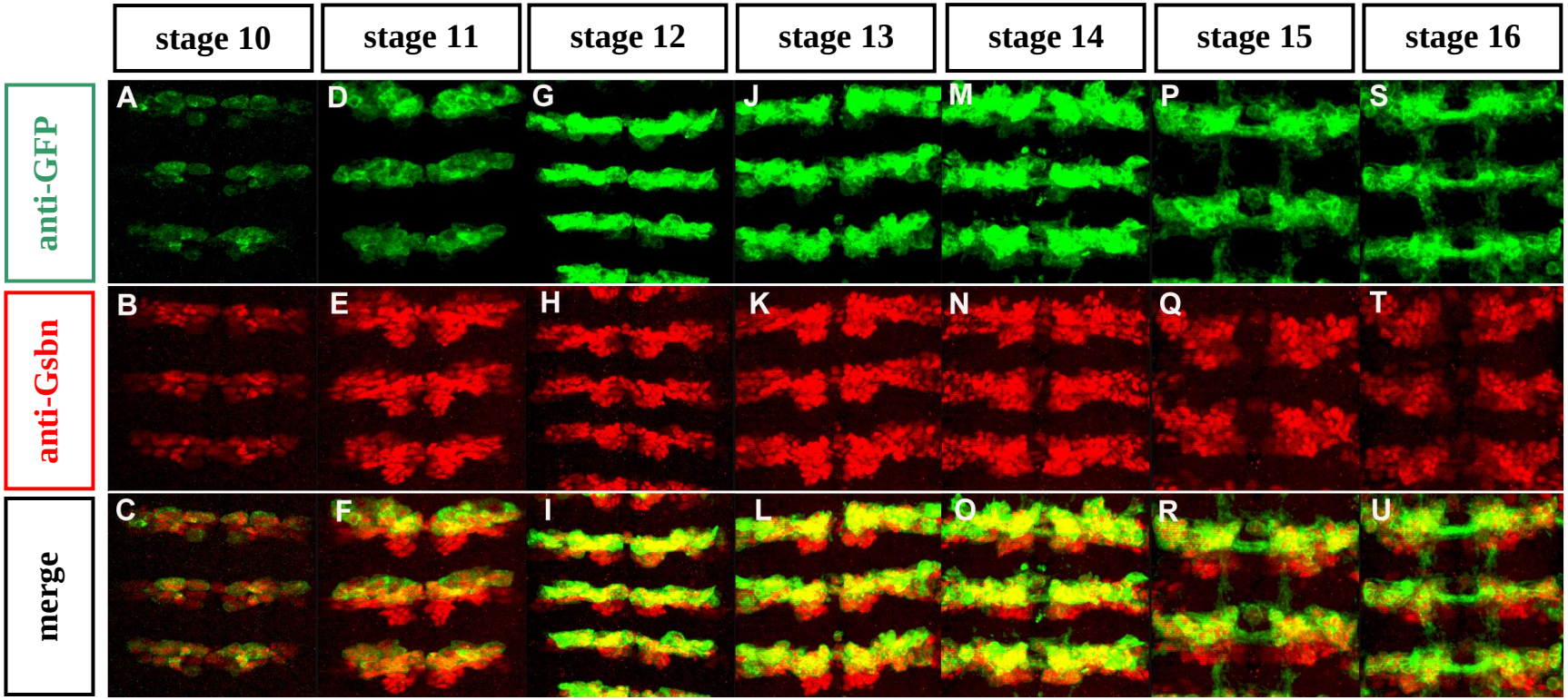

Fig. 2. The expression pattern of *gsbn-mCD8::GFP* in the CNS is similar to that of endogenous *gsbn*. Ventral views of VNCs of dissected and flat-mounted embryos with anterior up are shown. Embryos carrying *gsbn-mCD8::GFP* were double-stained with anti-GFP (A, D, G, J, M, P, and S) and anti-Gsbn (B, E, H, K, N, Q, and T).

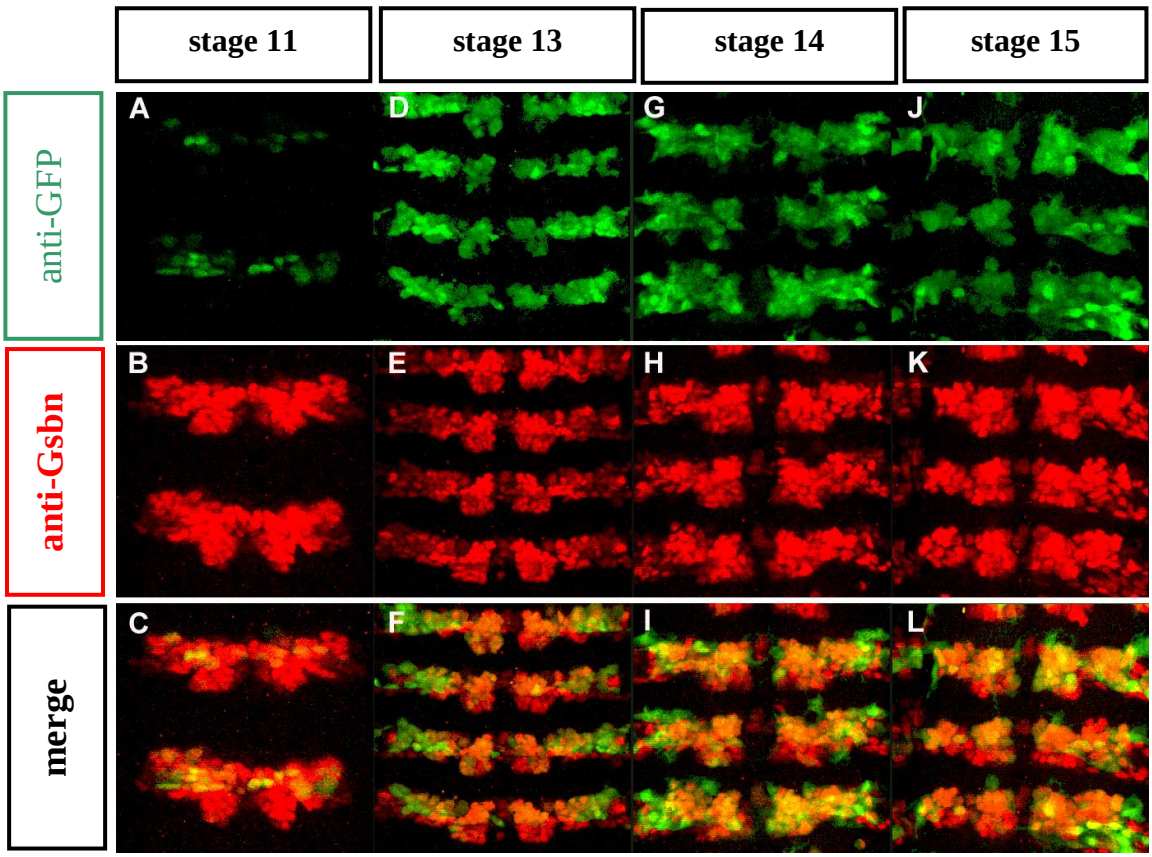

Fig. 3. *gsbn-Gal4* is expressed in the Gsbn-expressing cells. Ventral views of VNCs of dissected and flat mounted embryos are shown with anterior up. Embryos of *gsbn-Gal4/UAS-nlsGFP* were double-stained with anti-GFP (A, D, G, and J) and anti-Gsbn (B, E, H, and K). Due to the temporal delay of the GAL4/UAS system, the number of cells stained with anti-GFP is less than that of those stained with anti-Gsbn, particularly at early stages (cf. A with B).

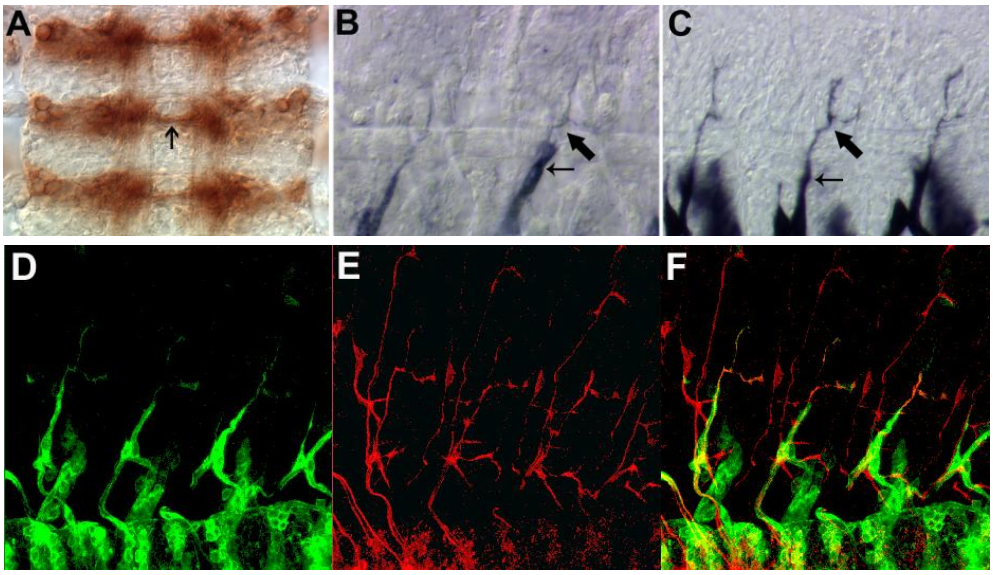

Fig. 4. Axonal projections of Gsbn-expressing neurons during embryogenesis. Ventral view (A) or lateral views (B-F) of dissected and flat mounted embryos with anterior up (A) or to the left (B-F) are shown. Stage 16 embryos carrying *gsbn-mCD8::GFP* (A, B) or *gsbn-Gal4* in combination with *UAS-mCD8::GFP* (C) were stained with anti-GFP. *gsbn-Gal4/UAS-mCD8::GFP* embryos were double-labeled with anti-GFP (D) and anti-Fasciclin II (MAb 1D4) (E). (F) is the merge of (D) and (E). Arrow in (A) indicates the posterior commissure. In (B, C) thick arrows point to the bifurcation of the SNa branch, thin arrows to the peripheral glial cell that enwraps it.

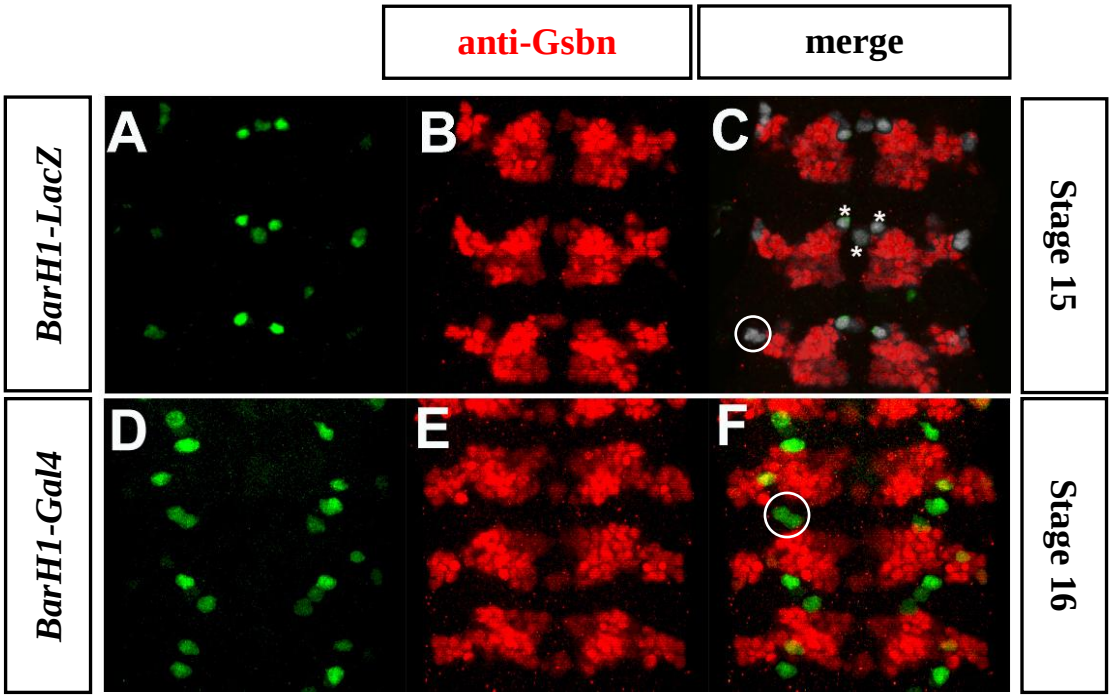

Fig. 5. *gsbn* is expressed in the dorsal subset of SNa MNs. Ventral views of VNCs of dissected and flat mounted embryos are shown with anterior up. Embryos carrying *BarH1-LacZ* (PL9 line) were double-labeled with anti-β-galactosidase (A) and anti-Gsbn (B). Embryos carrying *BarH1-Gal4* in combination with *UAS-nlsGFP* were double-labeled with anti-GFP (D) and anti-Gsbn (E). (C) is the merge of (A) and (B), (F) that of (D) and (E). Gsbn colocalizes with *BarH1-LacZ* in the dorsal SNa MNs (circle in panel C), and the three TH-positive cells per segment (asterisks in panel C). Gsbn is not expressed in the ventral SNa MNs (circle in panel F). The grey-colored cells in (C) indicate the colocalization of Gsbn with LacZ in these cells.

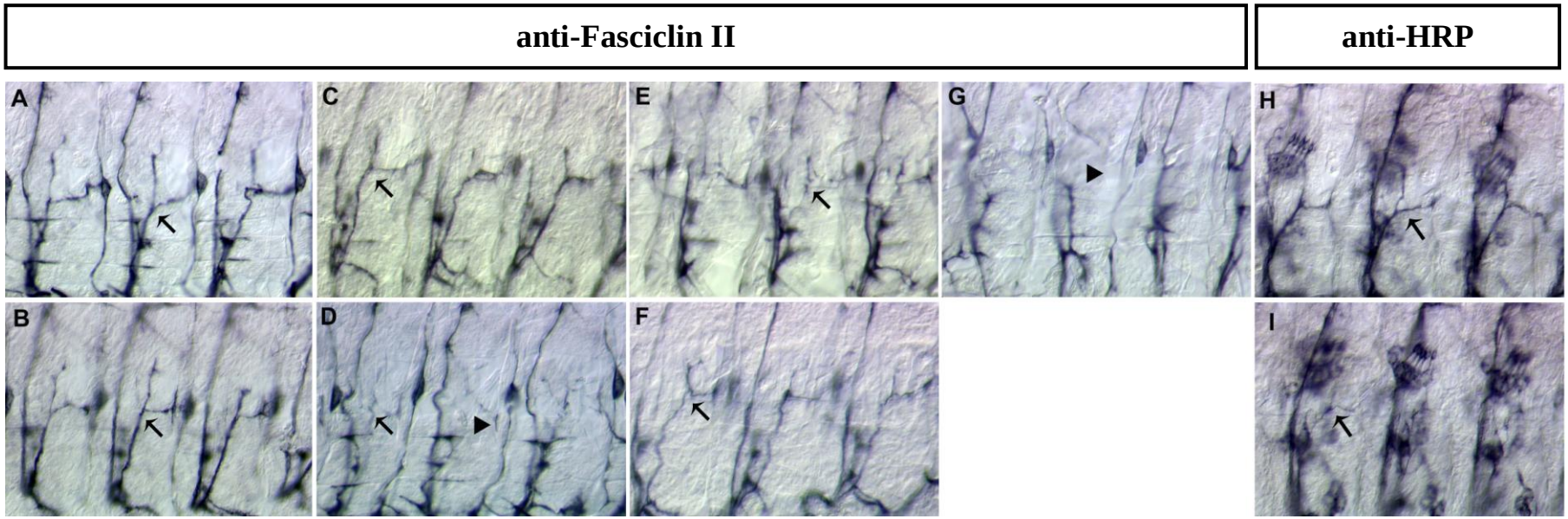

Fig. 6. *gsbn*$^{-}$ *gsb*$^{-/+}$ mutants show defects in innervation of lateral muscles by the SNa motor axons. Lateral views of three hemisegments of dissected and flat mounted late stage 16 embryos are shown, oriented with their anterior to the left, dorsal side up, and CNS to the bottom. Projections of motor axons were visualized by staining with anti-Fasciclin II (A-G) or with anti-HRP (H-I). Wild-type (A and H), *gsbn*$^{D\text{-}19A}$ (B), and *gsbn*^{del} (C) embryos exhibit normal SNa projections. In *gsbn*$^{D\text{-}19A}$*/Df(2R)IIX62* embryos (D and I) and *gsbn*^{del}*/Df(2R)GGG*^{d13} embryos (E), the SNa branch frequently shows the "thin" phenotype (arrows in D and E), and sometimes displays the "bifurcation missing" phenotype (arrowhead in D). In *gsb*^{525} mutants (G), the bifurcation of the SNa branch is frequently missing (arrowhead). In *gsbn*$^{D\text{-}19A}$*/Df(2R)IIX62* embryos carrying two copies of *gsbnRes-deltaIN3* (F), the SNa phenotype is rescued. Arrows point at the SNa branching point (bifurcation). For quantification of phenotypes, see Table 1.

Table 1. *gsbn* and *gsb* are required for the innervation of lateral muscles by SNa branch.

Genotype	SNa "bifurcation missing" phenotype	SNa"thin" phenotype	Number of hemisegments examined
y w	0	0.019	211
Df(2R)IIX62/+	0	0.033	240
$Df(2R)GGG^{d13}/+$	0	0.025	159
$gsbn^{D\text{-}19A}$	0	0.026	231
$gsbn^{del}$	0	0.056	197
$gsbn^{D\text{-}19A}/Df(2R)IIX62$	0.14	0.72	232
$gsbn^{D\text{-}19A}/Df(2R)GGG^{d13}$	0.11	0.75	194
$gsbn^{del}/Df(2R)GGG^{d13}$	0.16	0.75	174
$gsbn^{D\text{-}19A}/Df(2R)IIX62$; *gsbnRes-deltaIN3*	< 0.01	0.07	228
elav-Gal4/+; $gsbn^{D\text{-}19A}/Df(2R)GGG^{d13}$; *UAS-gsbn/+*	0	0.12	288
$gsbn^{D\text{-}19A}/Df(2R)GGG^{d13}$; *UAS-gsbn/+*	0.08	0.82	144

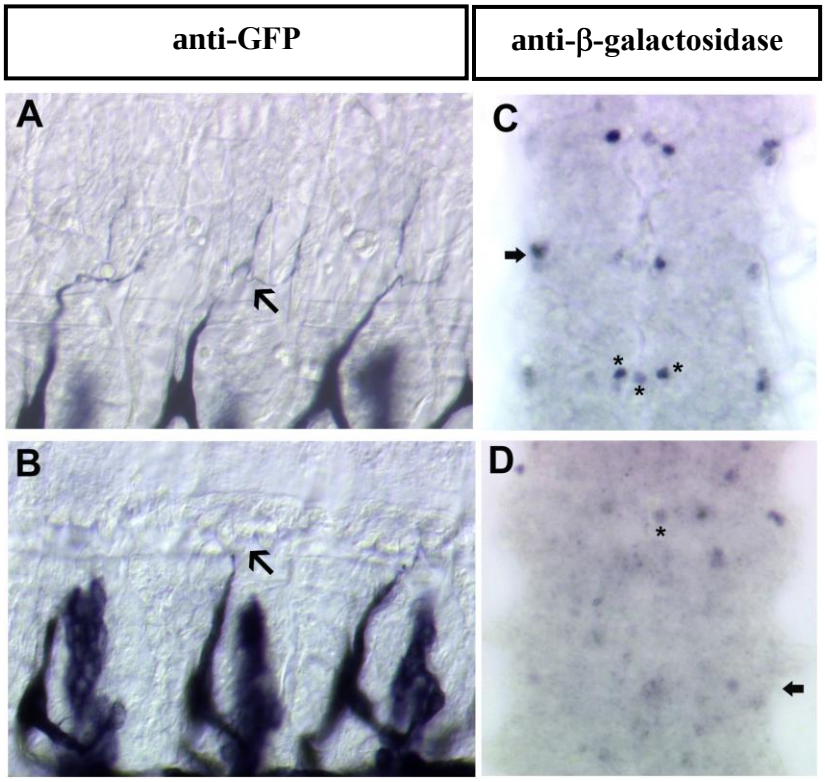

Fig. 7. *gsbn* and *gsb* are required for the differentiation of the dorsal SNa MNs. Lateral views of muscle fields of dissected, flat mounted embryos (A, B) or ventral views of isolated VNCs (C, D) are shown with anterior to the left, dorsal up, and CNS down (A, B), or with anterior up (C, D). Stage 16 embryos carrying *gsbn-Gal4* and *UAS-mCD8::GFP* in a *Df(2R)GGG*^{d13}/+ (A) or *gsbn*$^{D\text{-}19A}$/*Df(2R)GGG*^{d13} background (B) were stained with anti-GFP. (A) The dorsal SNa motor axons extend into the lateral muscle field and innervate their target muscles (arrow). (B) The dorsal SNa MNs fail to elongate their axons into the lateral muscle field (arrow). (C, D) Embryos carrying *BarH1-LacZ* in a wild-type (C) or *gsbn*$^{D\text{-}19A}$/*Df(2R)GGG*^{d13} background (D) were stained with anti-β-galactosidase. In wild-type embryos, *BarH1-LacZ* labels the dorsal SNa MNs (arrow in C) and TH-positive cells (asterisks in C). In a *gsbn*$^{D\text{-}19A}$/*Df(2R)GGG*^{d13} background, *BarH1-LacZ* expression in the dorsal SNa MNs (arrow in D) and the TH-positive cells (asterisk in D) is dramatically down-regulated. Embryos in (C) and (D) are at stage 14 and 15, respectively.

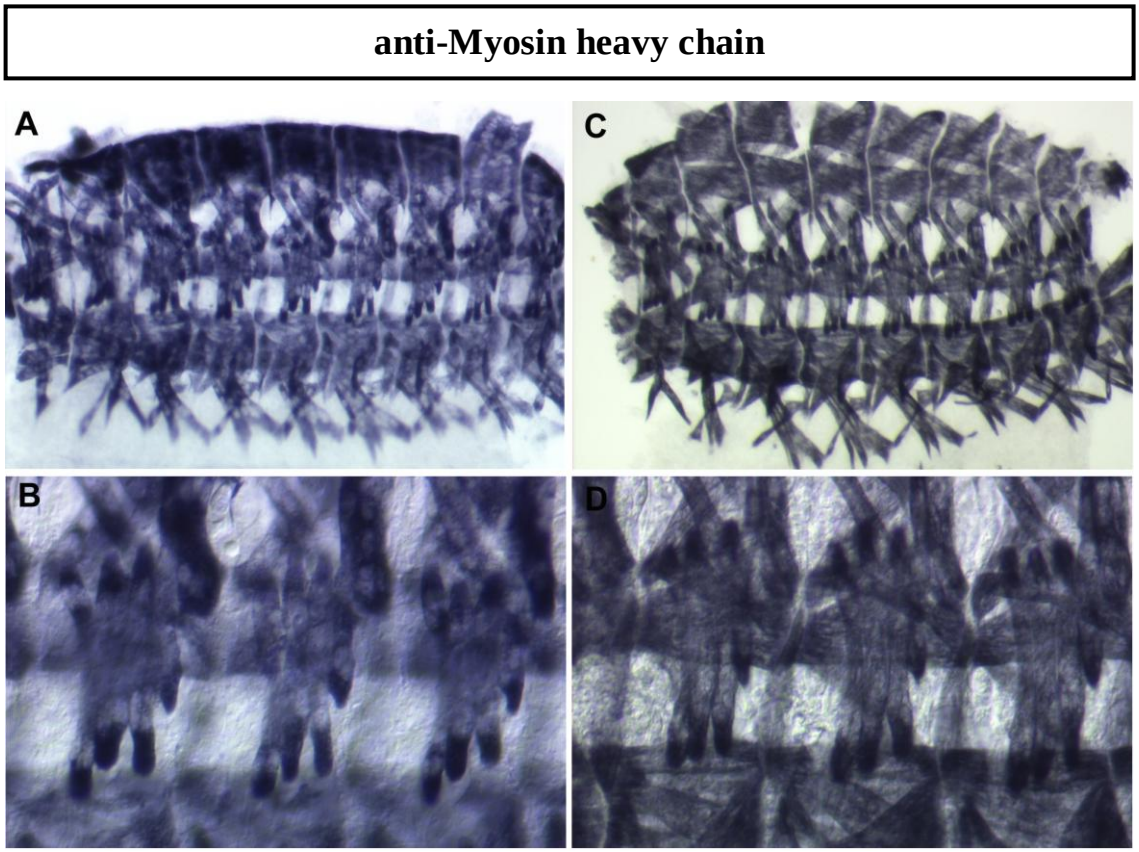

Fig. 8. *gsbn*$^{D\text{-}19A}$*/Df(2R)GGG*^{d13} embryos do not show defects in muscle development. Lateral views of body wall muscles of dissected and flat mounted embryos are shown. Embryos were oriented with their anterior to the left and dorsal side up. Wild-type (A, B) and *gsbn*$^{D\text{-}19A}$*/Df(2R)GGG*^{d13} (C, D) embryos at stage 16 were stained with anti-Myosin heavy chain (MHC). (B) and (D) show enlarged views of (A) and (C), respectively, for the lateral muscle fibers innervated by SNa motor axons.

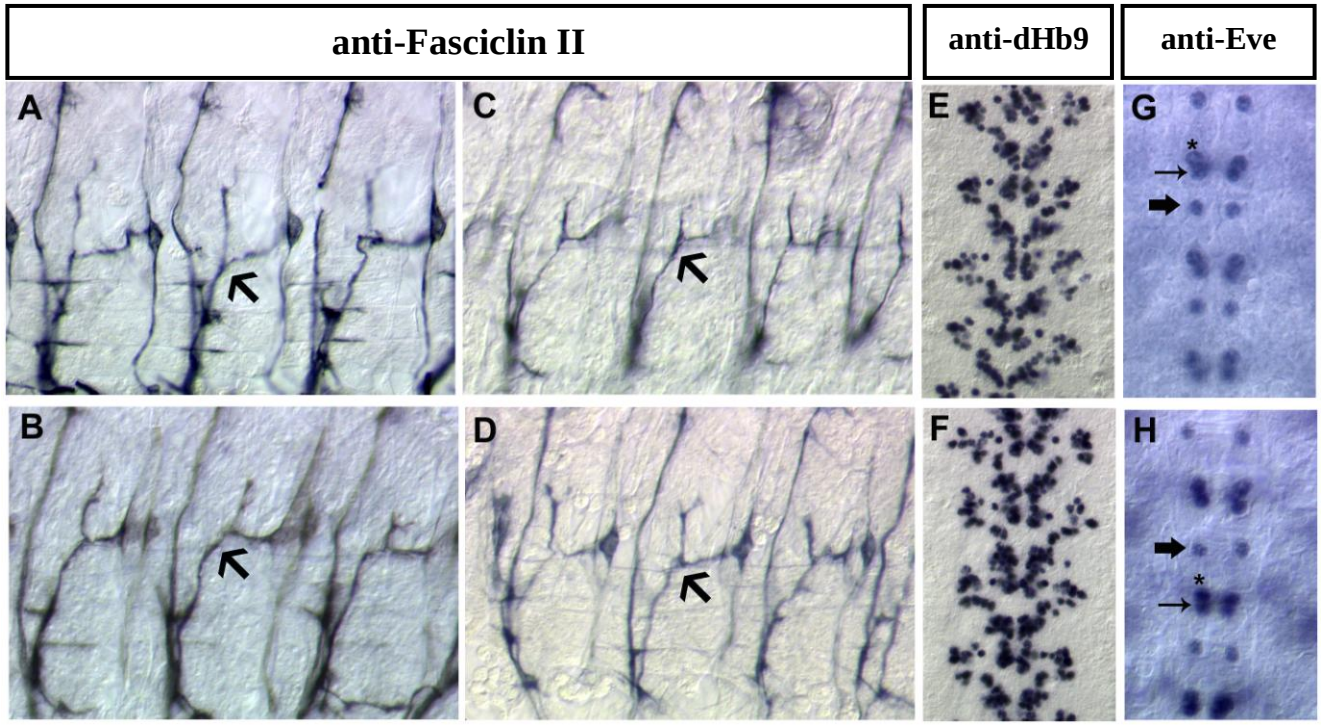

Fig. 9. Ectopic Gsbn does not transform the fate of other neurons into that of the dorsal SNa MNs. Lateral views of muscle fields (A-D) or ventral views of VNCs (E-H) of dissected, flat mounted embryos are shown with anterior to the left and CNS to the bottom (A-D), or with anterior up (E-H). Wild-type (A, E, and G), *elav-Gal4/+*; *UAS-gsbn/+* (B, F, and H), *elav-Gal4/+*; *UAS-gsbn* (two copies)/+ (C), and *UAS-gsbn* (two copies)/+; *ftz-Gal4/+* (D) embryos were stained with anti-Fasciclin II (A-D), anti-dHb9 (E, F), or anti-Eve (G-H). When Gsbn is over-expressed (B-D), the intensity of anti-Fasciclin II staining of SNa (arrows) is not increased as compared to wild type (A). The expression patterns of *dHb9* (F) and *even-skipped* (*eve*) (H) are not obviously altered when Gsbn is ectopically expressed. In (G, H), thin arrows point at the pCC neurons, asterisks mark the aCC neurons, and thick arrows point at the RP2 neurons.

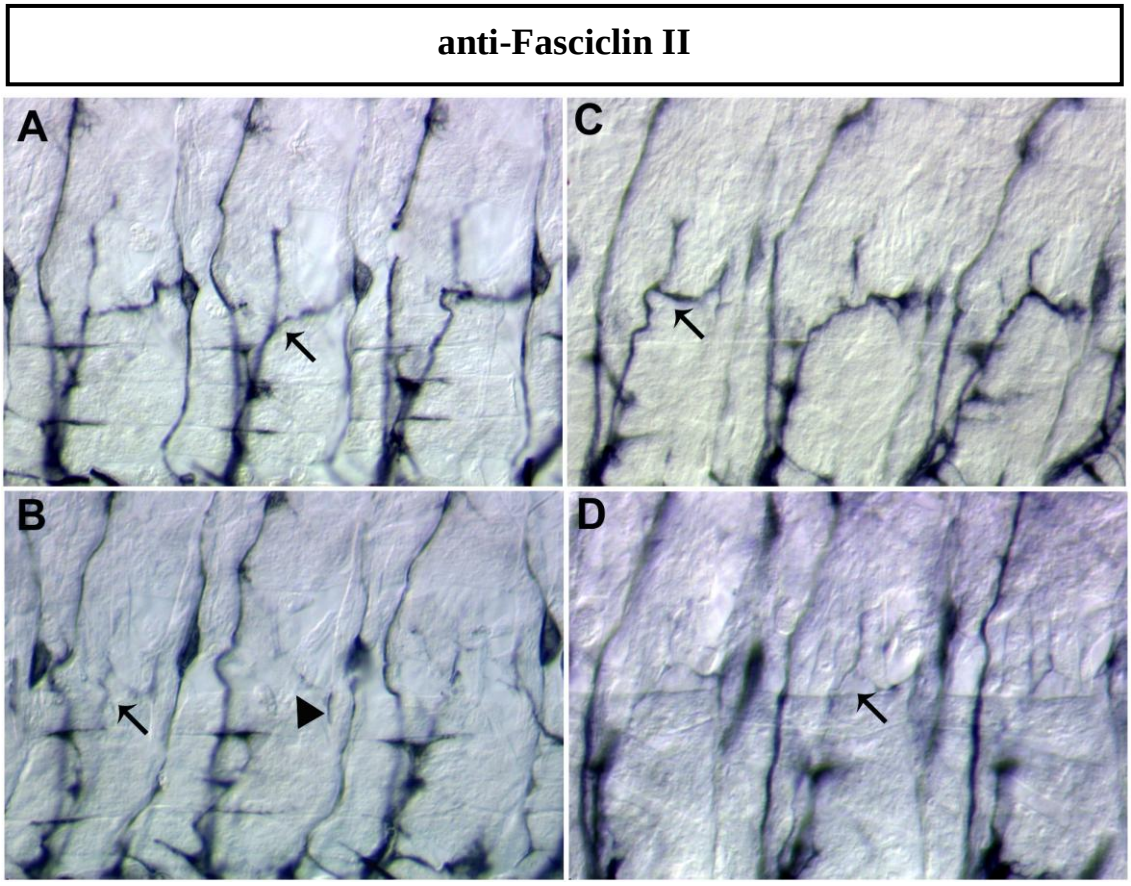

Fig. 10. Rescue of the SNa phenotype of *gsbn*$^{-}$ *gsb*$^{-/+}$ embryos by expressing Gsbn at the neuronal stage. Lateral views of three hemisegments of dissected and flat mounted late stage 16 embryos are shown with anterior to the left and CNS to the bottom. Wild-type (A), *gsbn*$^{D\text{-}19A}$*/Df(2R)IIX62* (B), *elav-Gal4/+*; *gsbn*$^{D\text{-}19A}$*/Df(2R)GGG*^{d13}; *UAS-gsbn/+* (C), and *gsbn*$^{D\text{-}19A}$*/Df(2R)GGG*^{d13}; *UAS-gsbn/+* (D) embryos were stained with anti-Fasciclin II. Arrows indicate the SNa branch (bifurcation shape). The SNa "thin" phenotype (arrow in B) and "bifurcation missing" phenotype (arrowhead in B) are rescued in *gsbn*$^{D\text{-}19A}$*/Df(2R)GGG*^{d13} embryos carrying *UAS-gsbn* and *elav-Gal4* (C), whereas *gsbn*$^{D\text{-}19A}$*/Df(2R)GGG*^{d13} embryos carrying only the *UAS-gsbn* transgene (D) still show the SNa phenotype. For quantification, see Table 1.

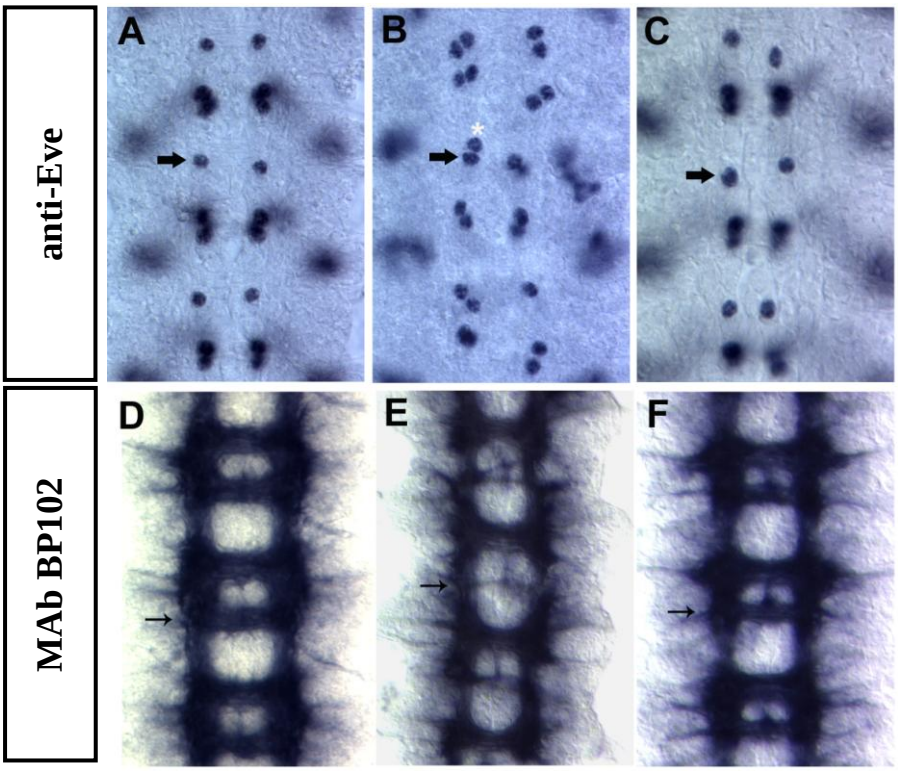

Fig. 11. *gsbn*$^{-}$ *gsb*$^{-/+}$ mutants show no neuronal precursor defects. Ventral views of VNCs of dissected, flat mounted embryos (A-C) or of dissected VNCs (D-F) are shown with anterior to up. Wild-type (A, D), *Df(2R)GGG*^{d13} (B, E), and *gsbn*$^{D\text{-}19A}$*/Df(2R)IIX62* embryos (C, F) embryos at stage 14 (B) or 15 (A, C-F) were stained with anti-Eve (A-C) or MAb BP102 (D-F). Arrows point at RP2 neurons (A-C) or at posterior commissures (D-F). In *Df(2R)GGG*^{d13} embryos, 80% of the hemisegments (n=116) show the "RP2 neuron duplication" phenotype (white asterisk in B), whereas none of the hemisegments (n=179) displays this phenotype in *gsbn*$^{D\text{-}19A}$*/Df(2R)IIX62* embryos (C). In *Df(2R)GGG*^{d13} mutants, the MAb BP102 staining in the posterior commissure is very weak (arrow in E), in contrast to wild-type (D) and *gsbn*$^{D\text{-}19A}$*/Df(2R)IIX62* (F) embryos.

Chapter 4

Partial redundancy of *gooseberry neuro* and *gooseberry* functions in embryonic segmentation of *Drosophila*

Summary

Although the main function of *gsb* as a segment polarity gene is the maintenance of *wg* expression at 6 h AEL through a *wg-gsb* autoregulatory loop, it remained uncertain whether the strong cuticular phenotype of *gsb* deficiency mutants can be attributed entirely to the loss of *gsb*. To address the role(s) of *gsb* and *gsbn* in segmentation, we examined the cuticular phenotypes of large deficiency mutants rescued by *gsbn*. Furthermore, a new strong allele specific for *gsb* was generated by imprecise excision of the P element from gsb^{P1155}. The results support the idea that *gsbn* is partially redundant with *gsb* in the development of the properly segmented epidermis, thereby implying that the strong cuticular phenotype of large deficiency mutants cannot be used to characterize *gsb* null alleles.

Introduction

The *gsb* locus was first identified in a systematic screen for mutations affecting segmentation and larval cuticle formation (Nüsslein-Volhard and Wieschaus, 1980). It has been shown that the main function of *gsb* as a segment polarity gene is to maintain *wg* expression at 6 h AEL (Li and Noll, 1993). Moreover, *wg* is also required for the maintenance of *gsb* expression after 4 h AEL, and the *gsb* enhancer responsible for *wg*-mediated maintenance has been identified (Li et al., 1993). Therefore, *wg* and *gsb* form a *wg-gsb* autoregulatory loop to ensure the spatiotemporal regulation of *wg* and *gsb* expression (Li and Noll, 1993).

The full rescue of cuticular phenotype of *Df(2R)IIX62* mutants by a *gsb* transgene and the strong *gsb* expression in the ectoderm raise the question whether this phenotype may be attributed solely to the loss of *gsb* (Gutjahr et al., 1993). Despite extensive efforts no mutations that affect only *gsb* and exhibit a strong cuticular phenotype have been isolated. Furthermore, the analysis of the segmentation function of *gsb* is complicated by the fact that undetectable levels of Gsb suffice to fully rescue this function (Duman-Scheel et al., 1997; Liu, 2003). Since all large deficiencies of *gsb* with strong cuticular phenotypes uncover not only *gsb*, but also *gsbn*, one possibility is that *gsbn* and *gsb* are partially redundant for the segmentation function. In this chapter, evidence is presented suggesting that *gsbn* may play a role in segmentation that is partially redundant with that of *gsb*.

Analysis of the *gsb* function is hindered to a large extent by the lack of a null allele specific for *gsb*. Therefore, hypomorphic *gsb* alleles have been combined with a large deficiency uncovering both *gsb* and *gsbn* to study the functions of *gsb*. However, this approach suffers from the following two limitations. First, the residual *gsb* activity from a hypomorphic allele might reduce the penetrance of, or completely mask, the mutant phenotype(s), an example of which is the *gsb* cuticular phenotype (Duman-Scheel et al., 1997; Liu, 2003). Second, since *gsb* and *gsbn* share overlapping functions, as shown in the preceding chapters of this thesis, the observed phenotype might result from the additional loss of one copy of *gsbn* uncovered by the large deficiency. This might not be a serious problem in the embryo where *gsbn* is expressed at very low levels in a *gsb*

mutant background. However, it is not clear whether *gsbn* expression also depends on *gsb* at postembryonic stages. Therefore, one has to be cautious in assigning solely to the loss of *gsb* function a postembryonic phenotype of transheterozygotes of a *gsb* hypomorphic allele over a large deficiency ($gsbn^{-/+}$ *gsb*). To overcome these difficulties, an attempt was made to generate *gsb* null alleles by screening for imprecise excisions of the P element from gsb^{P1155}. A *gsb* allele isolated from this screen, gsb^{J46}, appears to be a strong, if not a null, allele of *gsb*.

Results

Partial rescue of the strong gooseberry phenotype by a *gsbn* transgene

The finding that *gsb* and *gsbn* share overlapping functions for viability and motoneuron development led us to revisit the issue of the *gsb* cuticular phenotype. If *gsbn* is completely or partially redundant with *gsb*, one expects the cuticular phenotype of *gsb* null mutants to be weaker in the presence of two copies of *gsbn* than that of large deficiencies uncovering *gsb* and *gsbn*. Since all extant *gsb* null alleles are such large deficiencies, two copies of *gsbn* were provided by crossing the *gsbn* rescue transgene into the *Df(2R)IIX62* background. A *gsbn* transgene *gsbnRes-deltaIN3* was used, which not only recapitulates the *gsbn* expression pattern but also is transcriptionally regulated as endogenous *gsbn* (Fig. 4G, Chapter 2). In *Df(2R)IIX62* mutants, the naked posterior portion of each segment is deleted and replaced by the mirror-image duplication of denticle belts from the anterior portion with high penetrance and high expressivity (Nüsslein-Volhard and Wieschaus, 1980; Fig. 1B). However, in *Df(2R)IIX62* embryos rescued with two copies of *gsbnRes-deltaIN3*, 48% of the segments (n=273) showed partial or full rescue of the cuticular phenotype (Fig. 1E,F), which may imply a partial redundancy of *gsbn* with *gsb* in segmentation.

A *gooseberry* "modifier" in the vicinity of the *gsb* locus

Surprisingly, *Df(2R)GGG^{d13}*, which is smaller than *Df(2R)IIX62* and deletes only *gsbn*, *gsb*, and *gol*, exhibits a similar high penetrance, but variable expressivity with respect to the cuticular phenotype (Fig. 1C,D). This implies that the strong cuticular phenotype of *Df(2R)IIX62* results not only from the loss of *gsb* and *gsbn*, but also from other mutations on the *Df(2R)IIX62* chromosome. Since other large deficiencies in this region also showed the same expressivity of the gooseberry phenotype as *Df(2R)IIX62* (H.H. and M.N., unpublished data), it follows that the *gooseberry* "modifier" on the *Df(2R)IIX62* chromosome is located in the vicinity of the *gsb* locus and uncovered by *Df(2R)IIX62*, but not by *Df(2R)GGG^{d13}*. Furthermore, this *gooseberry* "modifier" appears not to be essential for the development of the epidermis since one copy of a *gsb* transgene fully rescues the strong cuticular phenotype of *Df(2R)IIX62* mutants (Gutjahr et al., 1993; Liu, 2003). To assess the partial rescue of the cuticular phenotype by *gsbn* without the effect caused by the *gooseberry* "modifier," we examined the cuticles of *Df(2R)GGG^{d13}* embryos rescued by two copies of *gsbnRes-deltaIN3* as well. As expected, the gooseberry phenotype in *Df(2R)GGG^{d13}*; *gsbnRes-deltaIN3* mutants is weaker than that of *Df(2R)IIX62*; *gsbnRes-deltaIN3* mutants (cf. Fig. 1G,H with 1E,F).

Isolation and characterization of the new *gsb* alleles

For historical reasons, the strong cuticular phenotype of *Df(2R)IIX62* (Nüsslein-Volhard and Wieschaus, 1980) was taken as a "gold standard" to be characteristic of a functional null allele of *gsb*. In light of the preceding result that a *gsbn* transgene can partially rescue the gooseberry phenotype, the failure of previous screens to isolate a *gsb* null allele affecting only *gsb* might have been caused by its relatively weak cuticular phenotype that could be easily overlooked in a large-scale screen. Therefore, in an attempt to isolate new *gsb* null mutations that do not affect adjacent genes, we carried out a screen using imprecise excision of *P{P1155}* which is inserted 54 bp upstream of the *gsb* transcription start site (Duman-Scheel et al., 1997; Liu, 2003), and particularly focused on mutants exhibiting the relatively weak cuticular phenotype. Figure 2 shows the scheme of the genetic crosses used to generate imprecise excision of *P{P1155}* and

isolate the *gsb* mutant stocks. Of 320 independent excisions in ry^- males, 92 cannot complement with gsb^{P1155}, and hence stocks were established. Cuticle preparations from each of the 92 lines were examined, and two lines, gsb^{J46} and gsb^{J62}, showed the gooseberry phenotype. The penetrance and expressivity of the cuticular phenotype is relatively low for both alleles. Only 7.7% of segments (n=273) showed a partial gooseberry phenotype for gsb^{J46} (Fig. 3C, D) and 6.2% (n=336) for gsb^{J62} (Fig. 3E,F). To further characterize the two new *gsb* alleles, mutant embryos were stained with an antiserum specific for Gsb. In gsb^{J46} embryos, Gsb protein is not detectable (Fig. 4C), whereas there is a weak staining of Gsb in the CNS of gsb^{J62} embryos (Fig. 4D). In contrast to gsb^{P1155} embryos, Gsb protein is not detected in the ectoderm of gsb^{J62} embryos (cf. Fig. 4D with 4B).

In a previous similar screen for *gsb* mutants by imprecise excisions of *P{P1155}*, no *gsb* mutant alleles could be recovered as only internal deletions of the P-element insertion were recovered (Duman-Scheel et al., 1997). To determine whether the P-element of *P{P1155}* is completely excised in gsb^{J46} and gsb^{J62}, gsb^{J46} and gsb^{J62} mutant embryos were stained with anti-β-galactosidase since *P{P1155}* includes a *lacZ* cassette (Duman-Scheel et al., 1997). Indeed, strong staining was observed in both gsb^{J46} and gsb^{J62} embryos (Fig. 5C-E), which demonstrates that the *lacZ* coding region of the P-element is retained in both *gsb* alleles. It appears that the *lacZ* expression pattern of gsb^{J62} is similar to that of gsb^{P1155} embryos at the extended germband stage (cf. Fig. 5E with 5A). Moreover, gsb^{J62} embryos exhibit the same strong *lacZ* expression pattern at late stages (not shown) as gsb^{P1155} embryos (Fig. 5B). The expression pattern of *lacZ* in gsb^{J46} embryos is very similar to that of Gsb in wild-type embryos (cf. Fig. 5C with 5F), but drastically distinct from that of *lacZ* in gsb^{P1155} embryos at late stages (cf. Fig. 5D with 5B).

By the use of a series of primers flanking or inside the *P{P1155}* insertion, the molecular lesions of gsb^{J46} and gsb^{J62} were characterized. gsb^{J46} retains 2,736 bp of the 5'-end of *P{P1155}* (including 2,147 bp of the *lacZ* coding region), 19 bp of unknown origin, and 15 bp of the 3'-end of *P{P1155}*. The sequences flanking the insertion site of *P{P1155}* are intact in gsb^{J46}. Since the polyA addition signal of *lacZ* is deleted, one

expects that *gsb*^{J46} produces a hybrid transcript that includes the N-terminal coding half of *lacZ*, 54 bp of the *gsb* promoter region, the 5'UTR of *gsb*, and the *gsb* coding region. The protein produced from this hybrid transcript most probably contains only the N-terminal half of LacZ because several stop codons in the *gsb* promoter region and in the *gsb* 5'UTR are in-frame with the truncated LacZ.

gsb^{J62} has a deletion extending 1,332 bp downstream from a site located 1,091 bp downstream of the *gsb* stop codon. The deletion inside the P-element of *gsb*^{J62} has not yet been determined, but the sequences flanking the insertion site of *P{P1155}* are intact. The stronger cuticular phenotype of *gsb*^{J62} than of *gsb*^{P1155} embryos probably results from the additional deletion in *gsb*^{J62} of an enhancer downstream of the *gsb* coding region that activates *gsb* in the ectoderm. In agreement with this interpretation, previous work has shown that a *gsb* transgene under the control of 3 kb downstream sequences is able to partially rescue the *gsb* cuticular phenotype (Liu, 2003).

Discussion

The partial rescue of the gooseberry phenotype in *Df(2R)IIX62* and *Df(2R)GGG*^{d13} embryos by *gsbnRes-deltaIN3* and the low penetrance of *gsb*^{J46} with respect to the cuticular phenotype suggest that *gsbn* and *gsb* have partially redundant functions in segmentation and development of the epidermis. Our results suggest that *gsbnRes-deltaIN3* is expressed in the epidermis of *gsb*$^{-}$ embryos at undetectable levels (Figure 4H of Chapter 2), similar to the endogenous *gsbn* gene of *gsb*^{J46} embryos (data not shown). In addition, *gsb*^{J46} embryos (Fig. 3C,D) and *Df(2R)GGG*^{d13} embryos rescued by *gsbnRes-deltaIN3* (Fig. 1G,H) show similarly weak gooseberry phenotypes. It follows that Gsbn is expressed at undetectable levels at stage 11 in the epidermis of both wild-type embryos, as previously described (Gutjahr et al., 1993), and *gsb*$^{-}$ embryos (consistent with Gsbn expression patterns of *gsb*^{J46} embryos, not shown) that are sufficient to largely rescue the gooseberry phenotype. Similarly, it has been shown that undetectable levels of Gsb protein produced by read-through at the ochre codon of *gsb*^{525} are sufficient to rescue the *gsb* segmentation function (Liu, 2003). This is not surprising in view of the

functional conservation of the proteins encoded by *gsb* and *gsbn* during evolution (Li and Noll, 1994).

It may be surprising that although both gsb^{P1155} and gsb^{J46} have exongenous sequences inserted in the same region of the *gsb* promoter, the effect of their insertions on *gsb* expression appears to be very distinct. The strong repression of *gsb* expression in gsb^{J46} embryos is probably mediated by a transcriptional interference mechanism. When transcription of the truncated *lacZ* mRNA progresses through the short *gsb* promoter region of 54 bp, the assembly of a pre-initiation complex for *gsb* transcription may be inhibited and the epigenetic information in the *gsb* promoter region altered. While it seems plausible that such a transcriptional interference is able to repress *gsb* expression driven by its cognate promoter completely, it remains uncertain. Therefore, gsb^{J46} might not be a null allele. Nevertheless, gsb^{J46} should be considered as a strong allele of *gsb* because of its cuticular phenotype that is stronger than that of any mutant alleles specific for *gsb* and because it does not express detectable levels of Gsb protein. It should be noted that the cuticular phenotype of gsb^{J46} embryos is weaker than that of $Df(2R)GGG^{d13}$ embryos rescued by two copies of *gsbnRes-deltaIN3*. This might result from a lower expression level of the transgene than of endogenous *gsbn*. Alternatively, it might be explained by the fact that *gsbnRes-deltaIN3* does not include the downstream enhancer of *gsb*, which might activate both *gsb* and *gsbn* in the ectoderm in the endogenous situation.

A puzzling aspect of the gsb^{J46} allele is that its *lacZ* expression pattern, which is very similar, if not identical to that of endogenous *gsb*, drastically differs from that of gsb^{P1155} and gsb^{J62}, particularly at late embryonic stages (Fig. 5). The expression pattern of *lacZ* in the CNS of late gsb^{P1155} and gsb^{J62} embryos appears to be similar to that of *gsbn* in wild-type embryos at a similar stage. Since Gsbn-expressing neurons are derived from the neuroblasts expressing Gsb (Gutjahr et al., 1993; Buenzow and Holmgren, 1995), one possibility is that the LacZ protein produced in gsb^{P1155} or gsb^{J62} embryos is more stable than the truncated LacZ produced by gsb^{J46} and thus perdures in the lineage derived from the neuroblasts. Another, though less probable, possibility is that the P-element sequences deleted in gsb^{J46} are somehow involved in the transcriptional regulation of *lacZ*. Whatever the explanation may be, the *lacZ* with expression pattern

faithful to *gsb* in gsb^{J46} is a valuable marker for the Gsb-expressing cells in a *gsb* mutant background.

Materials and Methods

Fly stocks

y; gsb^{P1155}/*CyO*, y^+ w^+; ry^-,

y w; $amos^{[Tft]}$/*CyO*, *PiggyBac{delta2-3.Exel}2* (Parks et al., 2004),

w; *Df(2R)IIX62/SM6B*,

y w; $Df(2R)GGG^{d13}$/*SM6B*,

y w; gsb^{J46}/*SM6B*,

y w; gsb^{J62}/*SM6B*,

y w; *Df(2R)IIX62*/*CyO*, y^+; *gsbnRes-deltaIN3*,

y w; $Df(2R)GGG^{d13}$/*CyO*, y^+; *gsbnRes-deltaIN3*.

Genetic procedure for imprecise excision of gsb^{P1155}

Females carrying *P{P1155}* (*y*; gsb^{P1155}/*CyO*, y^+ w^+; ry^-) were crossed with males carrying *PiggyBac{delta2-3.Exel}2* (*y w*; $amos^{[Tft]}$/*CyO*, *PiggyBac{delta2-3.Exel}2*). One or two male progeny carrying both *P{P1155}* and *PiggyBac{delta2-3.Exel}2* (*y*; gsb^{P1155}/*CyO*, *PBac{delta2-3.Exel}2*; ry^-/+) were crossed with *y*; gsb^{P1155}/*CyO*, y^+ w^+; ry^- virgins. Single offspring males that were y^+ and ry^- (*y*; *Ex{P1155}*/*CyO*, y^+ w^+; ry^-) from different fathers were test-crossed with *y*; gsb^{P1155}/*CyO*, y^+ w^+; ry^- virgins. Excision lines that fail to complement with gsb^{P1155} were maintained for further analysis (Fig. 2).

Cuticle preparation

0-6 hrs embryos were collected and aged at 25°C for 24 hours. Cuticles were prepared as described **(**Wieschaus and Nüsslein-Volhard, 1986**)**.

Immunostaining of embryos

Collection, fixation, and immunostaining of embryos were carried out as previously described (Gutjahr et al., 1993). The following antibodies were used: rabbit anti-Gsbn at a 1:50 dilution (Gutjahr et al., 1993), rabbit anti-Gsb at a 1:100 dilution (Gutjahr et al., 1993), and rabbit anti-β-galactosidase at a 1:1,500 dilution (Cappel).

References

Buenzow, D. E. and Holmgren, R. (1995). Expression of the *Drosophila gooseberry* locus defines a subset of neuroblast lineages in the central nervous system. *Dev Biol* **170**, 338-349.

Duman-Scheel, M., Li, X., Orlov, I., Noll, M. and Patel, N. H. (1997). Genetic separation of the neural and cuticular patterning functions of *gooseberry*. *Development* **124**, 2855-2865.

Gutjahr, T., Patel, N. H., Li, X., Goodman, C. S. and Noll, M. (1993). Analysis of the *gooseberry* locus in *Drosophila* embryos: *gooseberry* determines the cuticular pattern and activates *gooseberry neuro*. *Development* **118**, 21-31.

Li, X., Gutjahr, T. and Noll, M. (1993). Separable regulatory elements mediate the establishment and maintenance of cell states by the *Drosophila* segment-polarity gene *gooseberry*. *EMBO J* **12**, 1427-1436.

Li, X. and Noll, M. (1993). Role of the *gooseberry* gene in *Drosophila* embryos: maintenance of *wingless* expression by a *wingless--gooseberry* autoregulatory loop. *EMBO J* **12**, 4499-4509.

Li, X. and Noll, M. (1994). Evolution of distinct developmental functions of three *Drosophila* genes by acquisition of different *cis*-regulatory regions. *Nature* **367**, 83-87.

Liu, W. (2003). Redundancy in enhancers and functions of the *Drosophila gooseberry* gene. Ph.D. thesis. University of Zurich.

Nüsslein-Volhard, C. and Wieschaus, E. (1980). Mutations affecting segment number and polarity in *Drosophila*. *Nature* **287**, 795-801.

Parks, A. L., Cook, K. R., Belvin, M., Dompe, N. A., Fawcett, R., Huppert, K., Tan, L. R., Winter, C. G., Bogart, K. P., Deal, J. E. et al. (2004). Systematic generation of high-resolution deletion coverage of the *Drosophila melanogaster* genome. *Nat Genet* **36**, 288-292.

Wieschaus, E. and Nüsslein-Volhard, C. (1986). Looking at embryos. In *Drosophila, A Practical Approach*, (ed. D. B. Roberts), pp. 199-227. Oxford, UK: IRL Press.

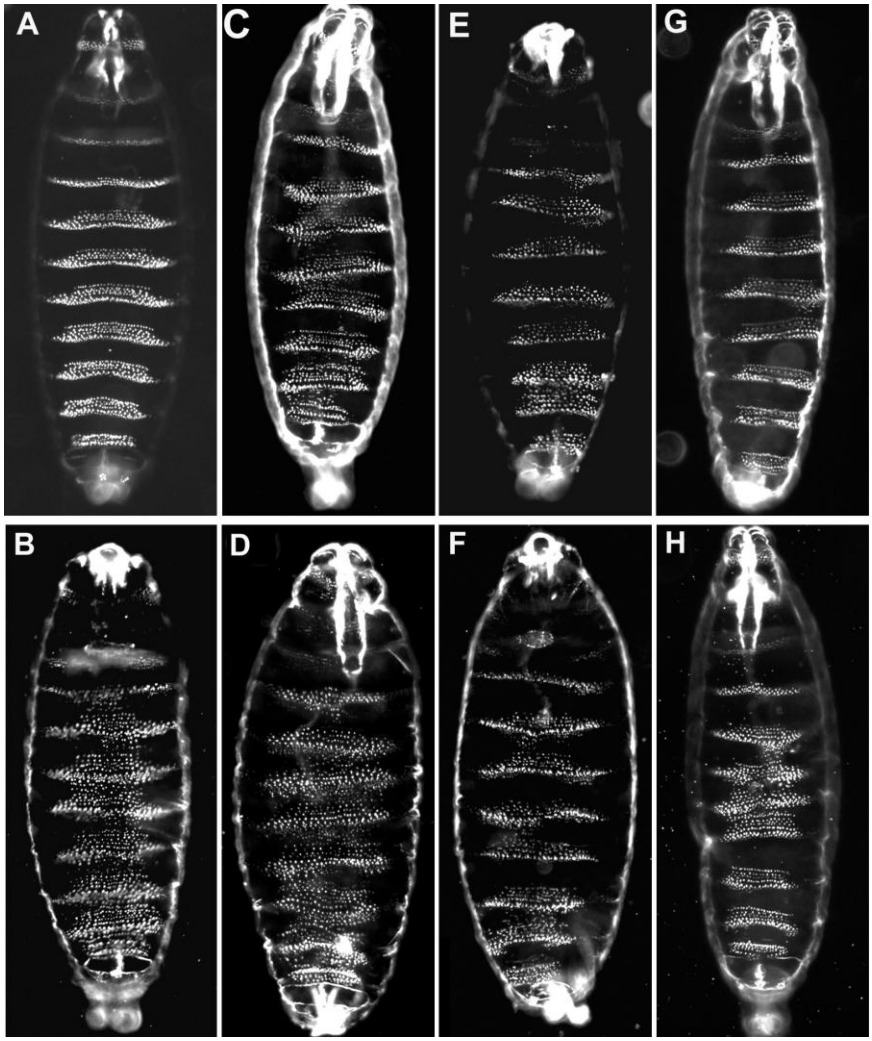

Fig. 1. Partial rescue of the gooseberry phenotype by *gsbn*. Cuticle preparations of wild-type (A), *Df(2R)IIX62* (B), *Df(2R)GGG*^{d13} (C, D), *Df(2R)IIX62*; *gsbnRes-deltaIN3* (E, F), and *Df(2R)GGG*^{d13}; *gsbnRes-deltaIN3* (G, H) embryos are shown under dark field illumination with anterior up. Note that the gooseberry phenotype of *Df(2R)GGG*^{d13} varies between low (C) and high (D) expressivity. Similarly, the partial rescue of the gooseberry phenotype by *gsbn* varies between low (E, G) and high (F, H) expressivity.

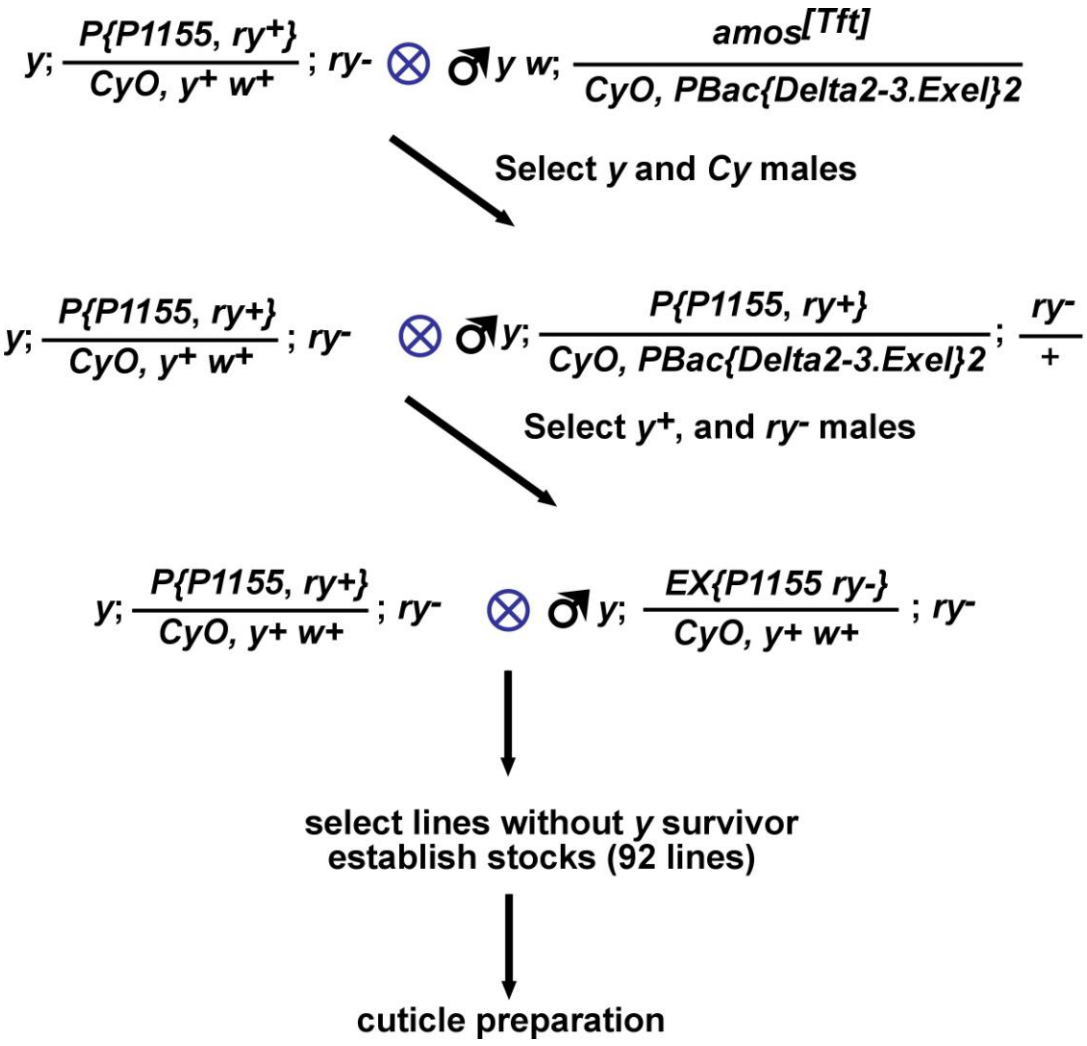

Fig.2. Crossing scheme for the generation of new *gsb* alleles.

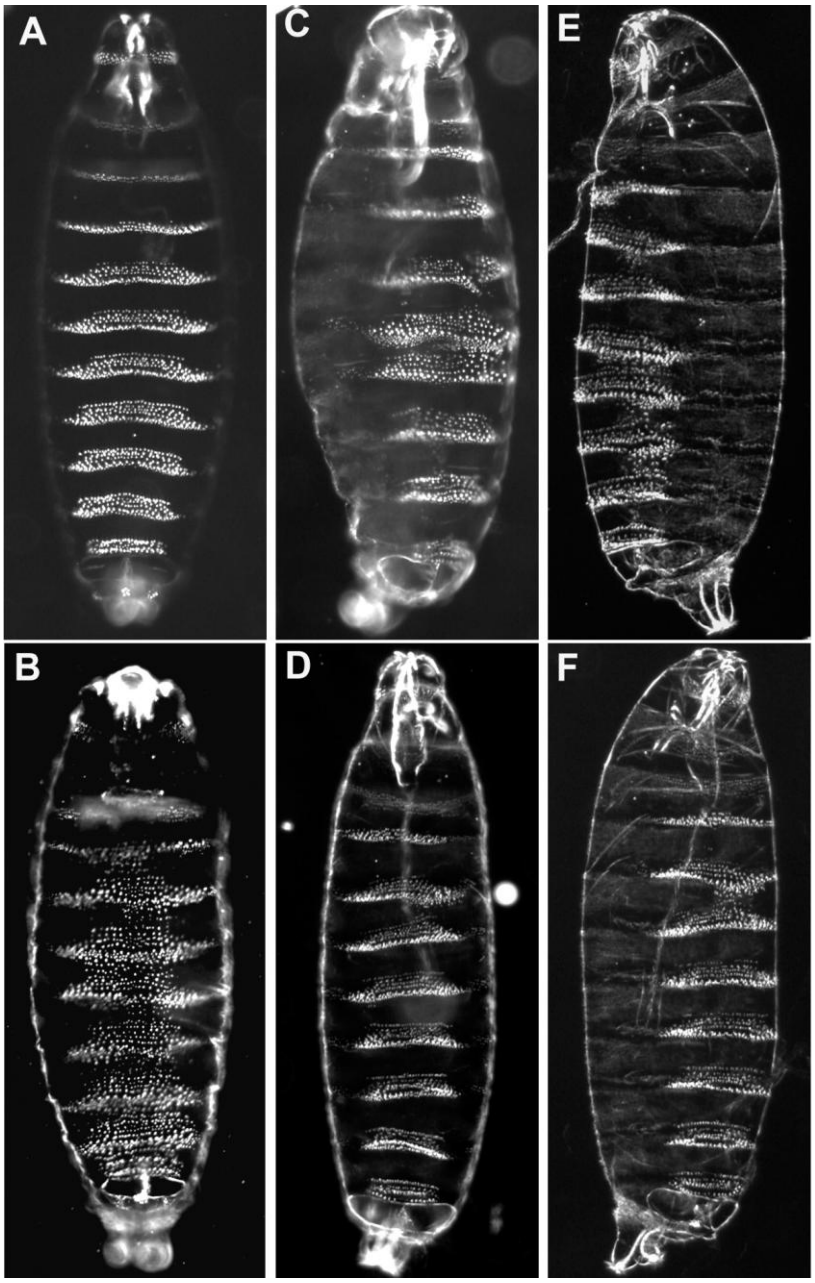

Fig. 3. The cuticular phenotype of the new *gsb* alleles. Cuticle preparations of wild-type (A), *Df(2R)IIX62* (B), gsb^{J46} (C, D), and gsb^{J62} (E, F) embryos are shown under dark field illumination with anterior up.

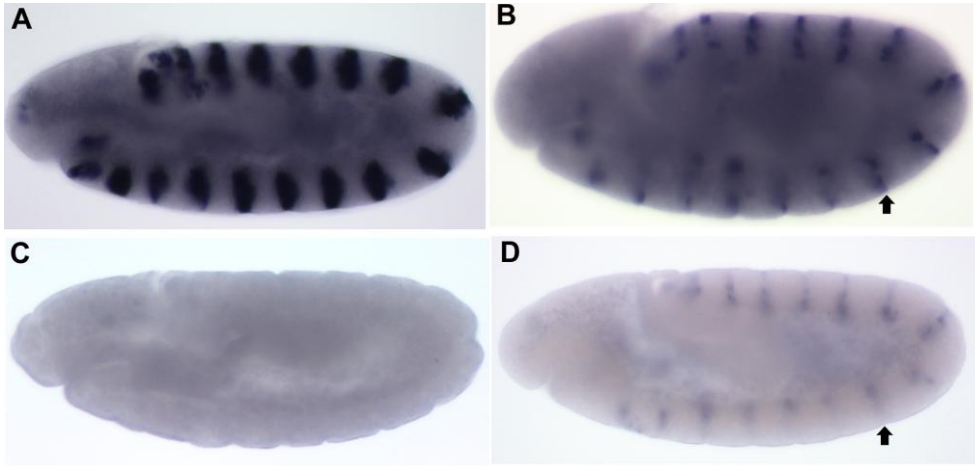

Fig. 4. Characterization of the new *gsb* alleles by anti-Gsb staining. Expression of Gsb protein in wild-type (A), gsb^{P1155} (B), gsb^{J46} (C), and gsb^{J62} (D) embryos at the extended germband stage is revealed by staining with anti-Gsb. Note that in contrast to gsb^{P1155} embryos, Gsb is detected only in the CNS but not in the epidermis of gsb^{J62} embryos (arrows in B and D). Embryos are oriented with their anterior to the left and dorsal side up.

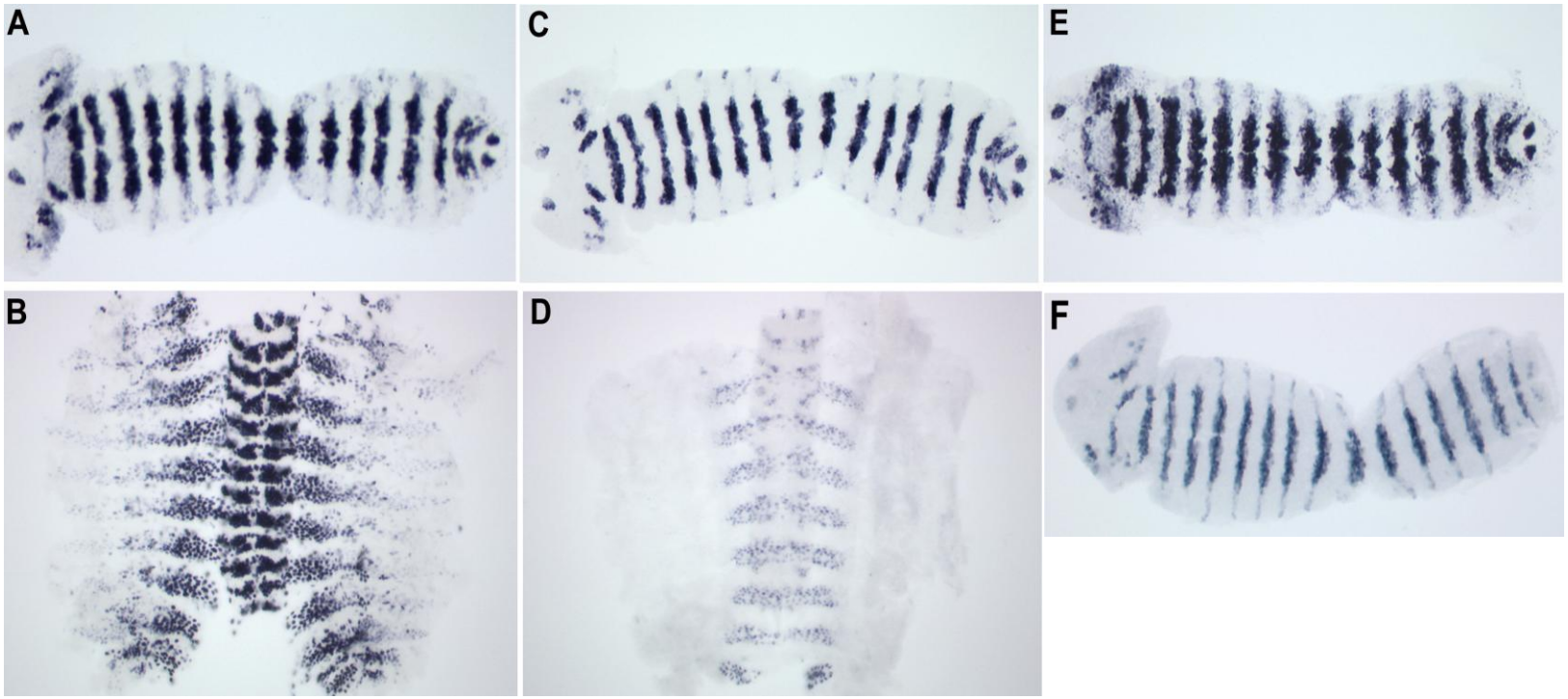

Fig. 5. Expression of *lacZ* in *gsb*^{J46} and *gsb*^{J62} embryos. Homozygous *gsb*^{P1155} (A, B), *gsb*^{J46} (C, D), and *gsb*^{J62} (E) embryos were stained with anti-β-galactosidase. For comparison, a wild-type embryo stained with anti-Gsb is shown in (F). Embryos in (A), (C), (E), and (F) are at stage 11, while embryos in (B) and (D) are at stage 16. Dissected and unfolded embryos are oriented with their anterior to the left (A, C, E, F) or up (B and D).

Acknowledgments

First of all, I would like to thank Prof. Markus Noll, my thesis advisor, for giving me the opportunity to pursue my Ph.D. studies in his lab. Not only his determined commitment to science strikes me, but also his thoroughness in research teaches me by example how to be a scientist. Apart from being an excellent advisor, Prof. Noll supports and helps me in many other ways. I am very grateful to the efforts he made for the reunion of my family.

Without many people's help, the work described in this thesis could not be completed. I am grateful to Prof. Walter Schaffner for being the member of my "Promotionskomitee." I thank Erich Frei for teaching me fly genetics and for stimulating discussions. Jianming Chen, Wei Liu, Yandong Shi, and Hai Zhang provided frequent help during the early stage of my work. I would also like to thank Werner Boll, Michael Daube, Cheng Zhang, and Sabarinadh Chilaka for technical support. My thank also goes to my fellow students in the lab: Sabarinadh Chilaka, Yanrui Jiang, Sreehari Kalvakuri, Jelena Georgijevic-Kühn, Dimitrije Krstic, Shilpi Minocha, Ivan Ostojic, Beijue Shi, and Cheng Zhang for stimulating discussions and friendship. I thank Dieter Egli and Huanfa Liu for sharing with me their experience of the fly knockout technique.

This thesis was thoroughly edited by Prof. Noll and carefully read by Yanrui Jiang to whom I am very grateful. I also thank Werner Boll for translating the "Zusammenfassung."

I thank people in Prof. Walter Schaffner's and Prof. Bernhard Dichtl's group for sharing the weekly progress and literature seminars, which were also an essential part of my training.

I thank Profs. Konrad Basler, Henri-Marc Bourbon, Barry Dickson, Chris Doe, Doug Dimlich, Peter Gallant, Alain Garces, Robert Holmgren, Henry Krause, Ward Odenwald**,** Walter Schaffner, James Skeath, Stefan Thor, and Joachim Urban for reagents.

I thank my wife, Liyun Yu, for her enduring love, support, and for translating the "Zusammenfassung." I close the acknowledgments by dedicating this thesis to my parents, with love and respect.

Curriculum Vitae

Surname:	HE
First name:	Haihuai
Date of Birth:	January 28, 1975
Place of Birth:	Zigong City, Sichuan Province, China
Nationality:	People's Republic of China
Address:	Alte Stationsstrasse 28, Oberglatt CH-8154, Switzerland

Education:

9/1990-7/1993	Shuguang Middle School, Zigong, Sichuan, China
9/1993-7/1997	Undergraduate student Department of Biological Science and Technology Nanjing University Degree: Bachelor of Science
9/1997-7/2000	Master student Institute of Virology, Chinese Academy of Preventive Medicine, Beijing, China Supervisor: Guodong Liang Title of thesis: Construction of infectious full-length cDNA clone of Sindbis virus XJ-160 Degree: Master of Science
8/2001-2007	Ph.D. student Institute for Molecular Biology, University of Zurich, Switzerland Thesis advisor: Prof. Markus Noll Title of thesis: Coupling of redundant *gooseberry neuro* and *gooseberry* functions in *Drosophila melanogaster*, an evolutionary strategy against an intrinsic haploinsufficiency of *gooseberry r*?

Working experience:

10/2000-6/2001 Case Western Reserve University, Cleveland, OH, USA
visiting fellow